UNIVERSITÀ
DEGLI STUDI
DI PADOVA

Sede Amministrativa: Università degli Studi di Padova

Dipartimento di Scienze Cardiologiche, Toraciche e Vascolari

CORSO DI DOTTORATO DI RICERCA IN: SCIENZE MEDICHE, CLINICHE E SPERIMENTALI
CURRICOLO: SCIENZE CARDIOVASCOLARI
CICLO 29°

ROLE OF CARDIAC MAGNETIC RESONANCE IN CLINIC AND ARRHYTHMIC PROGNOSTIC RISK ASSESSMENT IN NON-ISCHEMIC HEART DISEASES

Coordinatore: Ch.mo Prof. Gaetano THIENE
Supervisore: Ch.mo Prof. Martina PERAZZOLO MARRA

Dottorando: Dott. Manuel DE LAZZARI

Ensinar é mostrar que é possível. Aprender é tornar possível a si mesmo.

P. Coelho, O diario de um mago

"Teaching is only demonstrating that it is possible. Learning is making it possible for yourself."

P. Coelho, The Pilgrimage

INDEX

ABSTRACT

Currently, many diagnostic tools are available in the clinical arena helping physicians to achieve a diagnosis in non-ischemic heart diseases and now, the main issue is change into prognostic assessment both clinical and, above all, arrhythmic.

Cardiac magnetic resonance (CMR) has emerged as a clinically applicable and highly reproducible non-invasive imaging technique and so used extensively over the last years. Its value in term of diagnosis is well known and recently investigations are aimed at prognostic purposes and risk stratification. Many studies analyzed the impact of a scar as detected in vivo by contrast-CMR in hypertrophic cardiomyopathy in term of death and ventricular arrhythmias. The same concept was proved for dilated cardiomyopathy identifying a midwall stria as an adverse prognostic marker of cardiovascular death, arrhythmias and less robust marker of heart failure hospitalization. Junctional type of scar was investigated in hypertrophic cardiomyopathy and in right ventricle hypertrophy due to pulmonary artery hypertension, no data concerning its value in dilated cardiomyopathy are reported so far. This learning may be transferred into other kind of heart diseases.

Cardiac magnetic resonance tissue characterization doesn't deal with scar only but also with myocardial tissue edema. Myocardial edema was been strongly studied in acute myocardial infarction in term of area at risk, savage myocardium and to detect hemorrhagic myocardial infarct, but prognostic data regarding other heart diseases are missing.

The aims of our studies were the followings:

1. to evaluate the presence and the prevalence of junctional LGE in patient with dilated cardiomyopathy, the possible relationship between junctional LGE and hemodynamic data and the prognostic significance of this pattern in terms of specific endpoints (arrhythmic and heart failure outcome) in opposite of other type of LGE. In order to investigate this hypothesis, data disclosed in the clinical studio have been proved by ex vivo studies.
2. To evaluate the relationship between myocardial edema as evidenced by CMR and electrocardiographic data (T-wave inversion) in a series of consecutive patients admitted for clinically suspected acute myocarditis. Moreover, to evaluate the prognostic value of T wave inversion (as myocardial edema marker) during the acute/subacute disease phase in predicting LV dysfunction during follow-up.
3. To evaluate the presence of a myocardial substrate underlying life-threatening arrhythmias in young adults with mitral valve prolapse. In order to investigate this hypothesis, data collected in the clinical studio have been proved by pathological (ex vivo) study.
4. Since the proof of the relationship between ventricular arrhythmias and scar in specific area of left ventricle in mitral valve patients, to evaluate the morphological features of mitral valve apparatus underling arrhythmic mitral valve prolapse with fibrosis. In order to confirm these observations, data disclosed by the clinical study have been related by ex vivo results in the pathologic study.

Chapter 1

BACKGROUND

Cardiac Magnetic Resonance

Cardiac magnetic resonance (CMR) is a non-invasive imaging modality allowing not only for highly accurate quantification of right and left ventricular volumes and function, but also for myocardial tissue characterization, including differentiation of myocardial edema and necrosis/fibrosis, which may otherwise remain unrecognized (1). Furthermore, there is growing evidence delineating the strength and additive value of CMR in identifying patients at risk for sudden cardiac death (SCD) in all cardiomyopathies, beyond other traditional risk factors as ejection fraction (2).

The volumes and function information are obtained by steady state free precession sequences, the methods of choice for cine imaging. They allow high signal-noise ratio and excellent contrast between myocardium and blood pool. These features lead to an easy morphologic and functional analysis.

The most widespread used technique to detect myocardial edema are T2-weighted sequences even if they can have potential pitfalls that might be known

and recognized to avoid a misleading interpretation. Incomplete blood suppression with dark-blood techniques, regional variations in signal intensity from coil inhomogeneities, and signal loss from myocardial contraction and relaxation during acquisition are significant challenges for this technique in clinical practice. Thanks to recent technical developments (i.e. turbo inversion recovery magnitude sequences, Figure 1A) such challenges can be overcome most of the time. The special relevance that myocardial edema assessment has in a lot of clinical settings makes these information essential. Nowadays mapping techniques seem to be more accurate than classical T2-weighted but not widespread available (1).

The technique of late gadolinium enhancement (LGE) to detect myocardial scar/fibrosis (Figure 1B) was developed more than one decade ago and validated with histopathologic correlation (3). Gadolinium is an intravascular medium of contrast which can diffuse in the interstitial space following a pathologic insult. These agents have paramagnetic properties, and as such, they modify tissue properties that directly affect T1 and T2 signal intensities on CMR. As a consequence, contrast agents yield a bright signal in the damaged areas where they accumulate compared to normal myocardium on delayed post contrast imaging. From LGE distribution, we can recognize several “pattern” of LGE: a spot pattern if the area of LGE is small and focal, “patchy” if there are multiple irregular foci of LGE, “stria” if the area of LGE has a linear shape like a band and “transmural” if the LGE is involving the whole thickness of myocardium wall (4).

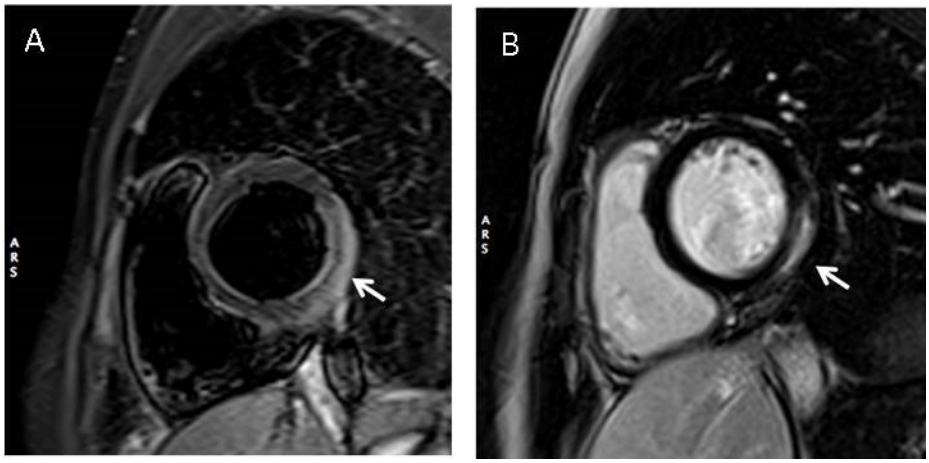

Figure 1; T2-weighted sequence to detect myocardial edema. Note the presence of myocardial edema in the epicardial layer of left ventricle lateral wall (A, white arrow); Delayed post contrast image (LGE) to detect myocardial fibrosis/necrosis. Note the presence of myocardial necrosis in the epicardial layer of left ventricle infero-lateral wall (B, arrow).

Current clinical application

In current clinical practice, CMR plays a central role in the diagnostic and decision making process in several cardiac disease/pathologies, including acute and chronic ischemic heart diseases, dilated cardiomyopathy, hypertrophic cardiomyopathy, acute myocarditis, infiltrative disease and cardiac masses.

Cardiac Magnetic Resonance has an expanding role also in prognostic risk assessment. The LGE (with a stria pattern, Figure 2A) in dilated cardiomyopathy is a promising predictor of cardiac death and ventricular tachycardia (5) even if in order to validate a biomarker as best predictor a vast multicenter clinical trial is needed. A recent meta-analysis showed that patients with LGE had increased overall mortality (odds ratio, 3.27; $P<0.001$), heart failure hospitalization (odds ratio, 2.91; $P=0.02$), and SCD/aborted SCD (odds ratio, 5.32; $P<0.001$) compared

with those without LGE (2). In the hypertrophic cardiomyopathy, left ventricle (LV) scar (Figure 2B) is demonstrated an independent predictor of inducible ventricular tachycardia, SCD (7,8), or cardiac death (9).

In Arrhythmogenic Ventricular Cardiomyopathy CMR plays an important role as diagnostic tool, even if so far the post contrast findings are not considered in current task force criteria (Figure 2C). Notwithstanding, post contrast imaging is an essential technique to identify an associated LV involvement or a left dominant disease. Finally the presence of LGE is associated with a high prevalence of appropriate ICD therapy and SCD reaching 48% (10).

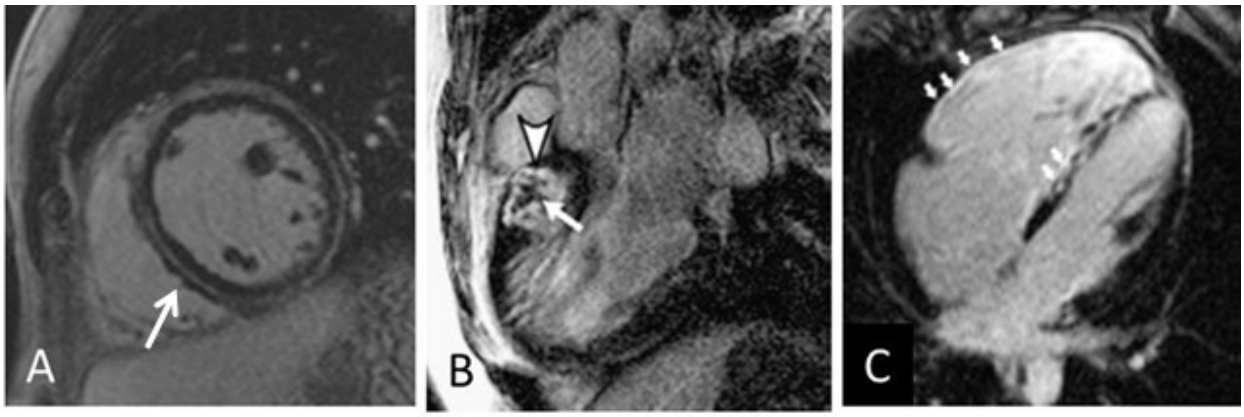

Figure 2. CMR post contrast images of (A) dilated cardiomyopathy with mid wall fibrosis stria (white arrow); (B) hypertrophic cardiomyopathy, note the black area (arrow head) within the LGE area (white arrow) corresponding to preserved isolated myocardium or microvascular damage; Arrhythmogenic cardiomyopathy (C) with fibrosis involving both right ventricle and interventricular septum, (arrows).

Chapter 2

COMPREHENSIVE AIMS

If the added clinical and prognostic value of tissue characterization endorsed by CMR is well known in several cardiomyopathies as previously described, some aspects of dilated cardiomyopathy and myocarditis as well as some old concepts regarding the challenging risk assessment in mitral valve prolapse are missing. I.e. the value of a focal LGE spot along the interventricular septum junctional points is not yet assessed in dilated cardiomyopathy. In acute myocarditis, the meaning about the prognostic value of negative T-wave is not studied, even this ECG pattern is considered benign in acute ischemic heart disease and in apical ballooning syndrome hence it might be represent an underlying transient myocardial edema. Finally, detection of myocardial scar may benefit the challenging risk assessment of mitral valve prolapse patients as seem to be true for non ischemic cardiomyopathy as described before.

The aims of our researches are to investigate the role of CMR in clinical and arrhythmic risk assessment in non ischemic heart disease such as:

- dilated cardiomyopathy focusing in the junctional pattern of LGE in opposition to classical stria, evaluating its prognostic role since analyzed its prevalence and the relationship with hemodynamic data obtained by simultaneous heart catheterization (Chapter 3).
- acute clinically suspected myocarditis focusing in myocardial edema as substrate of negative T waves and its implications in the follow up (Chapter 4)
- mitral valve prolapse focusing in the substrates associated with ventricular arrhythmias (Chapter 5 and 6).

Regarding the junctional pattern in dilated cardiomyopathy and the anatomic-morphological features of left ventricle and mitral valve annulus in mitral valve prolapse, the *in vivo* analysis performed by CMR have been compared with *ex vivo* pathologic and histopathologic studies.

Chapter 3

THE DIFFERENT PROGNOSTIC ROLE OF FIBROSIS IN DILATED CARDIOMYOPATHY.

Is not just a matter of Late Enhancement

3.1 Introduction

Dilated cardiomyopathy (DCM) is a common heart muscle disease, which is responsible for approximately one-third of the heart failure (HF) (11,12). Life-threating arrhythmias and sudden cardiac death (SCD) account for 30% of all fatalities in this kind of patients (13). Current risk stratification for SCD and indication to implant an ICD rely on reduction of LV (left ventricle) ejection fraction (EF), which is a recognized poor marker of ventricular electrical instability (14-16). Clinic-pathologic correlation studies have showed that the presence of myocardial fibrosis may provide a substrate for malignant ventricular arrhythmias and SCD (17,18).

As highlighted in the section before, CMR with LGE is a well established noninvasive tool that has the ability to accurately identify and quantify ventricular myocardial fibrosis (19). Previous CMR studies in patients with DCM have demonstrated that ventricular LGE heralds an adverse prognosis with regard to death and/or composite end point (i.e. heart failure-related hospitalization, arrhythmias). Also our group published a study designed with the aim of evaluate the role of the presence and the extent of LV LGE for predicting major arrhythmic events and SCD in a large population of patients with DCM diagnosed according to the WHO criteria (6). By study design, the hemodynamic patient profile encompassed the entire disease spectrum including subjects with severe LV dysfunction who meet criteria for ICD implantation and those with mild or moderate disease forms who did not. Dilated cardiomyopathy was classified as "non-ischemic" by coronary angiography findings, which is consistent with current clinical practice and allows the most accurate etiology definition for clinical research purposes. The major study results were that: 1) presence of LV-LGE is a powerful and independent predictor of arrhythmic outcome during a median follow-up period of 3 years; 2) presence of LV-LGE appeared to be superior in predicting major arrhythmic events and SCD to traditional LV EF ≤35%; 3) the absence of LGE characterized a low arrhythmic subgroup of patients with no SCD events over the follow-up. A sub-analysis of our data failed in disclosing an association between LGE and heart failure outcome. In the same year, Kuruvilla et al (2) published a metanalysis including 9 studies with a total of 1,488 patients and a mean follow-up of 30 months. Patients with LGE had increased overall mortality (OR 3.27, $p<0.001$) and an increased risk of SCD/aborted SCD (OR 5.32, $p<0.001$) when compared with those without LGE. Also the HF hospitalization was assessed but with a lower estimated odd ratio (OR 2.91, $p=0.02$) but, as the same authors declared, with a wide heterogeneity among the studies.

Of note, also the presence and extent of pulmonary hypertension (PH) is a well-established prognostic factor in heart failure (HF) in terms of increased mortality and hospitalization rates (20-24). At least two thirds of patients with severe LV systolic dysfunction have PH with associated right ventricular (RV) failure, and mortality in this group is 2-folder higher in comparison with isolated LV dysfunction (22). Hence, the potent prognostic impact of PH in HF suggests an important role for pre-clinical detection of signs indicating an ongoing RV dysfunction due to its remodeling.

The presence of a new pattern of LGE along the right ventricle (RV) junctional insertion point of the interventricular septum was recently described by CMR in patients with pulmonary artery hypertension (PAH). This pattern, the so-called junctional LGE was present in the majority of these patients (25-31), associated with a RV hypertrophy due to pulmonary artery pressure overload. These studies suggested a significant inverse correlation between the degree of junctional RV LGE and hemodynamics. The hypothesized mechanisms underlying junctional LGE in PAH includes myocardial ischemia, hypoxia, fibrosis, and mechanical wall stress, leading to the development of local fibrosis in those places where the RV muscular stress is unloaded and we can speculate that junctional LGE is related to gadolinium pooling within these area.

So far, a junctional type LGE pattern has been found beyond PAH, in other clinical conditions such as hypertrophic cardiomyopathy (32), congenital heart disease with RV overload (33,34), dilated cardiomyopathy (alone or associated with diffuse mid-wall LGE) (35,36), and moreover in endurance athletes (37). The association between hemodynamic parameters and junctional LGE have been studied in PH only in the setting of a precapillary PAH, characterized by a normal pulmonary capillary wedge pressure (PCWP) (25,31), and no data have been reported i.e. in patients with DCM and severe impairment of LV systolic function, characterized by end diastolic LV pressure overload/post capillary pulmonary

hypertension (Group 2) (38). If it could be demonstrated that junctional LGE pattern correlate with a worst hemodynamic parameters in term of end-diastolic LV pressure and/or post capillary pulmonary artery pressure, it will be a marker of incipient heart failure than other classical LGE pattern already analyzed (i.e. midwall stria, epicardic stria, patchy).

3.2 Aims

The aims of our study were: 1) to evaluate the presence and the prevalence of junctional LGE in patient with DCM, 2) to evaluate the possible relationship between LGE and hemodynamics obtained by a simultaneously right side catheterization, and 3) to evaluate the prognostic significance of this pattern in terms of major events and specific arrhythmic and heart failure outcome in opposite of other type of LGE.

3.3 Methods

Study population design

The present study included a consecutive series of patients referred to our clinic with diagnosis of DCM, based on the 1995 WHO/International Society and Federation of Cardiology criteria (39). To be enrolled, patients had to have 1) a reduced LV systolic function (LV EF <50%) on echo; 2) an angiographic study showing the absence of flow-limiting coronary artery disease (defined as ≥ 50% luminal stenosis on coronary angiography); 3) the absence of either valvular or hypertensive heart disease and congenital heart abnormalities.

Exclusion criteria were: recent onset of heart failure (<1 month); diagnosis of hypertrophic cardiomyopathy, restrictive cardiomyopathy, arrhythmogenic right ventricular cardiomyopathy, suspected infiltrative heart disease or other specific cardiomyopathies; contraindication to CMR (claustrophobia, pacemaker, implantable cardioverter defibrillator ICD, metallic clips, atrial fibrillation, severe obesity preventing the patient from entering the scanner bore; pregnancy); chronic renal failure with an estimated glomerular filtration rate < 30 ml/min. All subjects underwent a comprehensive diagnostic work-up including 12-leads electrocardiogram, echocardiography, biochemistry, CMR and cardiac catheterization (including coronary angiography), during the same hospitalization. The institutional review board approved the study, and all patients gave their informed consent.

Cardiac Catheterization

Diagnostic right heart catheterization was performed using a Swan-Ganz® Standard Thermodilution Catheters (Edwards Lifesciences) within 24 hours of CMR execution. The following measurements were obtained: mean right atrial pressure (RAP), systolic and end-diastolic right ventricular pressures, pulmonary artery systolic, mean and diastolic pressure (PASP, PAMP and PADP, respectively), and pulmonary capillary wedge pressures (PCWP). Blood samples for estimation of oxygen saturation were drawn from the superior and inferior caval veins, as well as right atrium, and that from the pulmonary and femoral arteries were used for screening for intra-cardiac shunts. Cardiac output was determined by thermodilution. Pulmonary vascular resistance (PVR) was calculated from the equation PAMP-PCWP (trans-pulmonary gradient) divided by cardiac output (CO). Using a pigtail catheter placed into the LV, LV end-diastolic pressure (LVEDP) was recorded. According with current guidelines (38), PH is definited as a PAMP ≥25 mmHg at rest, pre-capillary PH as PCWP is ≤15 mmHg, post-capillary PH as PCWP

>15 mmHg. Combinated post capillary and pre-capillary PH if the diastolic pressure gradient (definited as PADP – PCWP) ≥9 mmHg (38).

Cardiac Magnetic Resonance scan protocol and analysis

Cardiac magnetic resonance scan was performed on a 1.5-Tesla scanner (Magnetom Avanto, Siemens Medical Solutions, Erlangen, Germany). All patients underwent detailed CMR study protocol including post-contrast sequences. Images were acquired using a steady-state free precession sequence (true FISP) cine loops in sequential short axis views and 3 long- axis views.

After intravenous administration of contrast agent 2-dimensional segmented fast low-angle shot inversion recovery sequence after at least 10 minutes were acquired in the same views of cine images, covering the entire ventricles Inversion times were adjusted to null normal myocardium (typically 220-300 msec) and images were repeated in 2 separate phase-encoding directions to exclude artefacts (see Appendix section for details).

Global ventricular volumes, systolic function and LV myocardial mass were calculated from the short-axis cine images, excluding papillary muscles from the myocardium, using a dedicated software (CMR42, Circle Cardiovascular Imaging Inc). The presence, location and extent of LGE were assessed by two experienced observers who were blinded to clinical data and outcome; ambiguous cases were reviewed using a third expert. To exclude artefact, LGE was deemed present only if visible in two orthogonal views (short-axis and long-axis). To detect junctional LGE distinguishing from RV cavity or interventricular fat, post-contrast images were compared with balance steady-state free precession using frames acquired in the same position and in the same cardiac phase. Myocardial LGE was quantified by a semiautomatic detection and LGE mass (in grams) expressed as a percentage of total LV mass, according to previously validated methods (40) LGE was quantified using a signal intensity threshold of >3SD above a remote

reference region (41-44). The pattern of LGE distribution was characterized as either epicardial, mid-wall or patchy/junctional (35,36,42). Patients initially diagnosed as having DCM displaying a subendocardial or transmural pattern of LGE suggestive of myocardial infarction were excluded from the final analysis.

Follow up

The follow-up data were obtained prospectively during regular outpatient visits at 3, 6, 12,18 and 24 months. All events were adjudicated by the consensus of an independent committee blinded to the CMR results. The events collected were: hospitalization for decompensated heart failure (requiring inotropic and diuretics infusions), cardiac death/heart transplantation/ventricular assist devices and ventricular arrhythmias (composite by sustained ventricular tachycardia, sudden cardiac death, aborted sudden death, appropriate ICD intervention).

A 24-h ECG-Holter monitoring was obtained for each patient without ICD every 6 months. Routine ICD interrogation (at 1, 3 and 6 months, and every 6 months thereafter) and ECG recordings at the time of symptoms were used to document the occurrence of spontaneous ventricular tachycardia (VT) during follow-up. Sudden death was defined as any natural death occurring instantaneously or within one hour from symptoms onset. Sustained VT was defined as tachycardia originating in the ventricle with rate >100 beats/minute and lasting >30 seconds or requiring an intervention for termination. Appropriate ICD intervention was defined as a device shock or anti-tachycardia overdrive pacing delivered in response to a ventricular tachyarrhythmia and documented by stored intracardiac ECG data.

Statistical Analysis

Data are expressed as mean value ± standard deviation or median with 25 to 75 percentiles for normally distributed and skewed variables, respectively.

Normal distribution was assessed by Kolmogorov-Smirnov test. Differences between categorical variables were evaluated by the chi-square test or the Fisher exact test as appropriate. Categorical variable are expressed as percentiles. Paired and unpaired t test were used to compare normally distributed continuous variables respectively obtained from the same patient and different patients; paired and unpaired Rank Sum test were used for skewed continuous variables.
Regression analysis models were conducted on blocks of variables until regression final model with only significant variables were obtained in order to evaluate the independent predictive value of functional and hemodynamic parameters. Kaplan-Meier analysis was used to estimate the survival distributions. Cox model was used to identify predictors of events during follow up. Linear regression was used to assess the correlation between the 2 independent observes performing LGE planimetry. A p value <0.05 was considered significant. Statistics were analysed with SPSS version 19 (SPSS Inc, Chicago, IL).

3.4 Results

Baseline characteristics

A total of 144 with DCM were consecutively evaluated; 8 refused or had contra-indication to contrast-enhanced CMR and 5 did not perform right heart catheterization within 24-hours so these patients were finally excluded. Four patients were lost over the follow-up. The remaining 127 patients (97 men, median age 49 years) fulfilling the enrolment criteria constituted the final study population.
On the basis of LGE findings, out of 127 patients, 48 (38%) showed junctional LGE.

Table 1 shows baselines clinical characteristics of the enrolled patients. Thirty-one patients (24%) had a family history of DCM; 59 patients (47%) had a history of chronic HF. At the time of CMR, the majority of patients were NYHA class I or II and received a heart failure drug therapy, including angiotensin-converting enzyme Inhibitor (ACEI) or angiotensin II receptor blockers (ARB) (92%), and ß-blockers (94%). No differences on baseline characteristics were found between patients with or without junctional LGE.

Cardiac magnetic resonance findings

On morpho-functional CMR, the majority of patients (73%) showed an EF minor than 35% (median EF value 29%) (Table 1). No differences on LV and RV dimension were found between patients with or without junctional LGE. In the junctional LGE group, the patients had reduced RV EF (51% vs 57%, p<.001) and LV EF (27% vs 30%, p=0.003).

On post-contrast images, 58 (46%) patients had a midwall stria or a spot pattern of LGE. Contrast LGE was observed in the RV junctions (at the level of RV insertion points with septum) in 48 (38%) patients: in 17/48 patients LGE was confined only to the junctions points in 29/48 patients the junctional LGE was associated with mid-wall interventricular septal stria and 2 patient had junctional LGE associated with mid-wall stria on lateral free LV wall. Twenty-seven patients showed mid-wall/spot LGE pattern without junctional involvement.

The median extent of LGE was 2% [0-10%] of LV mass in the overall population. Among patients with LGE, the median extent of LGE was 10% [3-14%] and the median extent of junctional LGE was 1% [0-2%] of LV mass.

Linear regression analysis showed a high correlation between the 2 observers for planimetry of %LGE (r=0.95, p <0.01).

Table 1. Baseline characteristics of overall sample and according to results of Late Gadolinium Enhancement.

	Overall sample n = 127	**Junctional LGE present n = 48**	**Junctional LGE absent n = 79**	**p**
Age (years)	49 (37-61)	49 (37-62)	49 (33-60)	0.423
Male sex, No. (%)	97 (76)	37 (77)	60 (76)	0.884
Family history of DCM, No. (%)	31 (24)	13 (27)	18 (23)	0.585
Chronic heart failure (> 6 months), No. (%)	59 (47)	22 (46)	37 (47)	0.913
LBBB, No. (%)	43 (34)	16 (33)	27 (34)	0.922
NYHA class, No. (%)				
I-II	82 (65)	32 (67)	50 (63)	0.700
III-IV	45 (35)	16 (33)	29 (37)	0.700
Medications, No. (%)				
ACEI or ARB therapy	117 (92)	42 (88)	75 (95)	0.176
ß-blockers	119 (94)	45 (94)	74 (94)	0.762
Spironolactone	70 (55)	31 (65)	39 (49)	0.106
Diuretic	93 (73)	38 (79)	55 (70)	0.321
Amiodarone	20 (16)	9 (19)	11 (14)	0.506
Digoxin	18 (14)	9 (19)	9 (11)	0.265
NTproBNP (ng/L)	770 (381-1942)	1161 (694-3901)	662 (217-1487)	0.004
CMR				
LV EDV (mL/m^2)	113 (93-147)	111 (99-148)	113 (93-147)	0.542
LV EF (%)	29 (24-37)	27 (21-33)	30 (25-38)	0.033
LV EF< 35%, No. (%)	93 (73)	39 (81)	54 (68)	0.112
RV EDV (mL/m^2)	90 (82-100)	93 (82-118)	88 (83-97)	0.189
RV EF (%)	55 (48-60)	51 (45-56)	57 (52-61)	<0.001

LGE= Late Gadolinium Enhancement; DCM = Dilated Cardiomyopathy; EF= Ejection Fraction; EDV = End-Diastolic Volume; NYHA = New York Heart Association; ACE= Angiotensin-Converting Enzyme Inhibitors; ARB= Angiotensin II Receptor Blocker; LBBB = Left Bundle Branch Block; CMR= Cardiac Magnetic Resonance;

Categorical variables are presented as number of patients (%). Continuous values are expressed as median with 25% and 75%-iles.

Right heart catheterization hemodynamic and delayed enhancement

Right heart side catheterization demonstrated pulmonary hypertension, defined as a PAMP >25 mmHg, in 58 patients (46%) (Table 2); the majority of subjects showed increased LVEDP (69%) and 53% had increased PCWP. Patients with junctional LGE showed a worse hemodynamic profile in terms of pulmonary

hypertension (58% vs 38%; p=0.026), an increased value of PCWP (71% vs 42%; p=0.001) and LVEDP (88% vs 58%; p=0.001). According with the current European Society of Cardiology guidelines, among patients with PH with high PCWP, 54/58 patients had a combined post capillary and precapillary PH (Diastolic Pressure Gradient ≥7 mmHg).

In the junctional LGE group, a slight greater value of RAP (mean 6 mmHg vs 5 mmHg; p=0.019) were demonstrated.

Table 2. Hemodynamic characteristics on cardiac catheterization of overall sample and according to results of Late Gadolinium Enhancement.

	Overall sample n = 127	**Junctional LGE present n = 48**	**Junctional LGE absent n = 79**	**p**
PAMP > 25 mmHg	58 (46)	28 (58)	30 (38)	0.026
PCWP > 15 mmHg	67 (53)	34 (71)	33 (42)	0.001
LVEDP > 12 mmHg	88 (69)	42 (88)	46 (58)	0.001
CI (L/min/m^2)	2.6 (2.0-3.1)	2.5 (1.9-2.8)	2.6 (2.2-3.1)	0.460
PVR (Wood)	1.6 (1.1-2.5)	1.6 (1.1-2.5)	1.5 (1.5-2.1)	0.257
RAP (mmHg)	5 (3-8)	6 (4-10)	5 (2-8)	0.019

LGE= Late Gadolinium Enhancement; PAMP= Pulmonary Artery Mean Pressure; PCWP = Pulmonary Capillary Wedge Pressure; LVEDP = Left Ventricular End-Diastolic Pressure; CI = Cardiac Index; PVR = Pulmonary Vascular Resistance; RAP = Right Atrial Pressure.

Categorical variables are presented as number of patients (%). Continuous values are expressed as median with 25% and 75%-iles.

Among clinical and functional parameters both the value of RV and LV EF were significant in predicting junctional LGE (table 3), but only the RV EF resulted the independent one.

All right catheterization parameters indicating a worse hemodynamic status were significant on univariate analysis (table 3). The best variable at univariate analysis resulting with a higher HR in predicting junctional LGE was LVEDP.

In the final multivariate model RV EF and LVEDP resulted independent predictor of junctional LGE (LVEDP: OR 3.798; 95% CI 1.405-10.265, P= 0.009 and RV EF: OR 0.937; 95% CI 0.896-0.981, P=0.005).

Table 3. Clinical, functional and hemodynamic predictors of junctional LGE.

	Univariate analysis			Multivariable analysis*		
	OR	**CI**	**p**	**OR**	**CI**	**p**
Age (years)	1.009	0.986-1.033	0.441			
NYHA I-II	0.928	0.637-1.354	0.700			
LBBB	0.963	0.451-2.057	0.922			
LV EF (%)	0.956	0.918-0.995	0.027			
LV EDV (mL/m2)	1.005	0.995-1.015	0.313			
RV EF (%)	0.925	0.885-0.967	0.001	0.937	0.896-0.981	0.005
RV EDV (mL/m2)	1.015	0.995-1.036	0.140			
PAMP > 25 mmHg	2.287	1.100-4.754	0.027			
PCWP > 15 mmHg	3.385	1.537-7.285	0.002			
LVEDP > 12 mmHg	5.022	1.913-13.184	0.001	3.798	1.405-10.265	0.009

Abbreviations as in Table 1 and 2.
* final model.

Representative cases of a patient with post-capillary pulmonary hypertension and junctional LGE compared with a patient without pulmonary hypertension and no LGE is shown on Figure 3.

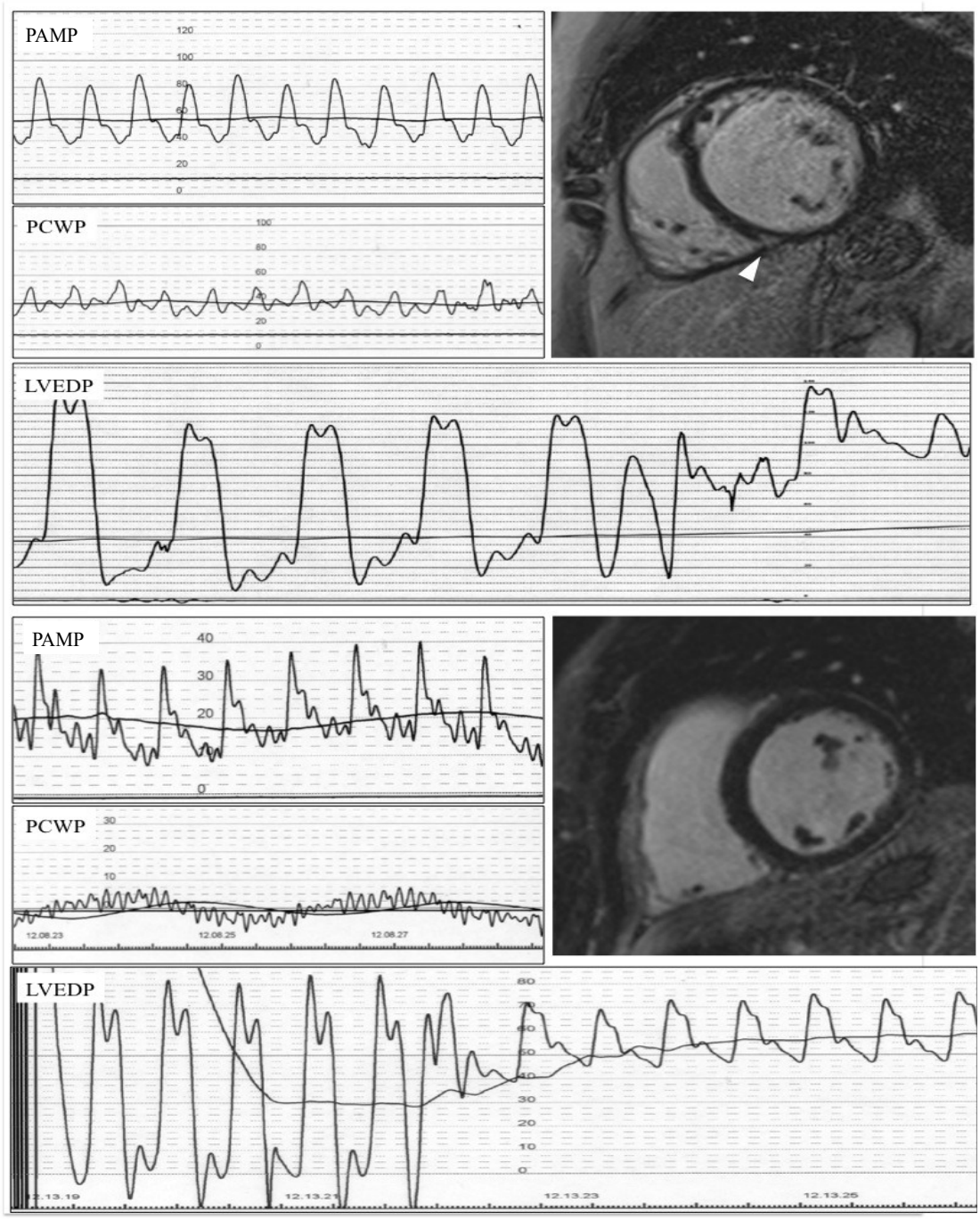

Figure 3. Hemodynamics data provided by right heart catheterization in patients with and without pulmonary hypertension and the corresponding post contrast CMR findings (short axis view). On the top a patient with post capillary pulmonary hypertension presenting a LGE area in the inferior ventricular junction (white arrow head). On the bottom, patient with normal pulmonary pressure values without LGE on post contrast CMR image. Abbreviations in the text.

Survival analysis

During a 24 months follow-up, 15 patients (12%) had death/heart transplantation/ventricular assist device, 7/48 (15%) in the junctional LGE group versus 8/79 (10%); 18 subjects (14%) had at least an episode of HF requiring intravenous administration of diuretics and inotropes, 14/48 (29%) among junctional LGE group versus 4/79 (5%). Ten patients (8%) experienced ventricular arrhythmias or sudden cardiac death, 4/48 (8%) in the junctional LGE group versus 6/79 (8%). Figure 4 shows Kaplan-Meier analysis of survival from heart failure end point (A and B), arrhythmic end point (C and D) and death/heart transplantation end point (E and F), each stratified both by the presence of junctional LGE and by non junctional LGE. Regarding HF end point both junctional LGE and non junctional LGE are associated with a worse follow up but only junctional type reaches the statistical significance. Regarding arrhythmic end point, only non junctional type seems to be a predictor of events.

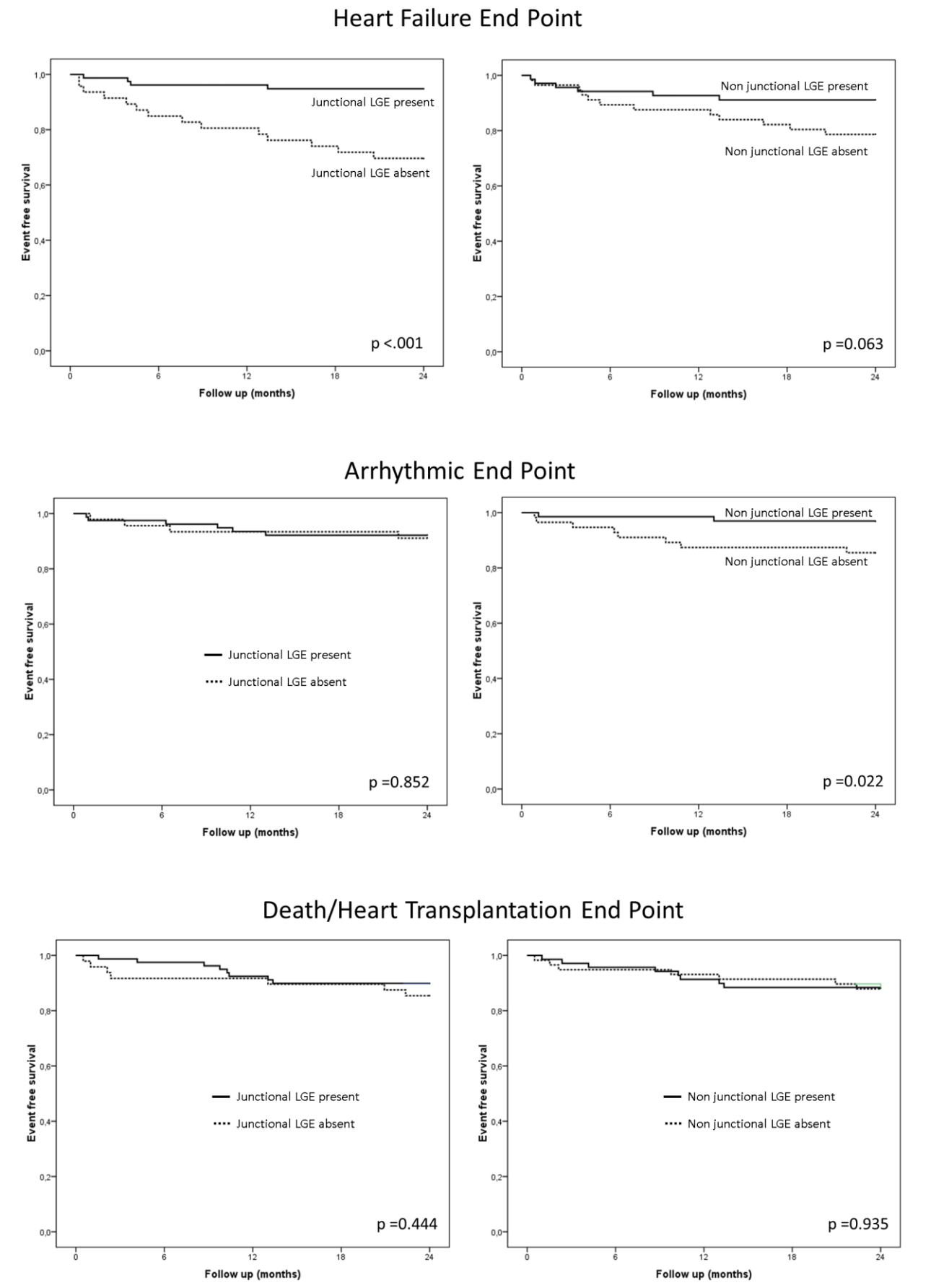

Figure 4. Kaplan-Meier analysis of survival from different endpoints. See text.

Autopsy data

During follow-up, 2 patients with junctional LGE previously demonstrated in vivo by CMR underwent heart transplantation. Comparison of the macroscopic appearance of the cut surface of the heart suggested fibrosis and interstitial expansion particularly affecting the right ventricular insertion points (Figure 5). There was excellent agreement between the pathological location of junctional expansion and the pre-mortem location of LGE on right ventricular insertion points with LV, so called “junctions”.

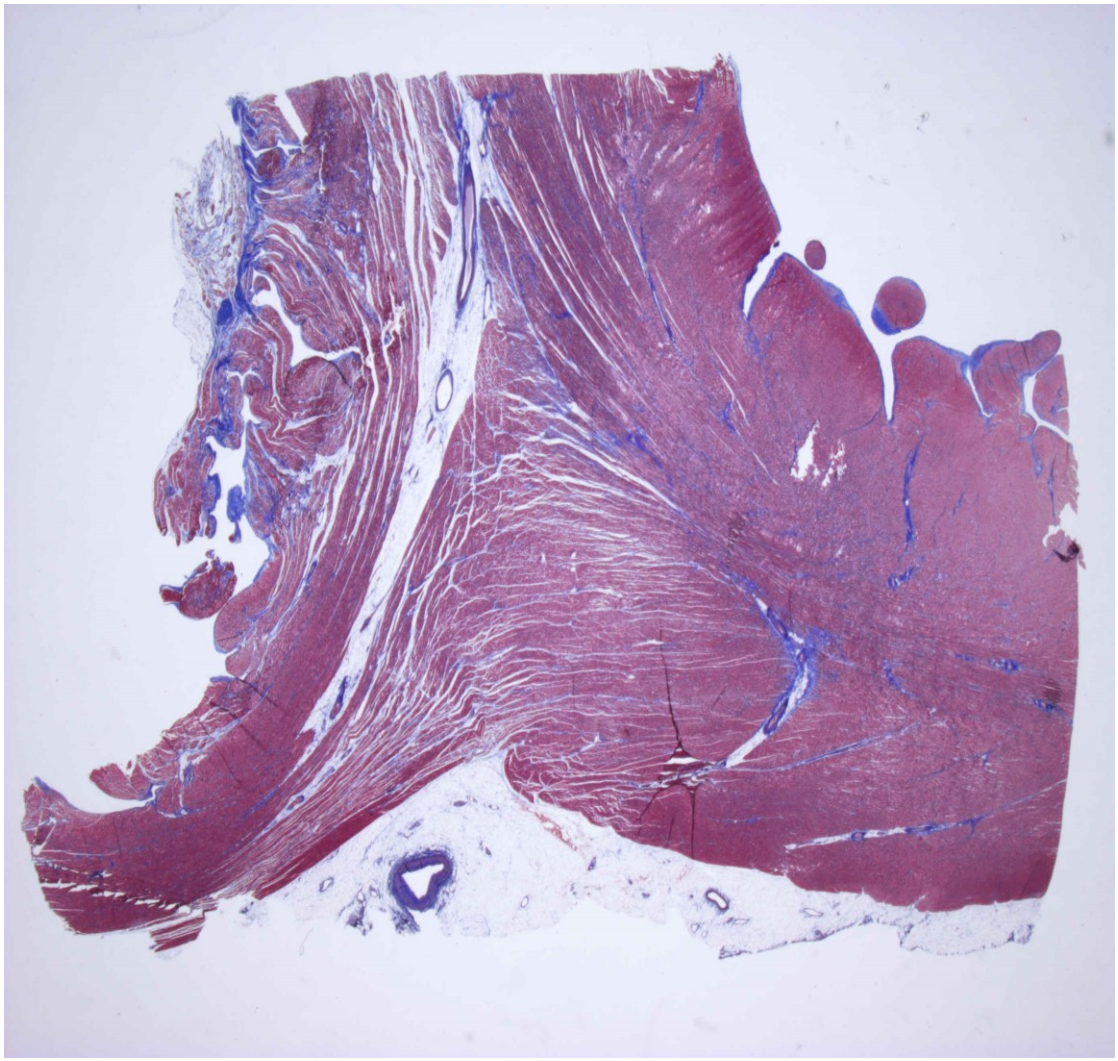

Figure 5. Representative histology of the RV-LV insertion point showing expansion of the interstitium and myocardial fibers with different orientation.

Cardiac Magnetic Resonance predictors of events

During a 24 months follow up both LV EF (HR 0.943; 95%CI 0.890-0.999; p= 0.044) and RV EF (HR 0.939; 95%CI 0.899-0.981; p= 0.005) were predictor of HF events during 24 months follow up. Also the presence of LGE (overall) seems to predict the occurrence of HF, as well the presence of junctional LGE (HR 6.566; 95% CI 2.16-19.955; p=0.001). Of note, dividing population by the presence of the classical LGE pattern (i.e. stria, without considering junctional involvement), the LGE fails to predict HF events (Table 5).

For the arrhythmic end point, only RV dysfunction (HR 0.925; 95% CI 0.872-0.980; p=0.008) and the presence of a non junctional LGE pattern (HR 5.102; 95% CI 1.081-23.809; p=0.040) were predictors of events (Table 6), instead junctional LGE fails.

Finally, regarding death/heart transplantation neither the presence of LGE or any pattern of LGE were able to predict events, but only RV and LV dysfunction (Table 7).

Table 5. CMR predictors of heart failure.

	Univariate analysis		
	HR	**CI**	**p**
LV EF (%)	0.943	0.890-0.999	0.044
LV EDV (mL/m^2)	1.005	0.993-1.018	0.415
RV EF (%)	0.939	0.899-0.981	0.005
RV EDV (mL/m^2)	1.031	1.007-1.055	0.011
LGE overall	6.113	1.405-26.589	0.016
Junctional LGE	6.566	2.160-19.955	0.001
Non junctional LGE	2.457	0.923-6.546	0.072

Abbreviations as in Table 1 and 2.

Table 6. CMR predictors of arrhythmias/sudden cardiac death.

	Univariate analysis		
	HR	**CI**	**p**
LV EF (%)	1.011	0.951-1.074	0.728
LV EDV (mL/m^2)	1.012	0.995-1.028	0.162
RV EF (%)	0.925	0.872-0.980	0.008
RV EDV (mL/m^2)	1.027	0.995-1.060	0.105
LGE overall	6.733	0.853-53.145	0.070
Junctional LGE	1.129	0.318-4.000	0.852
No junctional LGE	5.102	1.081-23.809	0.040

Abbreviations as in Table 1 and 2.

Table 7. CMR predictors of death/heart transplantation/assist device.

	Univariate analysis		
	HR	**CI**	**p**
LV EF (%)	0.900	0.836-0.969	0.005
LV EDV (mL/m^2)	1.011	0.997-1.024	0.131
RV EF (%)	0.934	0.899-0.980	0.006
RV EDV (mL/m^2)	1.026	1.000-1.054	0.052
LGE overall	1.090	0.388-3.062	0.870
Junctional LGE	0.665	0.241-1.835	0.431
No junctional LGE	1.005	0.358-2.822	0.993

Abbreviations as in Table 1 and 2.

We preferred no to do multivariable analysis because of the small number of events during follow up.

3.5 Discussion and conclusions

In this study we demonstrated that the presence of so-called “junctional LGE” in the right ventricular insertion points is a frequent CMR finding in DCM, up to 38% in our population. The strict relationship between all hemodynamic parameters indicating the presence of PH complicating the DCM with junctional LGE makes this peculiar CMR pattern not specific for pre-capillary PH as herein demonstrated, but related to all conditions of RV overload. The junctional LGE pattern on follow-up was able in our study to identify the patients at risk for developing heart failure in a short term follow up. Hence, since its relationship with PH, it might assume the role of an imaging marker of patients more likely to worsen clinically in terms of decompensated HF. The prognostic value of classical LE pattern (i.e. midwall stria) appears to be less specific in predicting HF hospitalization nevertheless is confirmed the strongest predictor of arrhythmias.

Junctional LGE and hemodynamics in dilated cardiomyopathy

The LGE in the right ventricular insertion points with interventricular septum has been described up to 65% of patients with pulmonary arterial hypertension (PAH) in whom chronic RV pressure overload may increase interventricular wall stress (26), independently from the underlying etiology. Contrast LGE of the septal right ventricular insertion points has also been reported in congenital heart disease with RV overload (33, 34). In transposition of great arteries, in which RV pressures may be similar to those in severe PAH, the extent of hyperenhancement also correlates inversely with RV ejection fraction (33). Recently a similar LGE junctional pattern has been recognized in endurance athletes up to 13% of subjects (37). The considerable increases in pulmonary pressures demonstrated in trained athletes during intense exercise suggest a similar physiological stress, albeit only transient (37). All these clinical conditions

are characterized by chronic or transient increased pulmonary pressure reflecting in a RV remodeling. However, PH is a heterogeneous entity with different causes leading to increased pressures in the pulmonary circulation. In fact, a combination of elevated LV filling pressures, reactive pulmonary arterial vasoconstriction, and pulmonary vascular remodeling results in PH secondary to left heart disease (45). A typical disease in which PH resembles this pathophysiological model is DCM. Among CMR studies evaluating the LGE pattern in DCM, a junctional contrast deposition has been describe since initial experience (35) through more recent paper (36). However, no relationship with hemodynamic parameters, in particular PH, has been investigated.

The novelty of our study is the comparison between right heart catheterization measures and CMR findings aimed to evaluate a possible explanation of junctional LGE in this specific patient population. In our study we demonstrated that the presence of so-called “junctional LGE” in the RV insertion points with septum, alone or associate with mid-septal stria, is not a rare CMR findings in DCM, up to 38% in our population. Moreover the percentage of subjects showing this peculiar pattern increased with the values of mean pulmonary artery pressure and wedge pressure. This observation confirms previous studies in which junctional LGE was associated with PH, but extent this association also in those with post-capillary PH as DCM. In the setting of DCM, has been recognized that increased LV filling pressures (measured by LVEDP), lead to pulmonary venous hypertension and post-capillary PH: when the elevation in venous pressure is chronic, excessive and persistent, it triggers a multistep adaptive process that involves not only the pulmonary vasculature, but also the RV remodeling. Under normal conditions, the RV operates against a low-impedance, high-capacitance, low-pressure system, with a short isovolumetric contraction period and a prolonged systolic ejection time (46). Although the RV is well suited to accommodate an increased in volume overload, it is exquisitely

afterload sensitive. Moreover, the RV and LV are connected in series and the impaired LV filling influences also the RV function as a cross talk or coupling between the right and left sides, referred to as diastolic ventricular interaction (46, 47). Left ventricle filling pressure directly measured by LVEDP and indirectly by PCWP, represents the downstream load imposed by the left heart on the RV. All these mechanisms are the basis of LV and RV remodeling due to PH, in particular in the DCM patients. Looking to right ventricular insertion points has been recognized that are regions of a particular mechanical stress as demonstrated by experimental studies that identified these regions, and later the interventricular septum, as the earliest sites of immune-reactive-atrial natriuretic peptide expression (48).

Anatomical basis of junctional LGE

In a normal heart, cardiac myofiber orientation plays a role in the uniform transmural distribution of mechanical stress and strain (49). The septum is a midline structure between the two ventricles and is composed of oblique fibers from two layers of the myocardial band able to provide the characteristic motion of “twisting” of the septum, with most dense cross at the level of insertion LV and RV regions. The RV insertion points with interventricular septum are regions of particular mechanical stress, even under normal physiological conditions. As demonstrated by previous histological studies, in the small area of junctions between the ventricular septum and RV free wall, myocite disarray and fibrosis were not so rare in control hearts (50). All conditions able to disrupt normal architecture by stretching the septum so that a more transverse, rather than oblique fiber orientation comprises its spatial configuration (51); as a consequence the alteration of myoarchitecture mostly in more “stressed” points in combination with alterations in the connective tissue matrix provide the structural basis for slow washout kinetics of gadolinium in diseased tissue.

Delayed contrast enhancement has been initially well characterized in relation to ischemic heart disease (52), in which the LGE represents the post-infarction scar. However, as experimentally demonstrated, the main mechanism of gadolinium deposition is the expansion of extracellular space such as myocites disruption, inflammation, increase in fat and fibrosis (as replacement type or interstitial). Moreover, previous clinic-pathological studies demonstrated that LGE in the setting of hypertrophic cardiomyopathy correlates not only with fibrosis and myocardial collagen, but also myocite disarray (32). So far, the histological basis of LGE in PAH have been proven only in a case report in which microscopy showed myocardial disarray, increased collagen and fat between fiber bundles without signs of replacement type of fibrosis (30). In another case, without CMR comparison, the specimen from interventricular septum of a woman affected by PAH showed extracellular expansion and edema with fibrosis (29).

In the setting of DCM, Assomul (41) provided a good correlation between circumferential LGE on pre-mortem CMR and fibrosis detected on autopsy, without a specific overview on junction section. In our study we provided the histological basis of LGE deposition in a patient with DCM complicated by reactive PH who underwent heart transplantation (Figure 5). Even in this case, as demonstrated in normal controls (50), the typical histological features previous seen in the right ventricular insertion points with interventricular such as disarray, fat, not pathologic fibrosis, and microvessels are expanded in this patient, probably due to mechanical stress, with edema: all conditions able to increase the distribution volume of gadolinium. Moreover, the at the junction site even in transplanted patient the traditional fibrosis findings are lacking, compared to lateral wall where the typical replacement type fibrosis also lead to LGE deposition.

In this study we demonstrated for the first time in the setting of DCM that junctional LGE reflects all hemodynamic adaptation of RV in this disease, as demonstrated by the strong association with WP and LVEDP.

Clinical significance of junctional remodeling in dilated cardiomyopathy

Increased mortality and hospitalization rates have been reported in HF patients with echocardiographycally estimated PH (22), and PAMP is an independent predictor of the need for cardiac transplantation (24) and the following outcome (46). On this basis, the final adaptive capability of the RV to the severity of pulmonary vascular disease seems a fundamental prognostic factor, regardless of LVEF and stage of HF. In our study we demonstrated that patients showing junctional LGE had a worse clinical outcome in terms of HF in a 2 years follow up. The prognostic significance of LGE has been recently demonstrated in the setting of DCM, in which its presence is related to worse clinical outcome, mostly as arrhythmic events. However, no specific association between typical LGE pattern and outcome has been demonstrated (42). In our population patients with junctional LGE had more episodes of HF compared with those with other pattern non including LGE at the level of the RV insertion points with septum; on the other hand, DCM with LGE, but not junctional, showed more arrhythmic events and all SCD occurred in this group. Thus, this observation confirm the role of LGE as predictor of outcome in DCM, but suggests that the role of junctional LGE in the arrhythmogenesis is limited, improving its significance in the detection of subject at risk of HF even treated with optimized medical treatment.

The identification in vivo of possible mechanism responsible for hypothetic reversible junctional LGE deposition may be useful to identify patients at risk for developing HF. In this context, the visualization of junction edema, leading later to contrast extravascular deposition, may be obtained using T2-weighted imaging,

so far not included in the CMR protocol of DCM study. Adding these information and future application on T1 and T2 mapping may provide further information.

Conclusions

Our study evaluated the features of so-called "junctional LGE" in the right ventricular insertion points. This is a frequent CMR findings in DCM, and it is related to all hemodynamic parameters indicating the presence of PH complicating the DCM, including RV systolic dysfunction, due to left side and so resulting not specific for pre-capillary PH.

Patients with junctional LGE are significantly more likely to worsen clinically in terms of decompensated HF, meaning that this peculiar CMR pattern may be a marker of incipient RV global impairment, instead doesn't represent a flag of arrhythmic risk.

Limitations

Further studies on larger populations, able to provide new insight in the comprehension of mechanism involved in the junctional LGE development in vivo, may be useful to confirm these data and, thereafter, monitor the efficacy of therapies.

Chapter 4

CLINICALLY SUSPECTED ACUTE MYOCARDITIS

The prognostic and expounder role of edema as detected by CMR

4.1 Introduction

Acute myocarditis is an inflammatory disease of the heart muscle most often caused by infectious agents such as viruses or autoimmune conditions. The majority of affected patients have a mild and transient cardiac involvement and favorable clinical outcome with complete clinical recovery; heart failure and arrhythmic sudden death are less common clinical presentations (53,54). The 12-lead electrocardiogram (ECG) is usually abnormal in myocarditis, although changes are neither sensitive nor specific. Most frequent ECG abnormalities in acute myocarditis consist of ST-segment displacement and negative T-waves, which may mimic those seen in acute coronary syndromes. The prevalence of T-waves inversion (TWI) ranges from 9 to 48% (54-61). The pathophysiologic

mechanisms and the prognostic meaning of TWI occurring in acute myocarditis remain to be elucidated. Cardiac magnetic resonance has become the gold standard imaging technique for tissue characterization and identification of myocardial lesions such as edema and fibrosis, which may represent the substrate for electrical disturbances leading to ECG changes in acute myocarditis (43). Previous CMR studies (which lacked T2-weighted sequences for myocardial edema) found that development of TWI in patients with acute myocarditis correlated with the extent of LV myocardial LGE (55,59). We previously demonstrated a pathophysiologic link between dynamic TWI and transient myocardial edema in Tako-tsubo cardiomyopathy, a condition which shows many similarities with acute myocarditis such as clinical presentation with chest pain, ST-segment elevation, TWI, myocardial enzymatic release and reversible ventricular dysfunction (62-65). Unlike Tako-tsubo cardiomyopathy, TWI is not observed in all patients with acute myocarditis: this provides an ideal study model to further test clinically the pathophysiologic link between myocardial edema (amount, regional distribution and transmural arrangement) and occurrence of TWI. Since Tako-tsubo cardiomyopathy, after passing acute phase, has a benign prognosis, we suggest that acute myocarditis presenting with TWI may represent a transient inflammation with a preponderant myocardial edema rather than myocardial fibrosis, as in tako-tsubo, and so a benign prognosis.

4.2 Aims

Our aims are to evaluate the relationship between TWI and myocardial edema as evidenced by CMR in a series of consecutive patients admitted for clinically suspected acute myocarditis. In addition, we investigated whether TWI during the acute/subacute disease phase predicted LV dysfunction during follow-up.

4.3 Methods

Study population

The study enrolled consecutive patients acutely admitted to our department between January 2012 and December 2014 for clinically suspected acute myocarditis (53) based on: 1) consistent clinical symptoms; 2) elevated Troponin I levels and 3) CMR imaging evidence of both regional increase of myocardial signal intensity in T2-weighted edema images and ≥1 local lesion in post-contrast inversion recovery T1-weighted images (late gadolinium enhancement, LGE) with non-ischemic regional distribution (43). Coronary artery disease was ruled out by coronary angiography or by stress-induced myocardial ischemia test in all patients. According to the American Heart Association/American College of Cardiology Foundation/European Society of Cardiology scientific guidelines on the role of EMB in cardiovascular diseases (66) confirmatory endomyocardial biopsy was reserved to the 8 patients presenting with heart failure symptoms and/or moderate to severe LV dysfunction. Six months after discharge, patients underwent a follow-up clinical evaluation including ECG and echocardiography. A CMR follow up scan was limited to the subgroup of patients showing LV dysfunction at 6-months follow up. Patients with rhythm and conduction disturbances such as atrial fibrillation, complete bundle branch block and atrioventricular block, as well as those with standard contraindications to CMR were excluded from the study. Each patient gave written informed consent to participate in the study.

Study protocol

A standard 12-lead ECG was recorded at the time of CMR, at a paper speed of 25 mm/s and an amplification of 10 mm/mV. Electrocardiographic data were evaluated by an observer who was unaware of clinical data and CMR results.

Standard measurements included heart rate; rhythm; PR interval; QRS axis, voltage, and duration; ST-segment and T-wave abnormalities. TWI was defined as the presence of negative T-waves of amplitude ≥1 mm in at least two contiguous ECG leads. The following locations of TWI across the 12 ECG leads were considered: 1) “anterolateral” for TWI in leads V1 through V4 extending to leads V5-V6, to leads I, aVL or both leads; 2) “inferolateral” for TWI in leads II, III, aVF extending to V5, V6; and 3) “diffuse” for TWI in both anterolateral and inferolateral leads. . In the subset of 13 patients who underwent a second CMR study during follow-up, we compared the sum of QRS voltages in limb leads, precordial leads and aVR lead of ECG recordings obtained at the time of acute and follow-up CMR studies.

CMR protocol and analysis

Cardiac magnetic resonance was performed on a 1.5-Tesla scanner (Magnetom Avanto, Siemens Medical Solutions, Germany) within 8 days from symptoms onset. All patients underwent a comprehensive CMR study protocol including cinetic, edema, early and delayed post-contrast sequences (1,5,43,64). See the Appendix for CMR acquisition details. The images of CMR were evaluated and analyzed independently by 2 observers, blinded to ECG and clinical findings, with the use of dedicated software (CMR42, Circle Cardiovascular Imaging Inc). In case of disagreement a third observer was consulted. Global ventricular volumes, systolic function and LV myocardial mass were calculated from the short-axis cine images, excluding papillary muscles from the myocardium. A 6 equiangular segmental approach for each short axis slice was used, finally resumed in the American Heart Association 17-segments-model. Slices with artifacts were not considered for edema assessment. The presence of myocardial edema on T2-weighted images was diagnosed using a dark blood sequence to reduce artifacts and, moreover, “slow flow artifacts” were excluded comparing T2-weighted

images with cine images side by side on the same cardiac phase. Myocardial edema was identified and quantified by semi quantitative analysis according to the workflow published in the Society for Cardiovascular Magnetic Resonance position statement (1) and all edematous regions were confirmed in two perpendicular views. Semi quantitative analysis was performed using regional T2-ratio method and the presence of myocardial edema was diagnosed when signal intensity (SI) was 2 or higher compared with that of the skeletal muscle. Myocardial edema was defined as "transmural" when it extended from the epicardium to the endocardium by more than 75% of the LV thickness in ≥2 adjacent segments. Early Gadolinium Enhancement was defined as global SI enhancement ratio of myocardium over skeletal muscle ≥ 4.0 or absolute value of myocardial SI enhancement ≥45% than pre-contrast myocardial SI. Myocardial LGE was assessed with an automated thresholding and considered present if SI was > 3 standard deviations above remote myocardium. Location of TWI across the 12 ECG leads and regional distribution of myocardial edema on CMR were considered concordant in the presence of: 1) TWI in the antero-lateral leads and myocardial edema localized in the anterior septum, anterior wall and/or antero-lateral wall, 2) TWI in the infero-lateral leads and myocardial edema localized (>75% of edematous LV segments) in the inferior septum, inferior wall and/or infero-lateral wall, 3) diffuse TWI (both anterolateral and infero-lateral leads) and diffuse myocardial edema (involving both the anterior septum, anterior wall and/or antero-lateral wall and inferior septum, inferior wall and/or infero-lateral wall).

Statistical analysis

Continuous variables were reported as median (25°-75° percentiles) and compared using the rank sum test because of the small size of subgroups. Categorical variables were analyzed with the chi-squared test or the Fisher's exact

test, as appropriate. Comparison between continuous variables was performed with the Mann-Whitney U test for unpaired samples and with the Wilcoxon signed rank test for paired samples. The presence of transmural edema, the number of segments with edema and the number of segment with LGE were entered into a multivariable binary logistic regression model for prediction of TWI. Concordance between localization of TWI and regional distribution of myocardial edema was evaluated by the Cohen kappa statistic test. The inter-observer agreement was evaluated by the Cohen kappa statistic test. A 2-tailed $p<0.05$ was considered statistically significant. All analyses were performed using SPSS 17 (SPSS Inc; Chicago, IL).

4.4 Results

Clinical and electrocardiographic findings

The patient population included 76 patients (87% male, median age 34 years). The baseline clinical characteristics of the study population are summarized in Table 8. Chest pain was the most common reason for seeking medical attention (N=67, 88%), dyspnea was the onset symptom in 3 subjects (4%), palpitation in 6 (8%). Coronary artery disease (i.e., coronary stenosis <50%) was excluded by coronary angiography in 56 (74%) patients. The remaining 20 (26%) patients did not undergo coronary angiography as they were considered as having a low pretest probability of coronary artery disease, because of young age, absence of coronary risk factors, and obvious recent gastrointestinal or respiratory infection; in these patients the absence of stress-induced myocardial ischemia was demonstrated by exercise testing and/or single-photon emission computed tomography. All patients had elevated troponin I levels with a median

peak of 9.9 ug/L. The echocardiography showed reduction of LV ejection fraction in 29 (38%) patients with a median value of 48% (43-51); a LV ejection fraction <45% was documented in 8 (11%) patients. A mild pericardial effusion was detected in 13 (17%) patients.

Table 9 summarizes ECG findings at the time of CMR. All patients were in sinus rhythm. None had a bundle branch block (median QRS duration 90 msec). Two patients (3%) had low amplitude (<0.5mV) of QRS complex in limb leads. TWI was observed in 21 (27%) patients. In the subset of 13 patients who underwent a second CMR study during follow-up, there was a trend towards a lower amplitude of QRS complexes on the acute ECG compared with follow-up ECG obtained at the time of CMR studies but, probably due to the small number, this was not statistically significant: from 61 mV (46-73) to 63 mV (44-73) in limb leads (p=0.34), from 86 mV (79-97) to 87 mV (78-98) in precordial leads (p=0.09), and from 10 mV (8-11) to 11 mV (8-12) in aVR lead (p=0.257).

Table 8. Clinical characteristics of population

	Overall (n=76)	**No TWI (n=55)**	**TWI (n=21)**	***p***
Male	66 (87)	49 (89)	17 (81)	0.45
Age, (years)	34 (26-43)	34 (24-42)	37 (26-49)	0.93
Recent flu	48 (63)	36 (66)	12 (57)	0.60
Clinical presentation				
Chest pain	67 (88)	51 (93)	16 (76)	0.11
Dyspnea	3 (4)	1 (1.8)	2 (9.5)	0.18
Palpitations	6 (8)	3 (6)	3 (14)	0.34
Laboratory data				
Peak Troponin I, ug/L	9.9 (4.4-20.2)	10 (4-20.2)	8.2 (6-23)	0.85
Peak C-Reactive Protein, mg/dL	26 (3.6-56)	30 (7.2-68)	20 (3.1-38)	0.16
Echocardiogram				
LV EDV, ml/m2	59 (52-67)	59 (54-67)	50 (46-62)	0.02
LV EF, %	57 (51-63)	58 (51-63)	56 (49-61)	0.86
Pericardial effusion,	13 (17)	10 (18)	3 (14)	1.0

Data are presented as median (1st-3rd quartiles) or N(%).

EDV= end-diastolic volume, EF=ejection fraction, LV=left ventricle, TWI=T-waves inversion.

Table 9. Electrocardiographic features at time of CMR

ECG features	Median (1st-3rd quartiles) or Number of patients (%)
Sinus Rhythm	76 (100)
PR interval, median msec	150 (145-170)
QRS duration, median msec	90 (90-100)
QRS axis, median degrees	50 (40-60)
QRS Low amplitude#	2 (3)
ST elevation	25 (33)
ST depression	0
Negative T-waves	21 (28)
Antero-lateral	10 (13)
Infero-lateral	9 (12)
Diffuse	2 (3)

#Low QRS amplitude if QRS mean voltage < 5mV in limb leads.

Cardiac Magnetic Resonance findings

The median interval between symptom onset and CMR was 5 (3-7) days. CMR findings are shown in Table 10. All patients had ≥ 1 LV myocardial segments showing myocardial edema on T2-weighted sequence and ≥ 1 LV myocardial segments showing non ischemic LGE on post-contrast sequences which fulfilled Lake Louise criteria for myocarditis (Table 3). The median number of LV segments showing any pattern of myocardial edema (transmural and non-transmural) was 3 (2-5). Thirty patients (39%) had ≥2 LV segments showing myocardial edema with a transmural pattern. We found an increased global myocardial early gadolinium enhancement ratio in 46 of 76 patients (61%). The median number of LV segments with LGE was 3 (2-5). The morphology of LGE was “stria” type in 41 (54%) patients and “patchy” type in 35 (46%).

Relationship between clinical, ECG and CMR features.

Baseline clinical characteristics and CMR features according with the presence of TWI are reported in Table 8 and 10. Patients with and without TWI did not differ with regards to LV ejection fraction, LV volume, LV mass and Troponin I peak values. At CMR, the number of LV segments with any pattern of myocardial edema (transmural and non-transmural), the number of LV segments with a transmural pattern of myocardial edema and the number of LV segments with LGE were higher in patients with TWI than in those without TWI. About early enhancement, its prevalence did not differ significantly among patients with and without TWI. Transmural edema of ≥2 LV segments was present in 17/21 (81%) patients with TWI versus 13/55 (24%) patients with no TWI ($p<0.001$). There was no association between repolarization abnormalities and specific LGE patterns ("stria" versus "patchy"). At multivariable analysis (Table 11) the presence of transmural myocardial edema of ≥2 LV segments remained the only independent predictor of TWI at the time of CMR.

Regional correlation analysis demonstrated that 6/10 (60%) patients with antero-lateral TWI showed myocardial edema confined to the antero-septal/anterior/antero-lateral LV segments, while 4/9 (44%) patients with infero-lateral TWI showed myocardial edema confined to the infero-septal/inferior/inferior-lateral LV segments; the other 2 patients with diffuse TWI showed myocardial edema in both LV regions. The overall concordance between TWI and myocardial edema (either transmural or non-transmural) was observed in 12 (57%; k=0.42) patients, while the other 9 (43%) patients had myocardial edema extending beyond LV segments explored by leads exhibiting TWI. A sub-analysis of topographic agreement among patients with TWI and a transmural pattern of myocardial edema showed a 100% concordance (8/8) in patients presenting with antero-lateral TWI and a 71% concordance (5/7) in patients with infero-lateral TWI; the 2 patients with diffuse TWI showed transmural myocardial

edema in both LV regions. Overall, the topographic agreement between TWI and a transmural pattern of myocardial edema was 88% (15/17; k=0.81). The two “discordant” patients had infero-lateral TWI and transmural myocardial edema both in the infero-lateral and the antero-lateral wall. Figure 6-7-8 show the electrocardiograms and the CMR findings in three patients.

Interobserver agreement on the presence of transmural edema was 95% (72/76, kappa=0.88). Interobserver agreement was 94% (16/17, kappa=0.88) for the presence of transmural myocardial edema in the anterior segments and 88% (15/17, kappa=0.77) for the presence of transmural myocardial edema in the inferior segments.

Table 10. CMR finding according to the presence of T-waves negative.

	Overall (n=76)	No TWI (n=55)	TWI (n=21)	P
Functional CMR				
LV EF, (%)	60 (55-64)	60 (55-64)	60 (54-60)	0,293
LV EDV, ml/m2	61 (54-70)	65 (56-70)	55 (50-64)	0.056
LV mass, g/m2	59 (55-65)	58 (55-63)	61 (55-66)	0.345
Number of patients with regional kinetic abnormalities	28 (37)	9 (43)	19 (90)	0.597
T2-w sequence analysis				
Median number of LV segments with any edema per patient	3 (2-5)	3 (2-4)	5 (3-7)	0.015
Number of patients with transmural myocardium edema in ≥2 LV segments	30 (39)	13 (24)	17 (81)	0.000
Median number of LV segments with transmural edema per patient	0 (0-3)	0 (0-1)	2 (2-3)	0.000
Early enhancement analysis				
Number of patients with increased EGE ratio	46 (61)	30 (55)	16 (76)	0.080
Late enhancement analysis				
Median number of LV segments with LGE per patient	3 (2-5)	3 (2-4)	4 (3-7)	0.002

Data are presented as median (25°-75° %iles) or N(%).
LGE=late gadolinium enhancement. Abbreviations: see table 1

Table 11. Multivariable analysis for predictors of T-waves inversion

	OR	95% CI	p
LV segments with any edema	1.05	0.77-1.43	0.752
Presence of transmural edema in ≥2 LV segments	9.96	2.71-36.6	0.001
LV segments with LGE	1.21	0.89-1.65	0.215

Abbreviations: see table 1-3

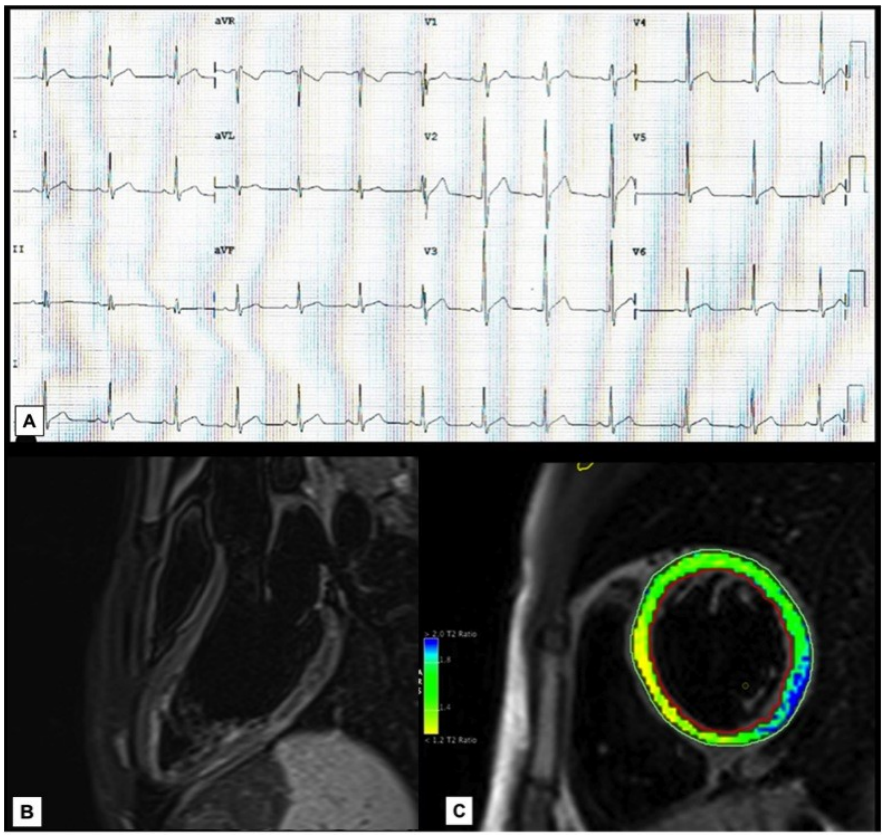

Figure 6 - Representative patient with no T-wave inversion. ECG at the time of CMR showing the absence of TWI (A). Long-axis 3-chamber view showing infero-lateral myocardial edema in T2-weighted sequences (B). Semiquantitive analysis by CMR42, showing the non-transmural arrangement of myocardial edema which is confined to the epicardial layer. The blue area depicts myocardial T2 intensity signal >2.0 compared with the skeletal muscle (C).

Figure 7 - CMR findings in a representative patient with inferior TWI. ECG at the time of CMR showing the presence of negative T waves in inferior leads (A). Long-axis three-chamber view showing infero-lateral myocardial edema in T2-weighted sequences (B). Semiquantitive analysis by CMR42, Circle Cardiovascular Imaging Inc. software showing the transmural arrangement of myocardial edema (C).

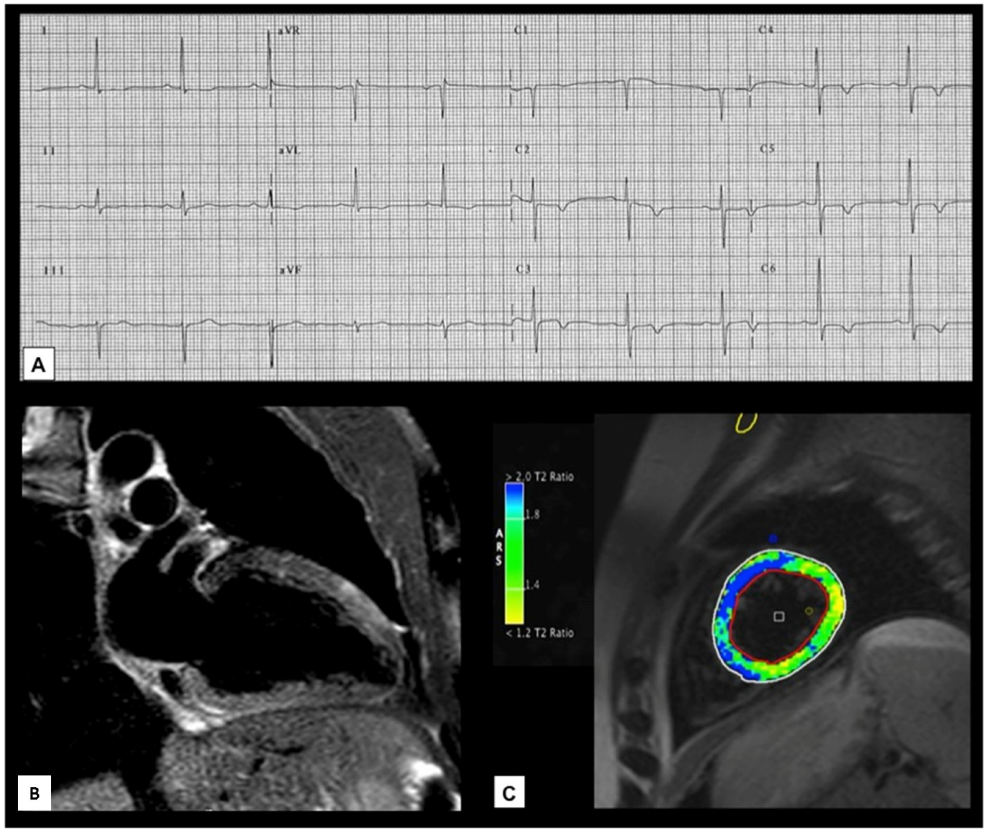

Figure 8 - CMR findings in a representative patient with anterior TWI. ECG at the time of CMR showing negative T waves in anterior leads (A). Two-chamber view showing anterior myocardial edema in T2-weighted sequences (B). Semiquantitive analysis by CMR42, Circle Cardiovascular Imaging Inc. software showing the transmural arrangement of myocardial edema (C).

Follow-up data

Follow-up data were available for 68 of 76 patients (18 of 21 patients with TWI and 50 of 55 without TWI). At a 6-month control ECG all patients exhibited normalization of T-waves polarity. Thirteen (19%) had reduced LV EF (<55%) on echocardiographic examination. At this time, a follow-up CMR study was performed in this subgroup of patients with echocardiographic LV dysfunction and demonstrated a complete normalization of SI value on T2-weighted sequences for myocardial edema, whereas a variable amount of non-transmural LV LGE was observed in all. Patients with a reduced LV EF at 6 months follow-up had during the acute phase significantly lower LV EF, higher LV end-diastolic volume and more severe LV wall motion abnormalities. At multivariable analysis

LV EF <55% at admission (OR=11.23; 95%CI=2.64-47.7; p=0.001) but no TWI (OR=1.61, 95%CI=0.33-7.77; p=0.555) predicted LV dysfunction at follow up (table 12).

Table 12 Clinical characteristics of population at admission according with the presence of left ventricular dysfunction at 6-month follow-up

	EF > 55% (n=55)	**EF < 55% (n=13)**	**P**
Male	46 (84)	12 (92)	0.67
Age, (years)	34 (26-42)	40 (30-54)	0.17
Recent flu	36 (66)	7 (54)	0.53
Clinical presentation			
Chest pain	49 (89)	10 (77)	0.36
Dyspnea	2 (4)	1 (8)	0.48
Palpitations	4 (7)	2 (15)	0.32
Laboratory data			
Peak Troponin I, ug/L	9.8 (4.4-16.5)	12 (6.6-49.8)	0.24
C-Reactive Protein, mg/dL	26 (4.1-38.1)	50 (3-94)	0.24
Echocardiogram			
LV EDV, ml/m^2	56 (48-62)	62 (59-70)	0.02
LV EF, %	60 (55-64)	46 (43-52)	<0.001
Pericardial effusion	9 (16)	3 (23)	0.69
ECG (at the time of CMR)			
ST segment elevation	17 (31)	6 (42)	0.34
ST segment depression	0	0	-
Negative T-waves	15 (27)	3 (23)	1.0
CMR			
Cine sequences			
LV EF, %	60 (52-66)	52 (50-55)	<0.001
LV EDV, ml/m2	60 (52-66)	68 (60-73)	0.045
Number of patients with regional kinetic abnormalities	12 (22)	11 (85)	<0.001
T2-w sequences			
Median number of LV segments with edema per patient	3 (2-5)	4 (3-4)	0.16
Median number of LV segments with transmural edema per patient	0 (0-2)	0 (0-2)	0.82
Post-contrast sequences			
Median number of segments with LGE per patient	3 (2-5)	3 (2-7)	1.0

Data are presented as median (25°-75° %iles) or n(%).

4.5 Discussion and conclusions

This study was the first to characterize the myocardial tissue changes underlying TWI in patients with a diagnosis of clinically suspected acute myocarditis, who underwent a comprehensive CMR protocol including T2-weighted and early/late gadolinium enhancement sequences. The major study suggestions, since the small number of subjects, were the following: 1) there was a significant association between quantitative parameters of LV myocardial edema as evidenced by T2-weighted sequences and TWI; 2) among the tissue characterization parameters, transmural extent of myocardial edema seems to be the only independent predictor of TWI suggesting that dispersion between epicardium and endocardium rather that the regional inhomogeneity of repolarization was the most involved electrophysiological mechanism; 3) there was an excellent topographic agreement between TWI location across the 12 ECG leads and regional distribution of transmural myocardial edema; 4) T-waves normalized in all patients and the presence of TWI during acute phase was not a unfavorable predictor of LV systolic dysfunction at 6-month period of follow-up.

T-wave inversion and myocardial edema in acute myocarditis

Our results confirm and extend previous CMR observations in patients with acute myocarditis by showing a significant association of TWI not only with the extent of LV LGE but also with quantitative parameters of LV myocardial edema as evidenced by T2- weighted sequences. However, on multivariable analysis, only transmural myocardial edema remained an independent predictor of TWI on the ECG at the time of CMR. A likely explanation of this finding is that in most of our study patients, LGE observed at the time of acute CMR evaluation could be a "reversible edema-related gadolinium myocardial enhancement". In this regard, experimental studies showed that a delayed washout of gadolinium may be

caused not only by permanent myocardial necrosis/fibrosis but also by increased interstitial water content such that associated with reversible myocardial edema (67). The pathogenic link between edematous myocardium and repolarization abnormalities remains to be elucidated. One can speculate that the acute inflammatory process causes myocyte repolarization inhomogeneity, either regional (between regions affected and those spared by myocardial edema) or transmural (i.e. between endocardial and epicardial layers), which gives rise to inversion of T-waves polarity. The observation that transmural extent of myocardial edema was the most powerful predictor of TWI suggests that dispersion of action potential duration between epicardium and endocardium of the LV wall, rather than regional inhomogeneity of repolarization, was the most involved electrophysiological mechanism in our study patients. This finding is in agreement with previous studies on either ischemic or non-ischemic dynamic TWI, showing that transmural myocardial damage is a prerequisite for T waves to become negatives (62-63). Whether there is a direct cause-effect relationship between myocardial edema and action potential changes or these phenomena are two parallel effects of the inflammatory myocardial lesion remains to be addressed by future experimental and clinical studies. A transient attenuation of QRS voltages concomitantly with myocardial edema has been previously reported in patients with tako-tsubo cardiomyopathy (68). In the subset of our patients with acute myocarditis undergoing both acute and follow-up CMR studies, we observed a non statistically significant trend toward an attenuation of QRS voltages on the acute ECG compared with follow-up ECG. The discrepancy may be explained by the lower number and patchy distribution of edematous LV segments in acute myocarditis compared with the homogeneous distribution and global involvement of mid-apical LV segments involved by myocardial edema in tako-tsubo cardiomyopathy.

LV segments with myocardial edema were not infrequently observed in LV regions different from those explored by the ECG leads showing TWI. Hence, the concordance between location of TWI on the ECG leads and the LV segments exhibiting any patterns of myocardial edema involvement was poor with an overall topographic agreement not exceeding 57%. This finding is in keeping with the results of previous CMR studies (lacking T2- weighted sequences for myocardial edema) which showed a weak topographic between ECG leads showing ST-T abnormalities and location of myocardial damage assessed by LGE (55, 56, 59). In our study, the sub-analysis of topographic concordance between TWI and transmural myocardial edema showed an excellent overall agreement (88%). This reinforces the concept that occurrence of TWI mostly depends on the transmural extent of LV myocardial edema.

Prognostic value of TWI

Previous studies reported that development of TWI in acute myocarditis was significantly and independently associated to the extent of myocardial LV LGE. Thus, it was suggested that TWI could be used for a noninvasive estimation of the amount of myocardial damage, and, by inference, owing its ability to identify patients with larger areas of myocardial fibrosis, as a marker for risk stratification. The present study demonstrated that the only independent predictor of echocardiographic reduction of LV ejection fraction at 6-month follow-up was LV dysfunction (EF < 55%) during the acute phase of the disease. Of interest, TWI was neither univariate nor multivariable predictor of a late impairment of LV systolic function. This finding provides further evidence that TWI reflects the underlying myocardial edema which is a completely (or almost completely) transient myocardial tissue change with no (or minimal) irreversible structural myocardial damage such as necrosis/fibrosis. In this regard, although we did not perform a control CMR study systematically, the analysis of the

subgroup of 13 patients undergoing CMR re-study at 6-month follow up because of a reduced LV EF, showed a complete resolution of myocardial edema in all, despite the presence of a variable amount of LV LGE.

Conclusions and clinical implications

Our study was the first to demonstrate a significant association between transmural myocardial edema as evidenced by CMR T2- weighted sequences and TWI in acute myocarditis. This finding obtained in patients with acute myocarditis provides further evidence that transmural myocardial edema is a common denominator which underlies both electrical and mechanical abnormalities of a series of conditions, either ischemic or non-ischemic, characterized by reversible ventricular dysfunction (stunned myocardium) and TWI. As an expression of reversible myocardial edema, TWI during acute phase of myocarditis does not represent a marker of unfavorable adverse prognosis because it underlies a transient impairment of myocardial function. The knowledge of this pathophysiologic link between repolarization abnormalities and transient myocardial edema may help to improve our diagnostic and prognostic assessment of patients presenting with “infarct-like” acute myocarditis. In this context, CMR may provide additional values

Limitations

The study population was relatively small because of the low disease prevalence and the limited number of affected patients with available and evaluable CMR study, including T2-weighted sequences. Although EMB is considered to be the “gold standard” for diagnosis of acute myocarditis, it was not performed in all our study patients but was reserved to patients presenting with symptoms of heart failure and/or moderate to severe LV dysfunction, according to international guidelines (66). Because most of our patients did not

have histological validation of diagnosis, we used thorough the manuscript the designation “clinically suspected acute myocarditis” which is the designation currently used to indicate a diagnosis of acute myocarditis based on clinical and CMR findings.

Chapter 5

THE MITRAL VALVE PROLAPSE

The arrhythmic landmark as evidenced by CMR

5.1 Introduction

Mitral valve prolapse (MVP) is characterized by typical fibro-myxomatous changes in the mitral leaflet tissue with superior displacement of one or both leaflets into the left atrium. Beside this general definition, the history of idiopathic MVP concealed a century of scientific debates, intuitions and pitfalls crossing all the last fifty years of Cardiology.

Mitral valve prolapse is the most common valve disease with an estimated prevalence of 2-3% in the general population (69). Although MVP is generally regarded as a benign condition (70,71), the outcome is widely heterogeneous and complications such as mitral regurgitation, atrial fibrillation, congestive heart failure, endocarditis and stroke are well known. Ventricular arrhythmias and SCD have been even reported (72-90).

From a pathologic anatomy point of view, accumulation of proteoglycans (myxomatous mitral valve) is the most common cause of MVP, accounting for

leaflet thickening and redundancy, interchordal hooding, chordal elongation and annular dilatation. While these valve abnormalities well explain mitral regurgitation and mechanical complications due to enhanced extensibility, the pathogenesis of ventricular arrhythmias/SCD in MVP remains unknown (82).

Since the estimated rate of SCD in MVP ranges from 0.2% to 0.4% per year on the basis of prospective follow-up studies (69,72), one of the major clinical concerns with MVP is the incidence of ventricular arrhythmia and the occasional occurrence of SCD.

Prevalence of arrhythmias in mitral valve prolapse

Arrhythmias have long been recognized to occur in patients with MVP (80-82). The prevalence of premature atrial complexes was reported to range from 35% to 63%, ventricular premature beats from 58% to 75%, and complex ventricular arrhythmias from 50% to 52% of MVP adult patients during prolonged ambulatory ECG recording. However other authors (83), analyzing unselect out of hospital patients found only a modest trend toward more complex/frequent ventricular premature beats in MVP group respect the control group, without reaching statistical significance. Of note, the definition of MVP to be enrolled was not the same across these studies, so the actual prevalence of complex arrhythmias in MVP depends on population-selection criteria.

Rare cases of SCD have been associated with MVP since its early recognition (84-86) and it has become generally accepted that a small but important subset of patients with MVP has complex arrhythmias that are potentially lethal. Malignant ventricular arrhythmias have been documented before fatal events in most instances and SCD is usually attributed to ventricular fibrillation (82, 87-90). This suggests that sudden death is a risk primarily in those patients with mitral valve prolapse who show frequent premature ventricular contractions. Demonstration of MVP as the only autopsy finding in some cases of sudden death (91, 92)

suggests the validity of this association even if does not prove mechanism or indicate cause and effect. Indeed, the strongest link between arrhythmias and sudden death in MVP comes from recognition of MVP as the only abnormality in survivors of cardiac arrest and in patients referred for management of refractory, symptomatic complex ventricular arrhythmias (93).

Although the risk of SCD in MVP is very low, with an estimated yearly rate of 0.4 %, the incidence is still twice that expected in the general population (69).

Despite a benign course of the disorder in most cases, predictive risk factors in patients with MVP have been lined out in clinical studies: in a long-term follow-up of 237 patients (mean duration of follow-up 6.2 years), Nishimura identified thickened and redundant mitral valve leaflets as a possible risk factor for sudden death or lethal complications (1.6% in higher risk groups versus 0.1% per year in lower risk group) (72). Moderate to severe mitral valve regurgitation is a well recognized predisposing factor for arrhythmias and SCD. The combination of severe mitral regurgitation, complex ventricular arrhythmias and LV dysfunction identifies a patient subgroup at particularly high risk (69). However, it should be noted that among the survivors of potentially fatal arrhythmia with MVP, mitral regurgitation has not been commonly reported (82,93,94). This might suggest that the proportion of SCD from MVP potentially associated with regurgitation is less than that observed by Davies (75): the pathogenesis of arrhythmic SCD in MVP patients with mild or no mitral regurgitation remains to be determined.

In the 2013, Ackerman investigates the prevalence of MVP and its association with ventricular arrhythmias in a cohort with “unexplained” out-of-hospital cardiac arrest. Ten patients had a bileaflet MVP among 24 idiopathic SCD (42%). The authors describe a “malignant” subset of patients with MVP who experienced life-threatening ventricular arrhythmias. This phenotype is characterized by bileaflet MVP, female sex, and frequent complex ventricular ectopic activity,

including premature ventricular contractions of the outflow tract alternating with papillary muscle or fascicular origin (95).

Pathogenesis of arrhythmias in mitral valve prolapse

Propensity for ventricular electrical instability has been related either to MVP in itself or to coexistent autonomic nervous system dysfunction (94), underlying cardiomyopathy (91,96,97) and or conduction system abnormalities (78).

Regarding mitral valve-related mechanisms, electrical instability can be due to:

1. the excessive traction on the papillary muscle by the prolapsing leaflets leading a mechanical stress and injury in the papillary muscle and in their insertional points (98,99).
2. the mechanical stimulation of the endocardium by the elongated cordae tendineae, their impact may produce a mechanical stimulus producing a ventricular ectopic beat. (100),
3. endocardial friction lesions and their myocardial extension: due arise as a result of friction between chordae and the LV mural endocardium which, in some instances, may lead to fibrosis of the mural endocardium. during early diastole the leaflets (87).

Of note, as previously described, Rizzon et al. observed how ventricular extrasystolic beats increase with the up-right position, exactly like the ausculatatory finding (101). In the 1997, Wilde studied a MVP patient with ventricular arrhythmias through intraoperatory endo and epicardic mapping: PVCs mostly originated from papillary muscle, could be elicited by manual traction on the chordae of the posterior papillary muscle (99, 102).

In conclusion, previous studies mostly focused on the potential relationship between structural/mechanical mitral valve alterations and potentially lethal ventricular arrhythmias while demonstration of the role of ventricular myocardial substrates remains unknown.

5.2 Aim

The aim of this study is to disclose the myocardial substrate underlying life-threatening arrhythmias in young adults with MVP, and demonstrate if it is detectable by contrast-enhanced cardiac magnetic resonance for risk stratification.

5.3 Methods

Study design

The study was divided in two arms: the first one (***A,*** *pathologic anatomy arm*) was designed as a retrospective revision of SCD victims' heart to analyse the pathological features of MVP-related deaths comparing with those for extracardiac causes; the second part (***B,*** *clinical arm*) was designed as prospective enrolment of MVP patients to detect any difference in term of in vivo tissue characterization between arrhythmic and no arrhythmic patients.

A) Pathologic anatomy arm: SCD victims with MVP

Population and Protocol of investigation

From 1982 to 2013, all the hearts of SCD victims ≤40 years old occurring in the Veneto Region, were collected, pathologically investigated and preserved. SCD is herein defined as witnessed sudden and unexpected death occurring within 1 hour of the onset of symptoms or death of an individual who had been seen in stable condition <24 hours before being found dead (21,22). Demographic, clinical and pathologic data were recorded in the electronic database of the Registry of Cardio-cerebro-vascular pathology which acts as referral centre for SCD of the North-East of Italy, supported by the Regional Health System. Charts were evaluated for age, sex, symptoms and clinical history. All the hearts were re-examined carefully according to a standardized protocol (21). SCD cases were selected in whom MVP due to myxomatous valve disease was the only cardiac abnormality found at autopsy. Myxomatous valve disease is defined as increased leaflet length and redundancy, with interchordal hooding and leaflet billowing toward the left atrium and chordae tendineae elongation (8). In the absence of extracardiac (cerebral, respiratory) or mechanical cardiovascular (pulmonary thromboembolism, aortic rupture, chordal rupture with pulmonary edema) causes, the cause of death was considered cardiac arrhythmic.

Exclusion criteria were clinical and/or pathologic evidence of more than mild mitral regurgitation, i.e. history of systolic murmur, echocardiographic report, and gross abnormalities such as left atrial dilatation, LV dilatation or chordal rupture. As controls, hearts from 15 sex and age-matched patients (10 females, mean age 30 years, range 18-40), who died suddenly for extracardiac causes (8 cerebral and 7 respiratory), were used.

Formalin fixed hearts were restudied according to a protocol previously reported (21). Leaflet involvement (whether anterior, posterior or bileaflet) and

the presence of endocardial fibrous plaque (friction lesion) on the LV infero-basal wall were assessed. Multiple samples of the entire LV and right ventricular free walls and septum, including the papillary muscles (PMs), were obtained for histology. Additional samples were taken in the infero-basal free wall of the LV, underneath the posterior mitral valve leaflet. Five µm- thick sections were stained with Hematoxylin-Eosin, Weigert-van Gieson, Heidenhain trichrome and Alcian-PAS. Morphometric analysis was performed using an Image-Pro Plus program (Version 4.0. Media Cybernetics, MD, USA) to quantify the fibrous tissue percent area of LV myocardium on Heidenhain trichrome stained sections at 25x magnification. Mean cardiomyocytes diameter was calculated on Haematoxylin-eosin stained sections at 400x magnification. Quantitative analysis was performed by two blind expert pathologists with an interobserver variability <5%.

B) Clinical arm : MVP patients with ventricular arrhythmias

Population and Protocol of investigation

The study included consecutive patients referred to the Inherited Arrhythmic Cardiomyopathy Unit of our Clinic, from 2010 to 2013 with complex ventricular arrhythmias detected on the basis of 12-lead 24-hour Holter monitoring and echocardiographic diagnosis of MVP, defined as >5 mm thickening and >2-mm displacement of one or both mitral leaflets into the left atrium as viewed in the LV outflow tract orientation (23). Twelve-lead ECG 24 hours Holter monitoring was requested due to the presence of either arrhythmic symptoms or 12-lead ECG changes. Complex ventricular arrhythmias consisted of ventricular fibrillation (VF) and ventricular tachycardia (VT), either non-sustained or sustained (24). The control group consisted of MVP patients with minor ventricular arrhythmias, i.e. isolated ventricular premature beats (VPB), couplets

and bigeminal VPB. Exclusion criteria were significant mitral valve regurgitation, tricuspid dysplasia or regurgitation, evidence of other cardiomyopathy or congenital heart abnormalities, hemodynamic unstable conditions and contraindication to CMR. The study was approved by the institutional review board, and all patients gave their informed consent.

All patients underwent cardiovascular evaluation including physical examination, 12-lead electrocardiogram (ECG), 2D-transthoracic echocardiography, 12-lead 24-hour Holter monitoring and CMR. Coronary angiography was performed in selected cases. The 12-lead ECG at rest and the 24-hour Holter monitoring were independently assessed by two experienced observers who were blinded to patient data.

The standard 12-lead ECG was recorded at rest; the following parameters were collected: PQ interval, QRS duration, ST-segment abnormalities, presence of T waves abnormalities (including inversion and biphasic morphologies, with corresponding regional distribution), QT corrected (QTc) duration according with Bazett's formula, QT dispersion, QT peak, presence of supraventricular premature beats (SVPBs) and finally, presence and morphology of VPBs. Twelve-lead 24-hour Holter monitoring was performed in all, with collection of the following parameters: presence of atrio-ventricular block, ST-segment abnormalities, number of SVPBs, number and morphology of VPBs. Non-sustained VT was defined as ≥ 3 consecutive VPBs with a rate > 100 bpm that lasted <30 seconds during 24-hour Holter monitoring. Sustained VT was defined as tachycardia originating in the ventricle with rate >100 beats/minute and lasting >30 seconds or requiring an intervention for termination.

Cardiac magnetic resonance was performed on a 1.5-Tesla scanner (Magnetom Avanto, Siemens Medical Solutions, Erlangen, Germany). All patients underwent detailed CMR study protocol (see Appendix for details), including ECG-gated cine steady state free processing (SSFP) images and T1 inversion recovery

post-contrast sequence. The presence and location of LGE were independently assessed by two experienced observers who were blinded to patient clinical data. To exclude artefact, LGE was deemed present only if visible in two orthogonal views (long-axis and short-axis). LGE was identified using a signal intensity threshold of >5SD above a remote reference region.

Statistical Analysis.

Data are expressed as mean value ± standard deviation or median with 25 to 75 percentiles for normally distributed and skewed variables, respectively. Normal distribution was assessed using Shapiro-Wilk test. Categorical differences between groups were evaluated by the chi-square test or the Fisher exact test as appropriate. Paired and unpaired t test were used to compare normally distributed continuous variables respectively obtained from the same patient and different patients; paired and unpaired signed rank test were used for skewed continuous variables.

A value of $P<0.05$ was considered significant. Statistics were analysed with SPSS version 19 (SPSS Inc, Chicago, IL). The minimal detectable effect that can be detected at a significance level of 5% and power at 80% is equal to 1 (with non parametric test) for quantitative variables (Cohen' Effect); for binary data an odds ratio of at least 10 can be detected if the proportion of the characteristic test is equal to 10% in the no CVA group (Fisher's exact test). A sub-analysis was done by dividing the MVP population with complex ventricular arrhythmias into two sub-groups, i.e. 3 beats run and >3 beats run.

5.4 Results

A) Pathologic anatomy arm: SCD victims with MVP.

Among 650 consecutive SCDs in young adults recorded in Cardiac Registry of the Veneto Region, 43 cases (26 females, median age 32 years, range 19-40) with MVP due to myxomatous valve disease were identified (7% of all SCD cases and 13% of women who died suddenly). Main clinical and pathologic data are reported in Table 13. SCD occurred mostly at rest or during sleep (n. 35, 81%). Twenty (47%) had an in vivo diagnosis of MVP, with auscultatory click in 18 (90%) and palpitations in 14 (70%). Nine (21%) were under beta-blockers therapy due to non sustained ventricular arrhythmias. ECG was available in 12 (28%), showing negative /isodiphasic T waves on inferior lead in 10/12 (83%) (Figure 9A,B); all had documented ventricular arrhythmias with right bundle branch block (RBBB) morphology (100%).

Macroscopically, MVP cases and controls did not differ in terms of heart weight, LV wall and septal thickness (all p=NS).

In SCD cases with MVP, mitral valve leaflets were always redundant, thick and elongated, with either isolated posterior (n. 13, 30%) or bileaflet (n.30, 70%) involvement (Figure 9C). The involvement of the posterior leaflet was diffuse in 23 (53%) and confined to the medial scallop in 20 (47%). Endocardial fibrous plaques in the postero-lateral wall were found in 25 (58%). At histology, diffuse myxoid degeneration of the spongiosa layer with Alcian PAS positive proteoglycans deposits, extending to the fibrosa and chordae tendineae, supported the gross diagnosis of MVP.

Microscopic examination of the LV myocardium showed an increase of endo-perimysial fibrosis and patchy replacement-type fibrosis at the level of PMs and adjacent free wall in all (Figure 9D,E and Figure 10). Similar findings, with a subendocardial-midmural layer distribution, were detected in the infero-basal

wall, underneath the posterior mitral valve leaflet, in 38 cases (88%). The mean fibrous tissue per cent area in SCD victims with MVP was 30.5% at the level of PMs and 33.1% in the infero-basal wall myocardium (vs. 6.3% and 6.4% respectively, in controls, $p<0.001$). In the same areas, the cardiomyocytes showed an increased diameter (19.2±6.0 micron vs. 12.8±0.4, $p<0.001$) and dysmorphic and dysmetric nuclei.

Table 13. Clinical and pathologic features of 43 patients who died suddenly with MVP due to myxomatous degeneration

Variables	SCD due to MVP 43 patients	Control 15 patients
Age, years median (range)	32 (19-40)	30 (18-40)
Female, n (%)	26 (61)	10 (67)
Athletes, n (%)	4 (9)	2 (13)
Marfan stigmata, n (%)	2 (5)	0
Pectus excavatum, n (%)	2 (4)	0
Pregnancy, n (%)	2/26 (8)	1/10 (10)
Circumstances of SCD, n (%)		
- on emotion/effort	8 (19)	4 (27)
- at rest	30 (70)	9 (60)
- during sleep	5 (12)	2 (13)
12 lead ECG available, n (%)	12 (28)	5 (33)
Inverted/biphasic T wave D2, D3, aVF n (%)	10 (83)	0
VAs, n (%)	12 (28)	0
VAs morphology, n (%)		
- RBBB	12 (100)	0
- LBBB	8 (67)	0
Antiarrhythmic therapy, n (%)	9 (21)	0
Gross features		
Heart weight (g), mean ±SD*	357±53	323±42
LV wall thickness (mm), mean±SD	12.6±1.3	12.5±3.6
VS thickness (mm), mean±SD	13.0±0.8	12.6±0.7
Patent foramen ovale, n (%)*	25 (58)	4 (27)
Oval fossa aneurysm, n (%)	10 (23)	1 (6)
Posterior MVP, n (%)	13 (30)	0
Bileaflet MVP, n (%)	30 (70)	0
Endocardial fibrous plaque, n (%)	25 (58)	0
Histology features		
LV scar		
- papillary muscles, n (%)	43 (100)	0
-infero-basal wall, n (%)	38 (88)	0
Fibrous tissue /myocardium (% area)		
- papillary muscles, mean ± SD †	30.5±10.7	6.3±1.6
- infero-basal wall, mean ± SD †	33.1±7.6	6.4±1.4
Cardiomyocytes diameter (μm), mean± SD †	19.2±6.0	12.8±0.4

Abbreviations: LV= Left Ventricle; MVP= mitral valve prolapse; RBBB= right bundle branch block; SCD= sudden cardiac death; VAs= ventricular arrhythmias; VS= ventricular septum.

† $p<0.001$

B) Clinical arm: MVP patients with ventricular arrhythmias.

The baseline clinical, electrocardiographic and functional and morphological CMR findings are summarized in Table 14. Fourteen MVP patients with minor ventricular arrhythmias, i.e. isolated ventricular premature beats (VPB), couplets and bigeminal VPB served as controls.

Thirty MVP patients (median age 41, range 28-43 years) with complex ventricular arrhythmias, i.e. ≥ 1 episode of VF (n.2) and VT (n.28) - either non-sustained (n.27) or sustained (n.1)- on 12-lead 24-hour Holter monitoring were collected. VT of LV origin (RBBB morphology) was present in all, with either inferior (43%) or superior (87%) axis. Among the 27 patients with non-sustained VT, the mean length in beats was 4 (ranging from 3 to 11 beats) and 15 (55%) had non-sustained VT ≥4 beats. Complex ventricular arrhythmias occurred at rest in 26/30 (87%). All patients had normal QTc (mean 423, range 409-440). Exercise stress test was performed in 20 and was negative for effort-induced ventricular arrhythmias.

Bileaflet MVP was present in 21 (70%) patients with complex ventricular arrhythmias vs. 5 (36%) of controls (p=0.031). On post-contrast sequences, LV-LGE was identified in 28 (93%) vs. 2 (14%) (p<0.001).

The LGE was localized on the PMs in 25 patients (83%), with a mid-apical distribution in 16 and/or basal adjacent free wall in 24 cases; and on the LV infero-basal segment, underneath the posterior valve leaflet, in 22 (73%) (Figure 11A-D). A segmental endocardial LGE, featuring the fibrous plaque, was found in 12 patients (40%). At quantitative analysis of LV LGE , the median LV LGE% was 1.2 in MVP with complex ventricular arrhythmias vs. 0 in in MVP without (p<0.01).

Two MVP patients experienced aborted SCD due to VF despite the use of anti-arrhythmic drug therapy with beta-blockers due to previous evidence of SVT.

Detailed invasive and non-invasive clinical and instrumental evaluation ruled out cardiac causes other than MVP. Both patients had ventricular arrhythmias with RBBB pattern and superior axis and T waves abnormalities on inferior leads. CMR, performed 6 and 10 months before aborted SCD, revealed LV LGE of PMs and of the infero-basal wall underneath the posterior mitral leaflet (Figure 11 E,F). Both patients received an implantable cardioverter defibrillator (ICD). One patient had pre-syncopal episodes despite antiarrhythmic therapy with bisoprolol. She underwent electrophysiological study with induction of sustained VT with the same RBBB morphology of VPBs (Figure 12A-C). The CMR showed a non-ischemic LGE pattern in the LV infero-basal wall (Figure 12D). She also underwent ICD implantation.

Of these three patients implanted with ICD (mean follow-up 10 months), two had NSVT: one patient with spontaneous interruption and the other one requiring anti-tachycardia pacing.

Table 14. Clinical, ECG and CMR features of 44 patients with MVP

Variables	MVP with CVA 30 pts	MVP without CVA 14 pts	p
Age, years median (range)	41 (28-43)	51 (24-64)	0.44
Female, n (%)	22 (73)	7 (50)	0.18
Symptoms, n (%)			
– aborted SCD	2 (7)	0	-
– palpitations	15 (50)	5 (36)	0.52
– syncope	2 (7)	0	1.00
– chest pain	2 (7)	1 (7)	1.00
– dyspnea	2 (7)	1 (7)	1.00
Therapy, n (%)			
– Beta-blockers	13 (43)	6 (43)	1.00
– Sotalol	3 (10)	0	0.54
– Other antiarrhythmic	1 (3)	1 (7)	0.54
12 lead ECG			
Inverted/biphasic T wave, n (%)	10 (33)	3 (21)	0.5
– D2, D3, aVF	9 (30)	2 (14)	0.46
– D1, aVL	2 (7)	1 (7)	1.00
QTc duration, msec	423 (409-440)	412(394-432)	0.19
ECG-Holter monitoring			
– VPB, n (%)	30 (100)	8 (57)	<0.01
– Bigeminal VPB	11 (37)	3 (21)	0.49
– NSVT, n (%)	27 (90)	0	-
SVT, n (%)	1 (3)	0	-
VF, n (%)	2 (7)	0	-
CVAs morphology, n (%)			
– LBBB inferior axis	0	0	-
– LBBB superior axis	1 (3)	0	-
– RBBB inferior axis	13 (43)	0	-
– RBBB superior axis	26 (87)	0	-

Abbreviations: SCD: sudden cardiac death; VPB: ventricular premature beats; NSVT: non sustained ventricular tachycardia; SVT: sustained ventricular tachycardia; VF: ventricular fibrillation; CVA: Complex ventricular arrhythmias; LBBB: left bundle branch block; RBBB: right bundle branch block.

Data are presented as median (1^{st}-3^{rd} quartiles) or N (%).

Table 14. Continued

Variables	MVP with CVA 30 pts	MVP without CVA 14 pts	p
CMR Morpho-functional Findings			
LV EDV, ml/m^2	91 (89-103)	91 (83-91)	0.13
LV EF, %	64 (60-65)	66 (64-69)	<0.01
LV mass, gr/m^2	62 (60-63)	63 (49-63)	0.48
RV EDV, ml/m^2	77 (71-79)	77 (76-78)	0.35
RV EF, %	64 (61-66)	64 (64-66)	0.43
Posterior MVP, n (%)	9 (30)	9 (64)	0.05
Bileaflet MVP, n (%)	21 (70)	5 (36)	0.05
Lengths MV leaflets, mm			
− Anterior	21 (19-26)	20 (17-25)	0.32
− Posterior	16 (13-18)	11.4 (9-14)	0.02
Prolapse distance, mm			
− Anterior leaflet	5 (2-8)	1 (0-3)	0.01
− Posterior leaflet	8 (4-12)	2 (2-4)	<0.01
CMR Post-contrast Findings			
LV LGE	28 (93)	2 (14)	<0.01
− papillary muscles	25 (83)	2 (14)	<0.01
− infero-basal wall	22 (73)	1 (7)	<0.01
LV LGE amount (%)	1.2 (0.8-2.1)	0	<0.01

Abbreviations: LV:left ventricle; RV right ventricle; EF= Ejection Fraction; EDV = End-Diastolic Volume; MV: mitral valve; LGE= Late Gadolinium Enhancement.

Data are presented as median (1st-3rd quartiles) or N(%).

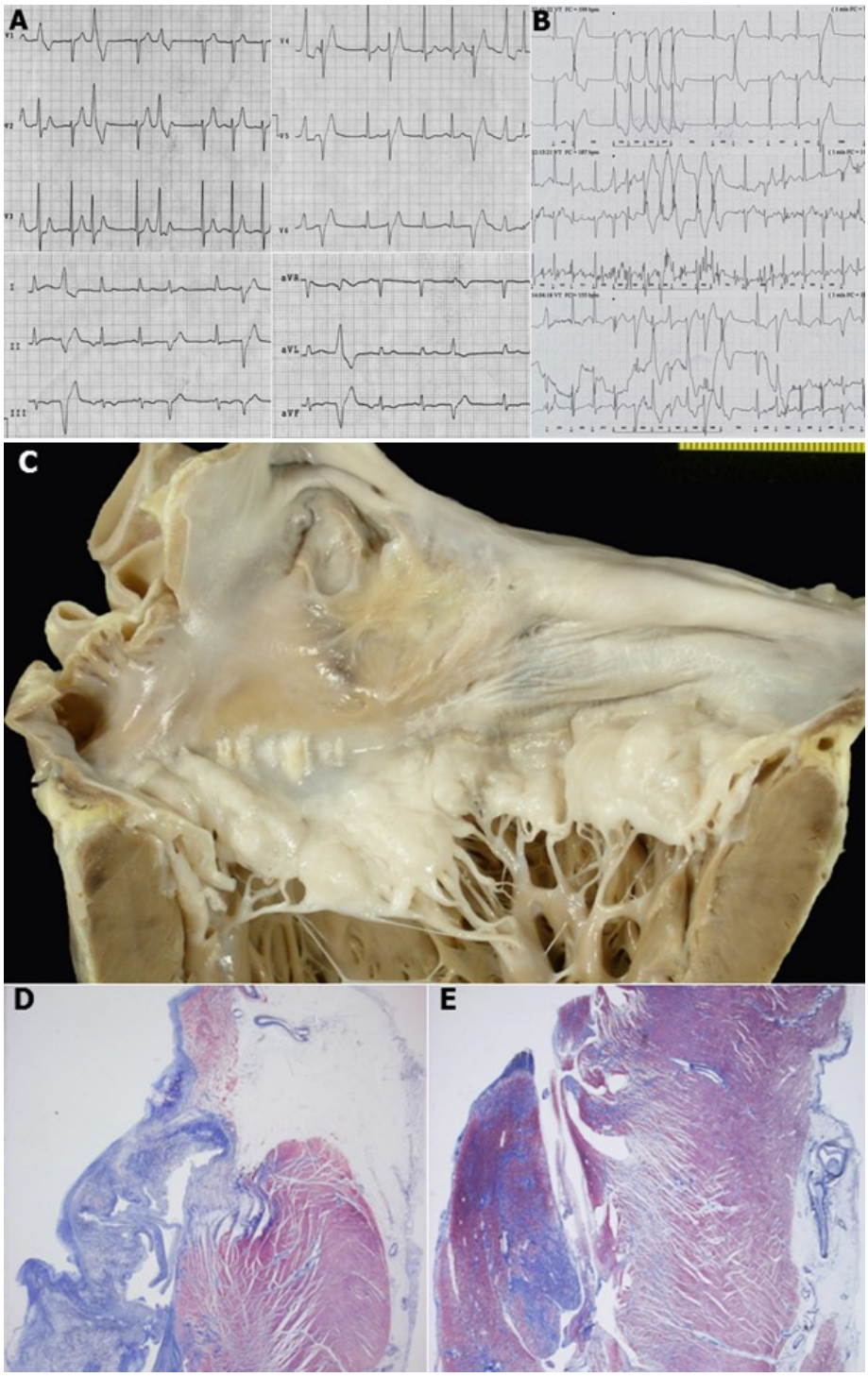

Figure 9. SCD in a 36 years old woman with in vivo diagnosis of MVP. A,B) 12-lead basal ECG at the time of emergency department admission for palpitations. Single and coupled VPBs with RBBB morphology are present; note the negative T wave on the inferior leads. At 24 hour Holter-ECG (B) NSVT is also recorded; C) At gross examination, myxomatous degeneration of both leaflets of the mitral valve with elongated chordae is visible; D,E). At histology, severe myxoid thickening of the posterior mitral valve leaflet and myocardial fibrosis of the LV infero-basal wall (D) and PM (E).

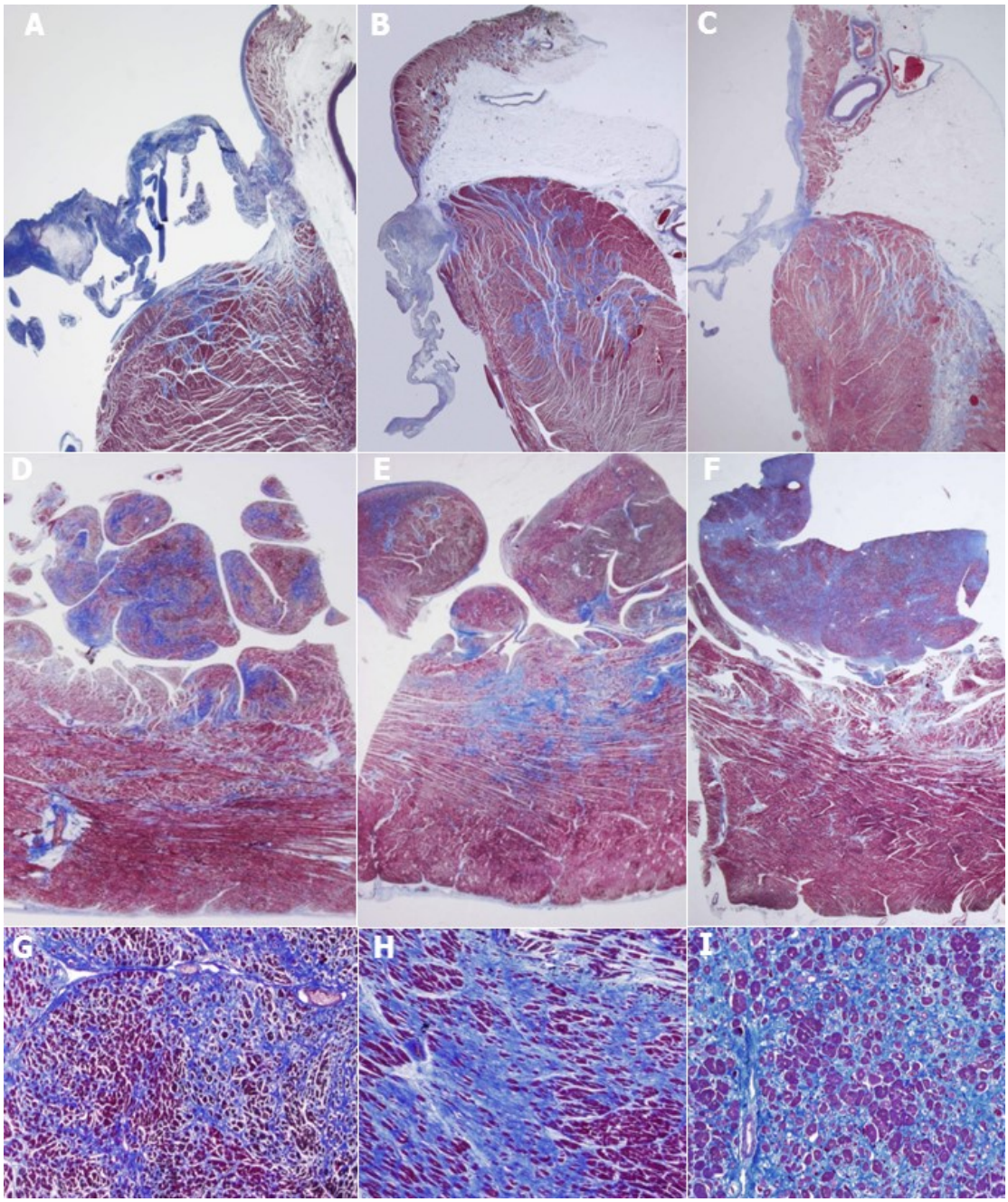

Figure 10. Histology of three representative SCD cases with MVP. Myocardial scarring is visible at the level of the infero-basal LV free wall, underneath the posterior mitral valve leaflet (A,B,C) and of the PMs plus adjacent free wall (D,E,F). Close-up of the scarring areas showing endo-perimysial and patchy replacement-type fibrosis with interspersed cardiomyocytes (G,H,I).

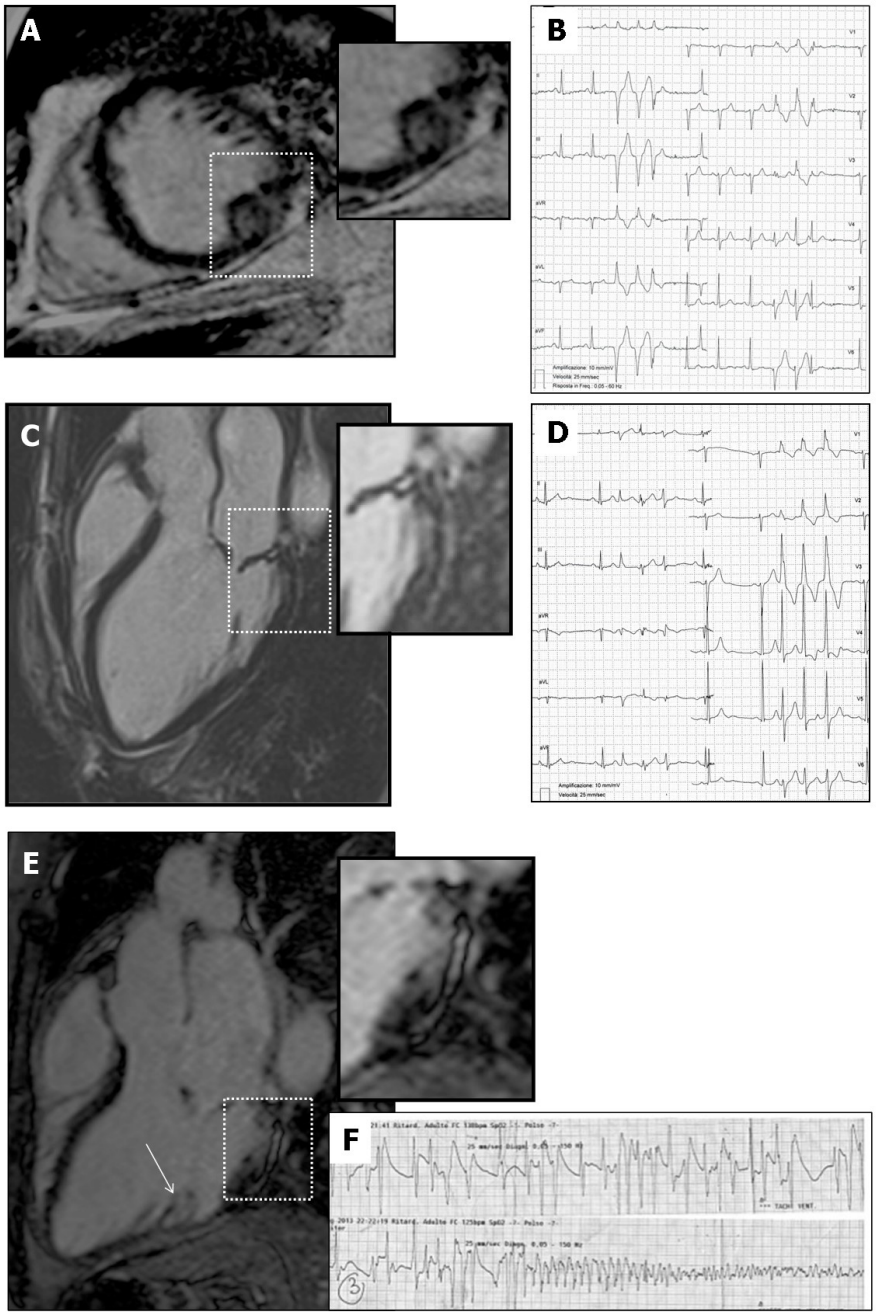

Figure 11 CMR findings in MVP patients with complex ventricular arrhythmias and aborted SCD. A,B) A 30 years old woman with MVP and complex ventricular arrhythmias. LGE of the PM is visible on mid-short axis view (A). The 12 lead ECG (B) shows the presence of NSVT with RBBB morphology originating from the posterior PM (superior axis). C,D) A 33 years old woman with MVP and complex ventricular arrhythmias. LGE of the LV infero-basal region, underneath the posterior valve leaflet, with endocardial-midmural extension, is visible on 3-chamber long axis view (C). The 12 lead ECG demonstrates NSVT with RBBB morphology originating from the LV infero-basal wall near the mitral annulus (inferior axis) (D). E, F) A 38 years old man with MVP and aborted SCD. CMR, performed 6 months before cardiac arrest, shows LGE in the infero-basal region of the LV on long-axis view (E). ECG recording of polymorphic SVT degenerating into VF (F).

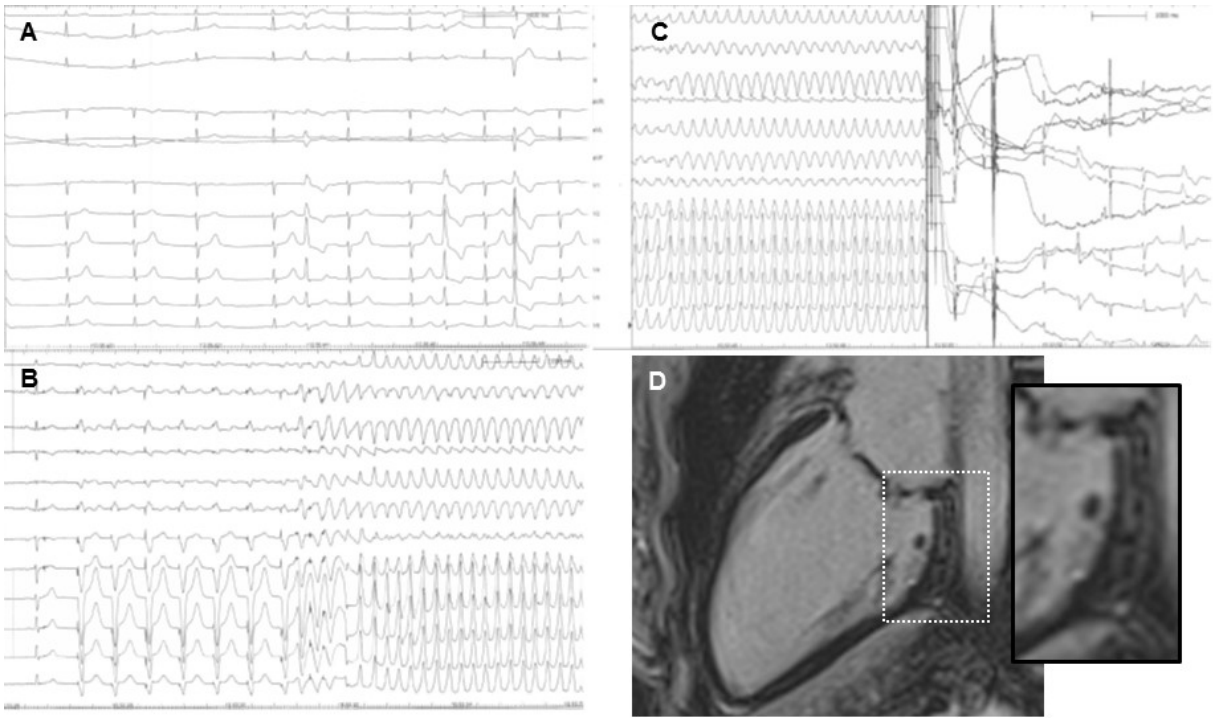

Figure 12 . A 34 years old woman with pre-syncopal episodes despite antiarrhythmic drug therapy.

A) Basal ECG shows isolated VPBs with two RBBB morphologies, indicating a LV origin from the PMs and the infero-basal wall close to the mitral anulus. B,C) Electro-physiologic study with programmed stimulation and induction of sustained VT with the same morphology of VPBs originating from the posterior mitral annulus, terminated by electrical cardioversion.

D) On CMR, LGE at the level of the LV infero-basal wall is visible.

5.5 Discussion and conclusions

MVP is an under-recognized cause of SCD in young adults, accounting for 7% of total fatal events and 13% of female victims in our large Cardiac Registry experience. Clear cut evidence of a substrate of electrical instability in MVP is herein provided for the first time and consists of myocardial scarring targeting the PMs and the infero-basal LV free wall, underneath the posterior leaflet, well in keeping with the site of origin of RBBB-type ventricular arrhythmias, showing either inferior or superior axis. The LV myocardial fibrosis observed at histology in SCD victims was then confirmed in the clinical arm of the study, with evidence of LGE at CMR in arrhythmic MVP patients, thus pointing to a promising role of this non invasive technique for risk stratification beyond traditional prognostic markers.

In MVP series with prolonged ECG recording, a variable prevalence of ventricular arrhythmias has been reported (80-82), reflecting the different MVP definition, the population studied and the complexity of ventricular arrhythmias considered. In particular, the clinical evidence of hemodynamically important regurgitation greatly impacts on the occurrence of ventricular arrhythmias (69).

However, the detection of MVP in survivors of life-threatening arrhythmias suggests that a true association between hemodynamically uncomplicated MVP and arrhythmic SCD may exist (76). Thus, we decided to focus on "pure" MVP, excluding MVP associated with valve incompetence and LV remodelling, not to defile the message and over-reporting ventricular arrhythmias. In the recent study of malignant MVP by Sriram et al (95), frequent VPBs originated from the outflow tract and PMs. Moreover, electrophysiology mapped the site of origin to the PMs, the LV outflow tract and the mitral annulus, as to suggest that VPBs arising close to the prolapsing leaflet and adjacent structures are the arrhythmic triggers.

From a pathophysiologic perspective, the mechanism of ventricular arrhythmias and SCD in MVP patients with trivial or absent mitral regurgitation remains speculative (76). MVP-related factors have been first advocated, such as the excessive traction on the PMs by the prolapsing leaflets; the mechanical stimulation of the endocardium by the elongated chordae, with after depolarization-induced triggered activity; the diastolic depolarisation of muscle fibres in redundant leaflets with triggered repetitive automaticity; and the endocardial friction lesions with their extension into the myocardium (98-100). Moreover, the coexistence of extravalvular diseases has been suggested, including autonomic nervous system dysfunction (94), conduction system abnormalities (78) and occult cardiomyopathies (77-91).

Previous pathology studies in MVP patients dying suddenly mostly focused on mitral valve structural alterations, suggesting a role for annular circumference, leaflets length and thickness and presence and extent of endocardial plaques (75,87-89). Surprisingly, no investigation did systematically address the LV myocardium in MVP patients dying suddenly to search for the substrate of electrical instability, except for a few anecdotic cases (87,90,99,124). For the first time, we extended the histopathology investigation beyond the valve in all SCD cases and provided convincing evidence of fibrosis in the LV myocardium which is closely linked to the mitral valve, i.e. the PMs with adjacent free wall and the infero-basal wall. The LV myocardial scarring is qualitatively different from that observed in ischemic heart disease, where it is usually compact and confluent, being instead patchy and interspersed within surviving, hypertrophic cardiomyocytes. Furthermore, we herein demonstrate that CMR detects LV- LGE in MVP patients with complex ventricular arrhythmias, overlapping in vivo the histopathologic features observed in SCD victims. At the level of PMs, two LGE deposition sites have been found, i.e. the mid-apical portion and the base/adjacent LV wall. Although PMs LGE has been reported by Han et al (111) in

MVP patients with a history of arrhythmias, most of these patients had moderate to severe mitral regurgitation. While confirming these data in purely arrhythmic MVP patients without hemodynamic impairment, we first provide convincing data on the presence of LGE in the infero-basal LV wall. The arrhythmogenic role of the LV myocardial scarring is supported by the morphology of arrhythmias and by electrophysiological studies in MVP indicating that the most common site of VPB origin is the infero-basal LV wall (95).

Many of the studies of CMR for risk stratification of SCD provide estimates of the percent of myocardium affected, with the notion that larger burdens of LGE are more relevant. Our preliminary quantitative data suggest that the volume of LV scarred tissue in MVP is relatively small but still significant. Thus, at difference from other conditions, LGE in MVP patients still predicts SCD risk despite the small burden. These findings are similar to those observed in dilated cardiomyopathy, where we demonstrated that LV-LGE is a powerful and independent predictor of malignant arrhythmic prognosis, while its amount and distribution do not provide additional prognostic value (5). Further studies with higher number of MVP patients are needed to confirm these preliminary quantitative data of LV LGE in MVP.

Since the early descriptions, abnormal LV contraction pattern and ECG abnormalities suggested that MVP has a significant myocardial involvement (116-119). The hypothesis that the so-called “MVP syndrome” is a cardiomyopathy, where regional hypercontractility acts as the primum movens of mitral valve geometry disruption, with abnormal tension on the chordae and leaflets and secondary increase in myxomatous tissue and leaflet thickening, has been even advanced. Our pathology and CMR data support the theory that LV abnormalities are rather the consequence of MVP, due to a systolic mechanical stretch of the myocardium closely linked to the valve, i.e. PMs and infero-basal wall, by the prolapsing leaflets and elongated chordae, accounting for a localized hyper-

contractility, with myocyte hypertrophy and injury leading eventually to fibrous tissue repair. The increased cardiomyocyte diameter in the same areas showing replacement-type fibrosis is in keeping with this theory.

Considering that performance of CMR in every case of MVP would be an expensive proposition, our study indicates some clinical markers that could target a high-risk subgroup of MVP patients destined for screening by CMR. These include ECG depolarization abnormalities on inferior or infero-lateral leads, complex ventricular arrhythmias (≥ 3 beats run) with RBBB morphology on 12-lead ECG Holter monitoring and a history of pre-syncope, syncope and aborted SD.

Finally, we recognize that our data support an association between anatomic substrate and risk, in an entity, i.e. MVP, that is under appreciated as a cause of SCD and also has a low enough incidence that any marker of increased risk might be of significant value to the clinician.

Current clinical practice suggests the use of generic drugs therapy (i.e. beta-blockers) in arrhythmic MVP patients. The fact that 21% of young adult SCD victims and two living MVP patients had aborted SCD despite beta-blocker therapy is intriguing. Prospective and multicentre studies are warranted to support the role of CMR and electrovoltage mapping for risk stratification and to assess the efficacy of traditional antiarrhythmic therapy and targeted catheter ablation in selected cases.

Limitations of the study.

The small number of enrolled MVP patients without complex ventricular arrhythmias could represent a limitation of the paper. However, we should recognize that it is difficult to collect “pure” MVP patients without either valve incompetence or ventricular arrhythmias. Prospective and multicentre studies enrolling a higher number of MVP with and without complex ventricular arrhythmias are needed to evaluate the exact prevalence of LGE in overall MVP population.

Conclusions.

MVP is a not so rare cause of SCD in young adults and is the leading one in women. Arrhythmic MVP patients are mostly female with ventricular arrhythmias of LV origin and frequent repolarization abnormalities on inferior leads. The hallmark of arrhythmic MVP is fibrosis of PMs and infero-basal LV wall, which well correlates with arrhythmia morphology, pointing to a myocardial stretch by the prolapsing leaflets and elongated chordae. CMR allows the identification of this arrhythmic substrate and is a promising non-invasive tool for risk stratification and SCD prevention.

Chapter 6

THE MITRAL VALVE PROLAPSE

The functional substrates underlying fibrosis

6.1 Introduction

As reported before in details, arrhythmic MVP seems to be characterized by LV fibrosis at the level of papillary muscles (PM) and inferobasal wall. We provided evidence of this structural substrate for electric instability both by histopathology in sudden cardiac death SCD patients with myxomatous mitral valve and by LGE on contrast-enhanced CMR in arrhythmic MVP patients, with the morphology of arrhythmias well correlating with the site of scarring (103). Thus, we hypothesized a localized mechanical stretch on the LV myocardium by the prolapsing leaflets producing replacement-type fibrosis. Myxomatous mitral valve is characterized by leaflet thickening and redundancy, interchordal hooding, chordal elongation, and annular dilatation because of accumulation of proteoglycans (75). In 1986, Hutchins et al (104) first advanced a role of the mitral annular disjunction (MAD), defined as a separation between left atrial (LA) wall at the level of mitral valve junction and the LV free wall, in disease pathogenesis. According to their hypothesis, this peculiar anatomy of the mitral annulus could trigger a mechanical stress on the leaflets, leading to myxomatous degeneration,

as a consequence of an excessive mobility of valve apparatus. Although MAD has been evaluated in MVP patients with severe valve regurgitation (105), its role in arrhythmic MVP remains to be elucidated.

6.2 Aim

Because MVP is a relatively common echocardiographic finding and only a small proportion of MVP patients is characterized by ventricular arrhythmias, the aim was to assess whether morphological and functional characteristics of the mitral valve apparatus could explain the propensity in some patients to develop a regional LV fibrosis at risk of electric instability. In order to investigate this hypothesis, the *in vivo* data collected by clinical study have been confirmed by pathological study.

6.3 Methods

Study populations

The study included consecutive arrhythmic patients (either right bundle branch block or polymorphic ventricular arrhythmias) referred to our Cardiology Clinic from January 2010 to July 2014 with echocardiographic diagnosis of MVP and who underwent CMR for the identification of LGE as previously defined. Complex ventricular arrhythmias consisted of ventricular fibrillation and ventricular tachycardia, either nonsustained or sustained.

MVP patients with LGE constituted our study population, whereas those without LGE, enrolled in the same period, served as control group. Patients with an echocardiographic diagnosis of MVP but without history of arrhythmias did not undergo CMR. Exclusion criteria were moderate-to-severe mitral regurgitation, tricuspid dysplasia or regurgitation, cardiomyopathies or congenital heart abnormalities, hemodynamic unstable conditions, and contraindication to CMR. The institutional review board approved the study, and all patients gave informed consent.

The pathology arm of the study included SCD patients with MVP and LV fibrosis (103). Hearts from sex- and age-matched patients who died suddenly as a result of extracardiac causes served as controls.

Protocols of investigation

A) Clinical arm

All patients underwent cardiovascular evaluation that included history, careful physical examination, 12-lead ECG, 2-dimensional transthoracic echocardiography, 12-lead 24-hour Holter monitoring, and CMR. Cardiac auscultation was performed in all patients, paying particular attention to the detection of midsystolic click and late systolic murmur, progressively anticipated in systole by postural changes (101,106,107). CMR was performed on a 1.5-T scanner (Magnetom Avanto, Siemens Medical Solutions, Erlangen, Germany). All patients underwent a detailed CMR study protocol (see appendix for details).

On CMR, a series of morphofunctional parameters were carefully evaluated. MAD was defined as a separation between the LA-valve junction and the atrial aspect of the LV free wall (104). According to this definition, the length of MAD (or elongated mitral annulus) was measured from the LA wall–posterior MV leaflet junction to the top of the LV inferobasal wall during end systole (108)

(Figure 13A). In particular, the upper limit of MAD was defined at the level of P2 scallop insertion to the LA wall, whereas the lower limit was defined at the level of LA connection with LV myocardium (105).

All these measurements were calculated from the 3-chamber view for the LV outflow tract long-axis view, equivalent to the transthoracic parasternal long-axis view, obtained by an image plane perpendicular to the mitral annular major axis centered at the aortic outflow track (109), and from 4-chamber view (110) (Figure 13) . According to previous studies on MVP (108-111), additional morphofunctional parameters were evaluated: 1) ventricular volumes; 2) lengths of MV leaflets; 3) prolapsed distance (measured as the maximum prolapsed distance during peak systole beyond the mitral annulus) (Figure 13B); 4) diastolic maximum MV leaflet thickness; 5) mitral annular diameter during end systole and end diastole; and 6) ratio of basal to midventricular end-diastolic wall thickness (Figure 13C).

Finally, the presence of the so-called curling, defined as an unusual systolic motion of the posterior mitral ring on the adjacent myocardium (112), was also evaluated. When present, a quantitative assessment of curling was provided, by tracing a line between the top of LV inferobasal wall and the LA wall–posterior MV leaflet junction, and from this line a perpendicular line to the lower limit of the mitral annulus was traced and expressed in millimetres (Figure 13D). Curling was defined as severe when the value was higher than the median value.

All these morphofunctional parameters were independently assessed by 2 experienced observers who were blinded to clinical data.

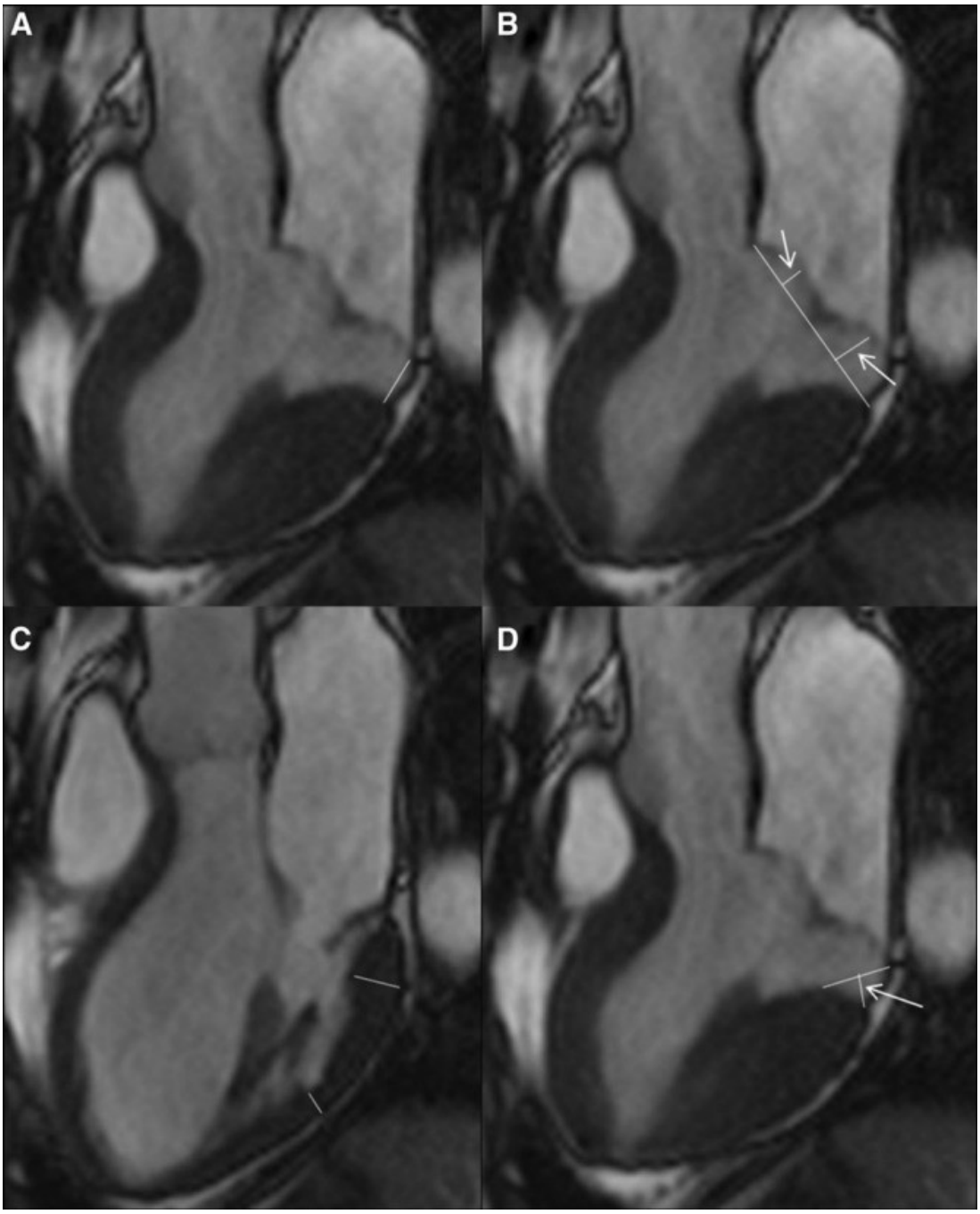

Figure 13.Cardiac magnetic resonance measures in patients with mitral valve prolapse. A, On 3-chamber, long-axis view, the length of mitral annulus disjunction (MAD; continuous white line) is measured from the left atrial (LA) wall–posterior MV leaflet junction to the top of the left ventricular (LV) inferobasal wall during end systole. B, On the same systolic frame, the prolapsed distance is measured as the maximum distance of the leaflet beyond the mitral annulus (white arrows). C, The LV thickness of basal and mid segments of the inferolateral wall is measured in the same long-axis view on diastole. D, The quantitative assessment of curling (white arrow) is provided by tracing a line between the top of LV inferobasal wall and the LA wall–posterior MV leaflet junction, and from this line, a perpendicular line to the lower limit of the mitral annulus during end systole.

B) Pathological Anatomy arm

Formalin-fixed hearts from patients who died suddenly with myxomatous MV degeneration and LV replacement-type fibrosis at the level of PM and inferobasal wall were examined to assess the presence of MAD, as previously defined. To this aim, longitudinal full thickness samples of the left atrioventricular junction along the lateral and posterior walls, including the LA wall, the LV wall, and the attachment of the posterior MV leaflet, were obtained for histology. Five-micrometer-thick sections were stained with hematoxylin–eosin, Weigert–van Gieson, and Heidenhain trichrome. Morphometric analysis was performed with an Image-Pro Plus program (version 4.0. Media Cybernetics) to measure the MAD at ×2 magnification expressed both in micrometers and millimeters. Quantitative analysis was performed by 2 blinded expert pathologists.

Statistical Analysis

Categorical data were expressed as number and percentage of population. Results were expressed as median and quartiles. In case of categorical variable, differences between groups were evaluated by the $\chi 2$ test or Fisher exact test as appropriate. Wilcoxon rank-sum test was used for quantitative variables. The interobserver agreement for CMR and histopathology measurements of MAD were evaluated with the Lin (113) Concordance Correlation Coefficient and the 95% confidence interval calculated with the bootstrap method considering 2000 resamplings. Ratio of basal to midventricular end-diastolic wall thickness was expressed both as continuous variable (millimeters) and as a cut off defined on the basis of median value. The linear correlation was expressed with Spearman correlation coefficient. In all the analyses, a value of $P<0.05$ was considered

statistically significant. Statistics were analyzed with SPSS version 19 (SPSS, Inc, Chicago, IL) and SAS 9.4 (SAS Institute, Inc, Cary, NC).

6.4 Results

A) Clinical arm

The baseline clinical and CMR findings of the 36 (27 female patients; median age: 44 years) arrhythmic MVP patients with LV fibrosis identified as LGE are summarized in Table 15. The control group consisted of MVP without LGE (n=16; 6 female patients; median age: 40 years).

A higher prevalence of midsystolic click (72% versus 38%; P=0.018), late systolic murmur (69% versus 25%; P=0.003), complex ventricular arrhythmias originating from the LV (32/36 [89%] versus 1/16 [6%]; P<0.001), and bileaflet MVP (26/36 [72%] versus 5/16 [31%]; P=0.005) was found in MVP patients with LV LGE as compared with those without. Moreover, MVP patients with LGE had a longer MAD (median: 4.8 versus 1.8 mm; P<0.001) and higher prevalence of curling (34 [94%] versus 3 [19%]; P<0.001). A representative case of a patient with curling and LV fibrosis is shown in Figure 14.

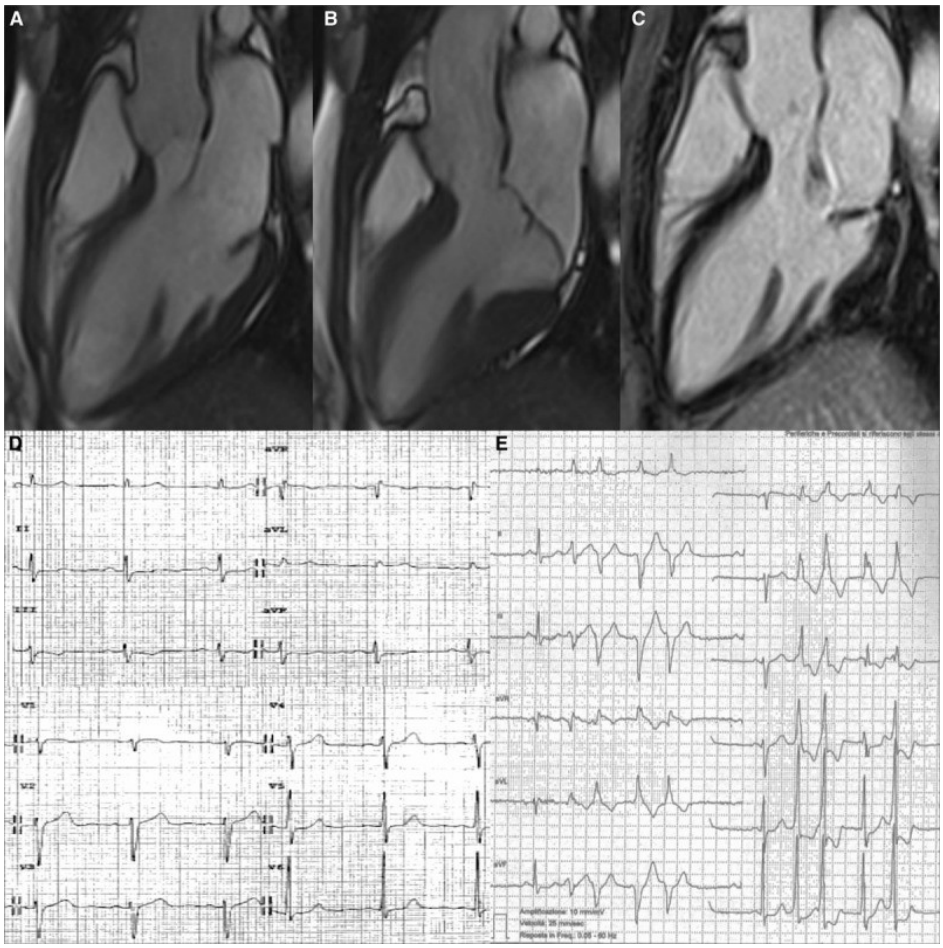

Figura 14 Representative case of arrhythmic MVP with mitral annular disjunction, curling, and late gadolinium enhancement (LGE). A 36-y-old woman with mitral valve prolapse and complex ventricular arrhythmias. On cine cardiac magnetic resonance (CMR) 3-chamber, long-axis view (diastolic frame A, systolic frame B), a mitral annulus disjunction is detectable; on contrast-enhanced CMR, a midmural LGE in the LV inferobasal region under posterior valve leaflet is visible (C). The 12-lead ECG (D) shows a negative T wave in III-aVF. Nonsustained ventricular tachycardia with right bundle branch block morphology originating from the LV inferobasal wall near the mitral annulus is also recorded in the 24-h Holter ECG (E).

The median value of the depth of curling was 3.5 mm in the overall population, with a statistically significant higher value in MVP patients with LGE (4.8 versus 0 mm; P<0.001). Using the median value as a cut off for severe curling, it was more prevalent in MVP patients with LGE (25% versus 1%; P<0.001). A linear correlation was found between MAD and curling (R=0.85; Figure 15) and

between MAD and extent of LGE (R=0.61; Figure 16). Patients with LV LGE showed an increased leaflet thickness both for anterior (median: 3.5 versus 3 mm; P=0.008) and posterior leaflet (median: 4 versus 3 mm; P=0.001) and a more pronounced prolapsed distance (anterior prolapsed distance median value: 4.9 versus 1 mm; P=0.004 and posterior prolapsed distance median value: 7.1 versus 2.1 mm; P<0.001). The median value of ratio between basal and mid portion of lateral wall thickness was 1.5 in the overall population, with no differences between the 2 groups. By applying the median value of 1.5 as a cut off for increased ratio, it was more prevalent in the LGE MVP group (22 [61%] versus 4 [25%]; P=0.016). Both end-systolic (median: 41.2 versus 31.5; P=0.004) and end-diastolic mitral annular diameters (median: 35.5 versus 31.5; P=0.042) differed between the 2 groups with a paradoxical increase of the mitral annulus diameter during systole versus diastole in the LGE group. Patients with bileaflet MVP (n=31) had a longer MAD (4.8 versus 2.5; P<0.001), higher prevalence of curling (28 [90%] versus 9 [43%]; P<0.001) and of LGE (26 [84%] versus 10 [48%]; P=0.005) as compared with patients with single (posterior) leaflet MVP (n=21).

Table 15. Clinical and CMR Characteristics.

Variables	MVP with LGE 36 patients	MVP without LGE 16 patients	p
Age, years	44 (36-55)	40 (23-53)	0.351
Female, n (%)	27 (75)	6 (38)	0.010
Complex Ventricular Arrhythmias, n (%)	32 (89)	1 (6)	<0.001
Physical Examination			
Mid-systolic click	26 (72)	6 (38)	0.018
Murmurs	25 (69)	4 (25)	0.003
CMR Morpho-functional findings			
LV EDV, mL/m^2	91 (89-99)	91 (81-93)	0.581
LV EF, %	64 (60-65)	67 (65-71)	0.001
LV mass, g/m^2	62 (59-64)	63 (49-64)	0.691
RV EDV, mL/m^2	77 (70-80)	77 (75-83)	0.527
RV EF, %	64 (62-68)	65 (64-68)	0.534
Posterior MVP, n (%)	10 (28)	11 (69)	0.005
Bileaflet MVP, n (%)	26 (72)	5 (31)	0.005
Mitral leaflets thickness, mm			
Anterior	3.5 (3-4)	3 (3-3)	0.008
Posterior	4 (3-4)	3 (2.5-3)	0.001
LV lateral wall thickness, mm			
Basal segment	8 (6.1-8.9)	8 (7.1-9.1)	0.834
Mid segment	5 (4-6)	5.3 (4.8-6.8)	0.154
Ratio LV lateral mid/basal wall thickness	1.7 (1.3-2)	1.3 (1.2-1.5)	0.168
LV lateral mid/basal wall ratio≥1.5, n (%)	22 (61)	4 (25)	0.016
Prolapsed distance, mm			
Anterior leaflet	4.9 (1.4-7.9)	1.0 (0-2.8)	0.004
Posterior leaflet	7.1 (4-11)	2.1 (2.0-3.7)	<0.001
Mitral annular diameter, mm			
End-systolic	41.2 (35.1-45.5)	31.5 (29-36.5)	0.004
End-diastolic	35.5 (31-38)	31.5 (26-33.5)	0.042
Systolic-Diastolic variation	6.2 (1.5-9.5)	1.5 (0.2-4)	0.016
Length of MAD, mm	4.8 (3.2-7)	1.8 (0-3.8)	<0.001
Curling, n (%)	34 (94)	3 (19)	<0.001
Curling, mm	4.8 (3-6)	0	<0.001
Severe curling (≥3.5 mm), n(%)	25 (69)	1 (6)	<0.001

Abbreviation: EDV= end-diastolic volume; EF= ejection fraction; LV= left ventricular; MVP= mitral valve prolapse; MAD= mitral annular disjunction; RV= right ventricular. Categorical variables are presented as number of patients (%). Continuous values are expressed as median with 25% and 75%-iles.

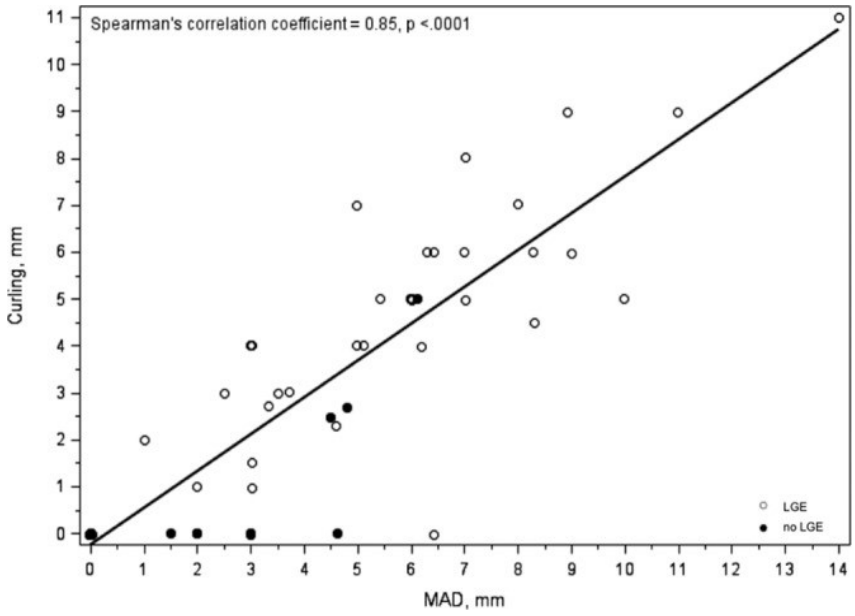

Figure 15 Relationship between length of mitral annular disjunction and curling in vivo. A significant correlation (*R*=0.85) between the depth of curling and length of mitral annulus disjunction (MAD; both expressed as mm) on cardiac magnetic resonance is observed. LGE indicates late gadolinium enhancement.

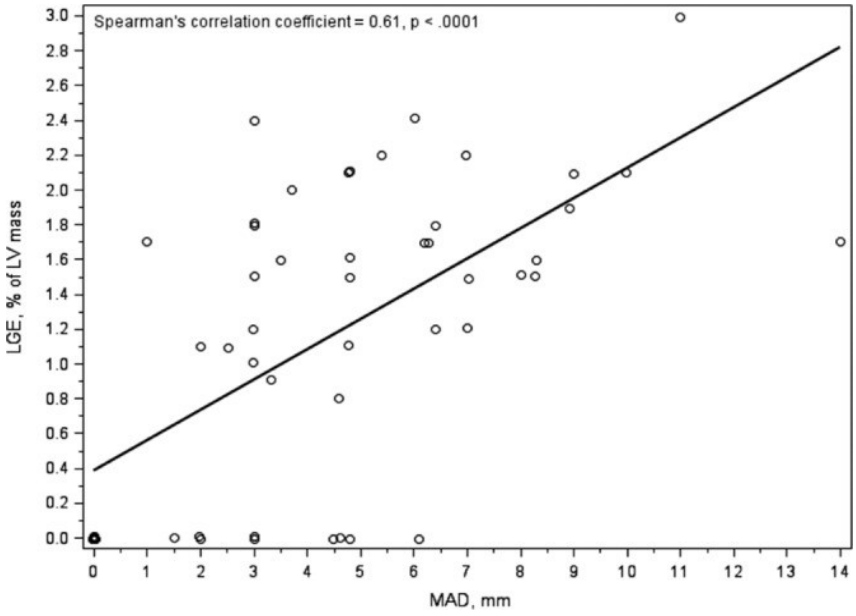

Figure 16 Relationship between length of mitral annular disjunction and amount of late gadolinium enhancement in vivo. A significant correlation (*R*=0.61) between the length of mitral annulus disjunction (MAD; expressed as mm) and the amount of late gadolinium enhancement (LGE; expressed as percentage of left ventricular [LV] mass) on cardiac magnetic resonance is observed.

On the basis of auscultatory findings, 32 MVP patients had a midsystolic click. Patients with midsystolic click showed an elongated MAD (median 4.8 versus 3 mm; P=0.1), curling (84% versus 50%; P=0.008), severe curling (≥4 mm in 63% versus 30%; P=0.023), LGE (81% versus 50%; P=0.018), and complex ventricular arrhythmias (75% versus 45%; P=0.029) as compared with those without click (Table 16)

Table 16. CMR findings according to mid-systolic click on auscultation.

Variables	**MVP with mid-systolic click** 32 patients	**MVP without mid-systolic click** 20 patients	**p**
Length of MAD, mm	4.8 (3-7)	3 (2.3-4.8)	0.089
Curling, n (%)	27 (84)	10 (50)	0.008
Curling, mm	4.8 (1.8-5.5)	1.2 (0-4)	0.009
Severe curling (≥3.5 mm), n(%)	20 (63)	6 (30)	0.023
LGE, n(%)	26 (81)	10 (50)	0.018
MV annulus systolic variation, mm	5.5 (0.8-9.5)	2.5 (-1.4-5.2)	0.042
Bileaflet MVP, n (%)	22 (69)	9 (45)	0.089
Prolapsed distance anterior leaflet, mm	4.9 (1-7.4)	1.8 (0-4.1)	0.050
Prolapsed distance posterior leaflet, mm	6.3 (3.5-11.4)	3.7 (2.1-5.8)	0.032
Complex Ventricular Arrhythmias, n (%)	24 (75)	9 (45)	0.029

LGE= Late Gadolinium Enhancement; MAD= mitral annular disjunction; MVP=mitral valve prolapse. Categorical variables are presented as number of patients (%). Continuous values are expressed as median with 25% and 75%-iles.

The 37 MVP with curling had a higher prevalence of negative T waves (32% versus 13%; P=0.3), LGE (92% versus 13%; P<0.001), and amount of LGE (1.6% of LV mass versus 0; P=0.001) as compared with those without curling.

B) Pathological arm

Mitral valve leaflets were redundant, thick, and elongated, with either isolated posterior (n=18, 36%) or bileaflet (n=32, 64%) involvement in a consecutive series of 50 SCD Patients (30 female patients; median age 36 years) with MVP and LV fibrosis. SCD patients with MVP had a longer MAD as compared with a series of 20 (14 female patients; median age: 34 years) SCD hearts without MVP (median: 3 versus 1.5 mm; P≤0.001; Figure 17).

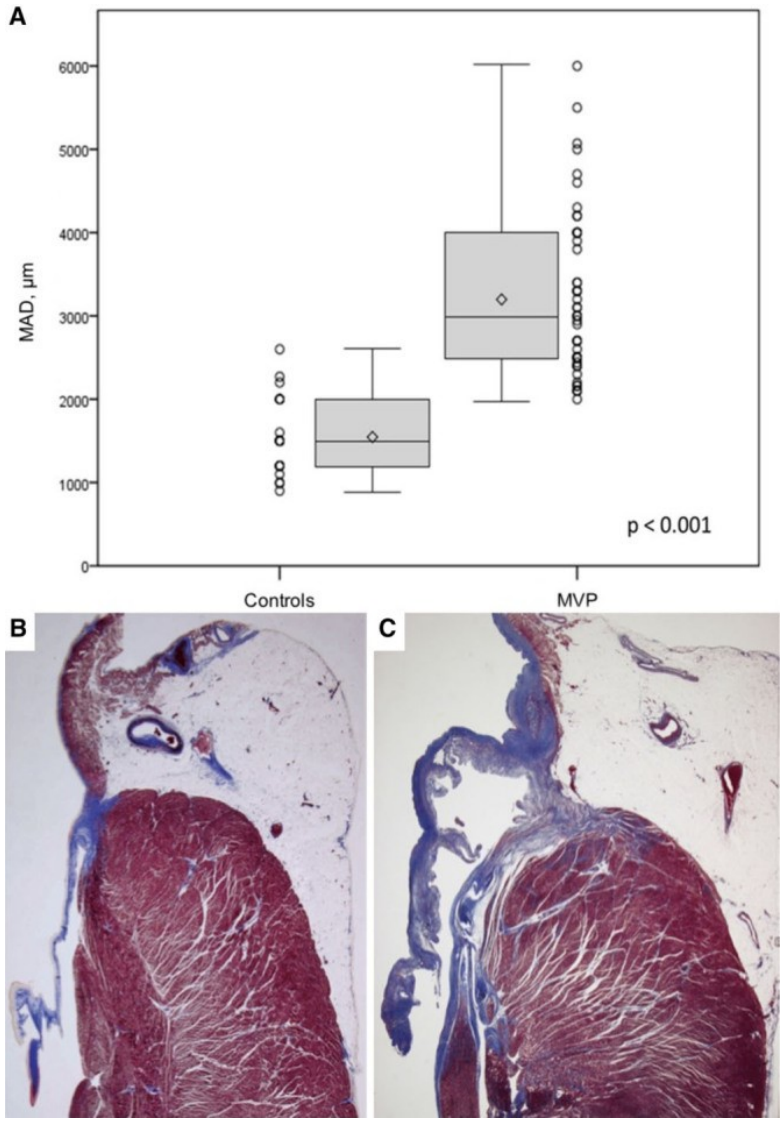

Figure 17 Length of MAD in SCD patients: controls vs mitral valve prolapse (MVP) patients. The length of MAD (measured as micrometers) in SCD patients with MVP is significantly higher than in controls (**A**). Representative histology of the mitral annulus showing the absence of MAD in a SCD control (**B**) as compared with an elongated MAD in a SCD patients with MVP (**C**).

6.5 Discussion and conclusions

Since arrhythmic MVP is characterized by myxomatous MV and LV fibrosis at the level of PM and inferobasal wall, as demonstrated before (103), the present study shows that MAD and systolic curling of the posterior MV leaflet are associated with LV fibrosis, accounting for the excessive mobility of the MV apparatus and systolic stretch of the myocardium closely linked to the valve. The specific distribution of LV fibrosis, as demonstrated by CMR, was in fact in keeping with a mechanical injury of the myocardium caused by the continuous traction of the prolapsing leaflets and elongated chordae.

The mitral annulus is a component of the MV apparatus and consists of a cord-like ring of collagen and elastic fibers distributed along the atrioventricular junction and giving support to the MV leaflets. It is conventionally divided into anterior and posterior portions, although the real annulus is the one that serves as hinge point for the mural posterior leaflet of the MV. The concept of MAD was originally introduced by Bharati (78) and then systematically investigated by Hutchins (104) in the 1980s, referring to an anatomic variation of the fibrous mitral annulus. In the latter pathological study of 900 hearts from adult autopsies, 25 (3%) had a morphologically typical floppy MV and 23 of them (92%) showed a MAD. This was defined as a variation in the attachment of the posterior MV leaflet, that accounts for a wide separation between the LA wall–MV junction and the LV attachment (104). In other words, the posterior annulus seemed stretched curtain-like, as compared with the normal cord-like structure (114). In the same series, MAD was rare in hearts without floppy MV (42 cases, 5%). Because these patients were significantly younger than those with a floppy MV, the authors suggested that this anatomic variation could play a role in the pathogenesis of

myxomatous valve degeneration, by means of increased mechanical stress induced by the excessive mobility of the MV apparatus (104).

To the best of our knowledge, this structural abnormality of the mitral annuls remained mostly forgotten and just a matter of speculation for pathologists up to 2005, when Eriksson (105) observed MAD by direct surgical inspection in some patients undergoing MV repair with advanced myxomatous disease. By applying a standardized transesophageal echocardiography protocol, the same authors found a 98% of prevalence of MAD in a surgical series of MVP patients with severe mitral regurgitation. Furthermore, a positive correlation between the severity of MAD and the number of diseased MV scallops was demonstrated, supporting the concept of an association between MAD and the severity of MVP. These authors also emphasized that impact of MAD on mitral annular function. In fact, in advanced MV disease, they did not observe any significant diastolic–systolic change in annular diameter, suggesting that not only mitral annulus geometry but also function is altered with loss of systolic contraction. On the basis of these findings, and the possible increased failure risk of MV repair because of an unrecognized MAD, Eriksson (105) modified their surgical repair technique to optimize long-term results.

Later on, Carmo (108) for the first time demonstrated that MAD is easily detectable and measurable also by routine transthoracic echocardiography. Using this technique in patients with myxomatous MV, including different degrees of mitral regurgitation, they found a MAD prevalence of 55%, more common in women (63% versus 38%) and often associated with chest pain. In this study, an association between MAD and mitral annulus dysfunction was also evidenced, with a paradoxical systolic increase of the mitral annulus diameter. Noteworthy, although sustained ventricular arrhythmias were not detected, an increased frequency of premature ventricular beats and nonsustained ventricular

tachycardia in patients with MAD versus those without was reported: the wider the magnitude of MAD, the higher the incidence of nonsustained ventricular tachycardia. In our study, we provide the evidence that MAD is associated with arrhythmic MVP, a theory previously only supposed (104,108). In our series, a quantifiable MAD was always detectable in both arrhythmic MVP patients with LV LGE (median: 4.8 mm) and SCD cases with LV fibrosis (median: 3 mm), mostly located close to the annulus in the inferobasal wall. The slight difference between CMR and histopathology MAD values is most likely the consequence of artifacts because of partial volume effects, as previously described in other echocardiographic studies (114,115). Moreover, the higher values reported by Eriksson (105) (10±3 mm) can be explained by their peculiar study population that included patients with severe mitral regurgitation, that, on the contrary, were excluded in our series. Interestingly, Carmo (108), by studying MVP patients with the entire spectrum of mitral regurgitation, demonstrated an intermediate value of MAD of 7.4±8.7 mm. The motion of the mitral annulus is passive and determined by the contraction and relaxation of adjacent atrial and ventricular musculature. As consequence, in normal condition, the posterior mitral ring and its adjacent myocardium move downward and anteriorly in systole, in synchrony with the remainder of the LV (114). Gilbert et al (112) in 1976 provided the first echocardiographic demonstration of a peculiar functional abnormality of the mitral annulus in MVP patients, describing an unusual systolic curling of the posterior mitral ring on the adjacent myocardium, so that the systolic movement of the ring was primarily downward with little, if any, anterior motion, thus resulting in a curled appearance when visualized in real-time motion. The authors concluded that the cause of curling in MVP was uncertain because, differently from previous reports, they did not visualize LV motion abnormalities either by echocardiography or angiography. In our series of arrhythmic MVP patients, we demonstrate for the first time that curling of the mitral annulus is associated with

MAD and accounts for annular hypermobility. Furthermore, a linear correlation has been found between the length of MAD and the severity of curling. These data create a link between the hypothesis made by Hutchins (104) and early angiographic observations of contractility abnormalities in MVP patients characterized by an arrhythmic profile, thus advancing the hypothesis of MVP as a cardiomyopathic condition (96,116,117).

A relative increase of the LV mass, which does not seem to be caused by mitral regurgitation, has been recognized in MVP since many years, suggesting that myocardial involvement is an integral part of arrhythmic MVP (118). On the basis of few observations of MVP patients with asymmetrical LV hypertrophy isolated to the inferobasal wall, Maron (119) even advanced the hypothesis of a novel form of hypertrophic cardiomyopathy. More recently, Zia (110) performed a CMR study demonstrating the existence of a relative concentric basal LV hypertrophy, focal and localized to the base in MVP patients as compared with controls. Moreover, they found a significantly increased ratio of basal to midventricular end-diastolic wall thickness mostly in the lateral wall, compared with all other segments. A positive correlation between the degree of relative basal LV hypertrophy and the excursion of the MV annulus, defined as the distance between the position of the annulus in end diastole and end systole, was also detected. All these findings are in keeping with a locally increased myocardial function adjacent to the prolapsed MV leaflet, eventually leading to focal hypertrophy of the LV base. The abnormal contractility of this LV region accounts in part for the so-called systolic curling motion. Noteworthy, original angiographic studies evidenced a bulging on the inferobasal wall, because of the abnormal contractility of the basal portion compared with the mid one, as to resemble the so-called ballerina-foot pattern (96, 120-125). In our arrhythmic MVP patients, we also found a relative hypertrophy of inferobasal wall, as compared with the adjacent mid portion. Moreover, a midmural LGE in the LV inferobasal wall was

demonstrated in 72% of cases, all with MAD and curling. On the contrary, in the study by Zia (110) no fibrosis as LGE was detectable in the context of basal hypertrophy. This discrepancy may be explained by the selection of MVP population, because we included MVP patients without mitral regurgitation, but with LGE and arrhythmic profile, differently from Zia who included retrospective patients with MVP and various degrees of valve regurgitation.

Although we demonstrated the role of LV fibrosis as a substrate of electric instability in arrhythmic MVP, a systematic investigation of morphofunctional abnormalities of the MV apparatus, capable to explain why a subgroup of MVP patients develop LV fibrosis, was still missing. The present study clearly demonstrates that, in arrhythmic MVP patients, the MV is characterized by MAD, systolic curling, and myxomatous leaflets thickening. On the basis of our previous observations in arrhythmic MVP (103) and the results reported in this study, the following cascade of events can be hypothesized. MAD is the cause of systolic curling motion; this morphofunctional alteration represents the basis for paradoxical increase of the MV annulus diameter during systole, myxomatous degeneration of MV leaflets, and myocardial stretch in the LV inferobasal segment. Our data in the subset of patients with arrhythmic MVP confirm, and further extend, the previous observation made by Hutchins et al. (104).

This impairment in the mitral annulus contractility not only influences the geometry and function of mitral ring and adjacent LV segments with relative hypertrophy but also involves a complex force balance of all MV components including PM. As a result of the abnormal contractility produced by MAD, the mechanical stretch is directly transmitted to PM that can also show LGE in the stretched areas. The regional area of hypercontraction, originally hypothesized and defined of unknown cause by Nutter (120), has a clear anatomic basis in the association of MAD with systolic curling. This association can increase wall stress in the inferobasal wall and PM, as evidenced by hypertrophy and replacement-

type fibrosis, both documented at postmortem by histology and confirmed in vivo as LGE by CMR in our previous study. The frequent observation of T-wave abnormalities on inferolateral leads at 12-lead ECG possibly suggests a disturbed repolarization of the area with abnormal contractility, as previously advanced (95,101,103).

The genesis of malignant arrhythmias in MVP probably recognizes the combination of the substrate (myocardial fibrosis) and the trigger (mechanical stretch) eliciting premature ventricular beats (99). Noseworthy (126) and Vaidya (127) reported a series of cases where the surgical correction of bileaflet MVP was associated with a reduction in malignant arrhythmia and appropriate implantable cardioverter defibrillator shocks. In other words, mitral valve repair could relieve the mechanical stretch of the myocardium, thus leading to a reduction, but no disappearance, of ventricular arrhythmias, as to confirm a key role of abnormal mechanical forces. When comparing bileaflet and single-leaflet MVP patients, the former have longer MAD and higher prevalence of curling and LGE. The fact that most of our arrhythmic patients had a bileaflet MVP is probably because of the entry criteria, since only patients with mild or absent mitral regurgitation were enrolled to exclude a confounding effect of hemodynamic impairment. In fact, it is likely that a retained coaptation of the leaflets does occur when both leaflets are involved.

In the past, following the original description of Barlow and Bosman (128,129), many studies addressed the syndrome of midsystolic click, late systolic murmur, and ballooning posterior mitral leaflet as a cause of distressing chest pain and life-threatening arrhythmias (86,90,96,101,124,130). More recently, because of the progressive disappearance of auscultation in the clinical setting (131), the role of midsystolic click as a marker of malignant MVP was overlooked. In our series, most of MVP patients with LGE had a midsystolic click on auscultation. Noteworthy, by reclassifying the population on the basis of presence

of midsystolic click, those with click had curling, LGE, and arrhythmias more frequently. In other words, MVP patients presenting with midsystolic click on auscultation, MAD, curling, and mitral annular abnormal contractility are those who need further evaluation for arrhythmic risk stratification through CMR. On the basis of our data, this auscultatory finding is likely because of the tension produced on the MV apparatus by the abnormal systolic curling (107). In light of these considerations, it is not surprisingly that in the early era of MVP, its diagnosis, being based on classical auscultatory findings, allowed the identification of patients with high prevalence of severe ventricular arrhythmias at risk of SCD (86,90,96,101,124,130). Arrhythmic MVP should be kept clearly distinct from the echocardiographic MVP, which is defined simply as single-leaflet or bileaflet prolapse of at least 2 mm beyond the long-axis annular plane. Although the latter is a relatively common condition with a benign behaviour (70,74,83,132,133), no data are available on the prevalence of the nosographic entity of arrhythmic MVP and further studies are needed.

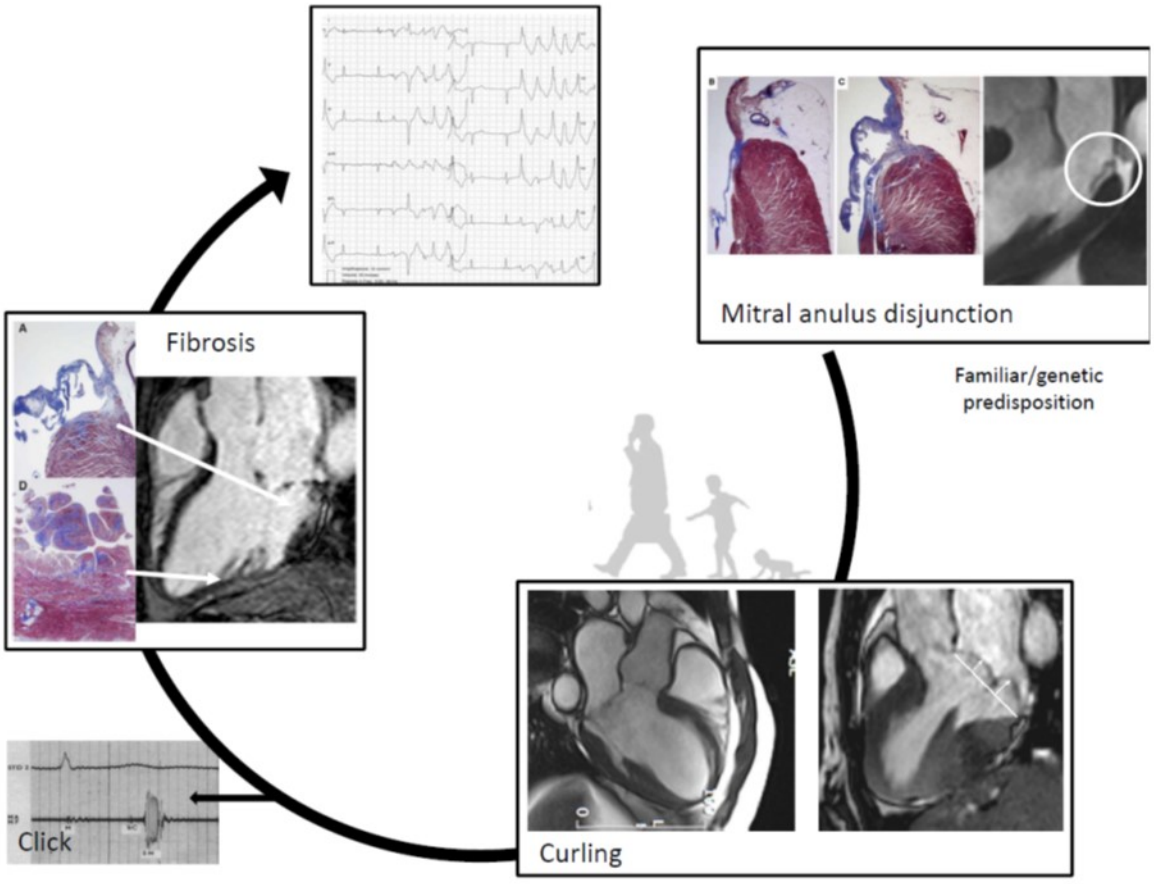

Figure 18. Phisiopathological hypothesis underling tissue characterization in MVP patients.

An association between MAD, curling, and LV fibrosis has been first detected by CMR in MVP patients with an arrhythmic malignant profile and then confirmed by histology in SCD patients with MVP. This unique annular morphology may account for the excessive mobility of the leaflets, as visualized by systolic curling and clinically suggested by auscultatory midsystolic click, and for the stretch-related myocardial remodelling of the inferobasal wall (Figure 18). Further studies are needed to confirm this hypothesis.

Chapter 7

CONCLUSIONS and LIMITATIONS

Cardiac magnetic resonance, due to its capability to provide both morphological, functional and tissue characterization information about any kind of heart disease “in vivo”, has become the linking between clinical issues and pathologist responses, allowing us to make diagnosis, suggesting hypothesis and making inference.

As in hypertrophic cardiomyopathy, dilated cardiomyopathy and in ischemic heart disease where the prognostic role of CMR is widely recognize, we herein demonstrated its value also in other and less studied heart disease.

We demonstrated as junctional fibrosis is not the classical myocardial scar and its association with higher LV filling pressure and/or right ventricular dysfunction make sense of its prognostic value for heart failure end point rather than ventricular arrhythmias.

Moreover, understanding the anatomical substrates underlying electrical issues (i.e. negative T waves), allows us to make inference about their prognostic value. Herein we demonstrated that transmural myocardial edema is associated with negative T waves in acute myocarditis as in tako-tsubo cardiomyopathy. Because

of its transitory nature, we hypothesized and confirmed that negative T-waves doesn't represent a marker of adverse remodeling in acute myocarditis (134) despite what are reported in literature.

Finally we investigated the linking between MVP and arrhythmias, disclosing that MVP cannot be defined simply as an excursion of one or both mitral valve leaflet into left atrium but probably we need to come back to Barlow and Gilbert's definition. An abnormal mitral insertion along the atrium-ventricular junction, the so called *disjunction,* perhaps associated with familiar/genetic predisposition, can be responsible of a non physiological leaflet protrusion into left atrium. This may lead to an abnormal valve and chordal progressive stretching that can be the responsible of a mixomatose valvular degeneration which perpetuates the vitium, according to Laplace theory. The chordae elongation yield the mid/late systolic click and the loss of coaptation of the billowing leaflet may produce the regurgitant murmur. The progressive development of "*curling*", due to the weak disjunction, represent the most sensational sign of the valve prolapse, leading an impairment of muscular contraction in these point where the stress is bigger (i.e. the papillary muscle and its insertion point and the basal LV). The tissue stretched leads to myocardial fibrosis may represent an arrhythmogenic substrate for MVP (103,135).

Some limitations about results are regarding the small population samples since the single center data. Further multicenter studies should be scheduled to confirm the conclusions obviously. On the other hand, the added value of these works is the closely relationship with in vivo and ex vivo findings: for what we explore in vivo by CMR, we find proofs in ex vivo pathologic studies.

APPENDIX

Detailed CMR acquisition protocols

- **Dilated Cardiomyopathy Study (chapter 3):**

Functional assessment and kinetic images: steady-state free precession sequence (true FISP) cine loops in sequential short axis views (slice thickness 6 mm, no gap; repetition time 2.5 to 3.8 ms; echo time 1.1 to 1.6 ms, average in-plane resolution 1.5x2.4 mm, flip angle 45° to 60°, temporal resolution 40 to 45 ms) and 3 long- axis views (2-chamber view, 3-chamber view, 4-chamber view).

Post contrast images: intravenous administration of gadobenate dimeglumine (Multihance, Bracco, 0.2 mmol/kg of body weight). Two-dimensional segmented fast low-angle shot inversion recovery sequence after at least 10 minutes were acquired in the same slices positions of cine images, covering the entire ventricles (repetition time 5.4 to 8.3 ms, echo time 1.3 to 3.9 ms, average in-plane spatial resolution 1.4 to 1.5 x 2.2 to 2.4 mm, 6- mm slice thickness, no gap, and flip angle 20° to 25°). Inversion times were adjusted to null normal myocardium (typically 220-300 msec). Images were repeated in 2 separate phase-encoding directions to exclude artefacts.

- **Acute Myocarditis study (chapter 4):**

Functional assessment and cinetic images: steady-state free precession sequence (true FISP) cine loops in sequential short axis views (slice thickness 6

mm, no gap; repetition time 2.5 to 3.8 ms; echo time 1.1 to 1.6 ms, average in-plane resolution 1.5x2.4 mm, flip angle 45° to 60°, temporal resolution 40 to 45 ms) and 3 long- axis views (2-chamber view, 3-chamber view, 4-chamber view).

Detection of myocardial edema: triple inversion recovery (TIRM) sequences were applied before contrast administration and acquired at the same location of cine images. Long axis views (2-chamber view, 3-chamber view, 4-chamber view) and sequential short axis views (slice thickness 6 mm, no gap): echo time 61 ms, average in-plane resolution 1.5x2.5 mm, flip angle 180°) .

Detection of early gadolinium enhancement: free-breathing black blood fast spin echo (FSE) T1-weighted sequence with an acquisition time of 3–4 min was acquired in four identical axial slices, both before and after (without any change in the parameters in between) intravascular injection of contrast agent (gadobenate dimeglumine, Multihance, Bracco, 0.2 mmol/kg of body weight).

Detection of LGE: ten minutes after intravenous administration of contrast agent 2-dimensional segmented fast low-angle shot inversion recovery sequences were acquired in the same views of cine images, covering the entire ventricles. Inversion times were adjusted to null normal myocardium using the Look-Locker sequence and images were repeated in 2 separate phase-encoding directions to exclude artefacts.

- **Mitral Valve Prolapse studies (chapter 5-6)**

Functional assessment and cinetic images: steady-state free precession sequence (true FISP) cine loops in sequential short axis views (slice thickness 6 mm, no gap; repetition time 2.5 to 3.8 ms; echo time 1.1 to 1.6 ms, average in-plane resolution 1.5x2.4 mm, flip angle 45° to 60°, temporal resolution 40 to 45 ms) and 3 long- axis views (2-chamber view, 3-chamber view, 4-chamber view).

Post contrast images: intravenous administration of gadobenate dimeglumine (Multihance, Bracco, 0.2 mmol/kg of body weight). Two-

dimensional segmented fast low-angle shot inversion recovery sequence after at least 10 minutes were acquired in the same slices positions of cine images, covering the entire ventricles (repetition time 5.4 to 8.3 ms, echo time 1.3 to 3.9 ms, average in-plane spatial resolution 1.4 to 1.5 x 2.2 to 2.4 mm, 6- mm slice thickness, no gap, and flip angle 20° to 25°). Inversion times were adjusted to null normal myocardium (typically 220-300 msec). Images were repeated in 2 separate phase-encoding directions to exclude artefacts.

REFERENCES

1. Schulz-Menger J, Bluemke DA, Bremerich J, et al. Standardized image interpretation and post processing in cardiovascular magnetic resonance: Society for cardiovascular magnetic resonance (scmr) board of trustees task force on standardized post processing. J Cardiovasc Magn Reson. 2013;15:35
2. Kuruvilla S, Adenaw N, Katwal AB, et al. Late Gadolinium Enhancement on Cardiac Magnetic Resonance Predicts Adverse Cardiovascular Outcomes in Nonischemic Cardiomyopathy. A Systematic Review and Meta-Analysis. Circ Cardiovasc Imaging. 2014 7:250-258.
3. Kim RJ, Chen EL, Lima JA, et al. Myocardial Gd-DTPA kinetics determine MRI contrast enhancement and reflect the extent and severity of myocardial injury after acute reperfused infarction. Circulation 1996 94:3318–26.
4. Sechtem U, Mahrholdt H, Vogelsberg H. Cardiac magnetic resonance in myocardial disease. Heart 2007;93:1520–1527
5. Klem I, Weinsaft JW, Bahnson TD, et al. Assessment of myocardial scarring improves risk stratification in patients evaluated for cardiac defibrillator implantation. J Am Coll Cardiol. 2012 60:408–420.
6. Perazzolo Marra M, De Lazzari M, Zorzi A, et al. Impact of the presence and amount of myocardial fibrosis by cardiac magnetic resonance on arrhythmic outcome and sudden cardiac death in nonischemic dilated cardiomyopathy. Heart Rhythm. 2014 May 11:856-63
7. Green JJ, Berger JS, Kramer CM et al. Prognostic value of late gadolinium enhancement in clinical outcomes for hypertrophic cardiomyopathy. J Am Coll Cardiol Img 2012;5:370–7.

8. Chan R, Maron BJ, Olivotto I et al. Prognostic utility of contrast-enhanced cardiovascular magnetic resonance in hypertrophic cardiomyopathy: an international multicenter study. J Am Coll Cardiol 2012 59:E1570.
9. Bruder O, Wagner A, Jensen CJ et al. Myocardial scar visualized by cardiovascular magnetic resonance imaging predicts major adverse events in patients with hypertrophic cardiomyopathy. J Am Coll Cardiol 2010 56:875–87.
10. Bhonsale A, James CA, Tichnell C et al. Incidence and predictors of implantable cardioverter-defibrillator therapy in patients with arrhythmogenic right ventricular dysplasia/cardiomyopathy undergoing implantable cardioverter-defibrillator implantation for primary prevention. J Am Coll Cardiol 2011 58:1485–96.
11. Jefferies JL, Towbin JA. Dilated cardiomyopathy. Lancet 2010;375:752-62.
12. Maron BJ, Towbin JA, Thiene G, et al. Contemporary Definitions and Classification of the Cardiomyopathies. An American Heart Association Scientific Statement From the Council on Clinical Cardiology, Heart Failure and Transplantation Committee; Quality of Care and Outcomes Research and Functional Genomics and Translational Biology Interdisciplinary Working Groups; and Council on Epidemiology and Prevention Circulation 2006;113:1807-1816.
13. Felker GM, Thompson RE, Hare JM, et al. Underlying causes and long-term survival in patients with initially unexplained cardiomyopathy. N Engl J Med. 2000;342:1077-84.
14. Goldberger JJ, Buxton AE, Cain M, et al. Risk stratification for arrhythmic sudden cardiac death: identifying the roadblocks. Circulation. 2011;123:2423-30.

15. Stecker EC, Vickers C, Waltz J, et al. Population-based analysis of sudden cardiac death with and without left ventricular systolic dysfunction: two-year findings from the Oregon Sudden Unexpected Death Study. J Am Coll Cardiol. 2006;47:1161-6.
16. Passman R, Goldberger JJ. Predicting the future: risk stratification for sudden cardiac death in patients with left ventricular dysfunction. Circulation. 2012;125:3031-7.
17. Wu TJ, Ong JJ, Hwang C, et al. Characteristics of wave fronts during ventricular fibrillation in human hearts with dilated cardiomyopathy: role of increased fibrosis in the generation of reentry. J Am Coll Cardiol. 1998;32:187-96.
18. Pogwizd SM, McKenzie JP, Cain ME. Mechanisms underlying spontaneous and induced ventricular arrhythmias in patients with idiopathic dilated cardiomyopathy. Circulation. 1998;98:2404-14.
19. Mewton N, Liu CY, Croisille P, Bluemke D, Lima JA. Assessment of myocardial fibrosis with cardiovascular magnetic resonance. J Am Coll Cardiol. 2011;57:891-903.
20. Butler J, Chomsky D, Wilson JR. Pulmonary hypertension and exercise intolerance in patients with heart failure.J Am Coll Cardiol 1999;34:1802-1806.
21. Abramson SV, Burke JF, Kelly JJ Jr Pulmonary hypertension predicts mortality and morbidity in patients with dilated cardiomyopathy. Ann Intern Med 1992;116:888-895.
22. Ghio S, Gavazzi A, Campana C, et al. Independent and additive prognostic value of right ventricular systolic function and pulmonary artery pressure in patients with chronic heart failure. J Am Coll Cardiol 2001;37:183-188.

23. Saxon LA, Stevenson WG, Middlekauff HR et al. Predicting death from progressive heart failure secondary to ischemic or idiopathic dilated cardiomyopathy. Am J Cardiol. 1993 Jul 1;72(1):62-5.
24. Rickenbacher PR, Trindade PT, Haywood GA et al. Transplant candidates with severe left ventricular dysfunction managed with medical treatment: characteristics and survival. J Am Coll Cardiol. 1996 Apr;27(5):1192-7.
25. Blyth KG, Groenning BA, Martin TN et al. C ontrast enhanced-cardiovascular magnetic resonance imaging in patients with pulmonary hypertension. Eur Heart J. 2005 Oct;26(19):1993-9
26. McCann GP, Gan CT, Beek AM et al. E xtent of MRI delayed enhancement of myocardial mass is related to right ventricular dysfunction in pulmonary artery hypertension. AJR Am J Roentgenol. 2007 Feb;188(2):349-55.
27. Sanz J, Dellegrottaglie S, Kariisa M et al. Prevalence and correlates of septal delayed contrast enhancement in patients with pulmonary hypertension. Am J Cardiol. 2007;100(4):731-5
28. Shehata ML, Lossnitzer D, Skrok J et al. Myocardial delayed enhancement in pulmonary hypertension: pulmonary hemodynamics, right ventricular function, and remodeling. AJR Am J Roentgenol. 2011;196(1):87-94
29. McCann GP, Gan CT, Beek AM et al. Extent of MRI delayed enhancement of myocardial mass is related to right ventricular dysfunction in pulmonary artery hypertension. AJR Am J Roentgenol. 2005 Feb;188(2):349-55.
30. Bradlow WM, Assomull R, Kilner PJ et al. Understanding late gadolinium enhancement in pulmonary hypertension. Circ Cardiovasc Imaging. 2010 ;3(4):501-3
31. Sato T, Tsujino I, Ohira H et al. Paradoxical interventricular septal motion as a major determinant of LGE in ventricular insertion points in pulmonary hypertension. PLoS ONE 8(6): e66724 .

32. Moon JC, Reed E, Sheppard MN et al. The histologic basis of late gadolinium enhancement cardiovascular magnetic resonance in hypertrophic cardiomyopathy. J Am Coll Cardiol. 2004;43(12):2260-4
33. Babu-Narayan SV, Goktekin O, Moon JC t al. Late gadolinium enhancement cardiovascular magnetic resonance of the systemic right ventricle in adults with previous atrial redirection surgery for transposition of the great arteries. Circulation. 2005 Apr 26;111(16):2091-8.
34. Babu-Narayan SV, Kilner PJ, Li W et al. Ventricular fibrosis suggested by cardiovascular magnetic resonance in adults with repaired tetralogy of fallot and its relationship to adverse markers of clinical outcome. Circulation. 2006 Jan 24;113(3):405-13
35. McCrohon JA, Moon JJC, Prasad SK, et al. Differentiation of heart failure related to dilated cardiomyopathy and coronary artery disease using gadolinium-enhanced cardiovascular magnetic resonance. Circulation 2003;108:54-9.
36. Neilan TG, Coelho-Filho OR, Danik SB, et al. CMR quantification of myocardial scar provides additive prognostic information in nonischemic cardiomyopathy. J Am Coll Cardiol Img 2013;6:944-54.
37. La Gerche A, Burns AT, Mooney DJ et al. Exercise-induced right ventricular dysfunction and structural remodelling in endurance athletes. Eur Heart J. 2012;33(8):998-1006
38. Galiè N, Humbert M, Vachiery JL et al. 2015 ESC/ERS Guidelines for the Diagnosis and Treatment of Pulmonary Hypertension. Eur Heart J. 2016 Jan 1;37(1):67-119
39. Richardson P, McKenna W, Bristow M, et al. Report of the 1995 World Health Organization/International Society and Federation of Cardiology Task Force on the Definition and Classification of cardiomyopathies. Circulation. 1996;93:841-2.

40. Amado LC, Gerber BL, Gupta SN, et al. Accurate and objective infarct sizing by contrast-enhanced magnetic resonance imaging in a canine myocardial infarction model. J Am Coll Cardiol 2004;44:2383.
41. Assomull RG, Prasad SK, Lyne J, et al. Cardiovascular magnetic resonance, fibrosis, and prognosis in dilated cardiomyopathy. J Am Coll Cardiol. 2006;48:1977-85.
42. Lehrke S, Lossnitzer D, Schöb M, et al. Use of cardiovascular magnetic resonance for risk stratification in chronic heart failure: prognostic value of late gadolinium enhancement in patients with non-ischaemic dilated cardiomyopathy. Heart. 2011;97:727-32.
43. Friedrich MG, Sechtem U, Schulz-Menger J, et al. Cardiovascular magnetic resonance in myocarditis: A JACC White Paper. J Am Coll Cardiol 2009;53:1475-87.
44. Iles L, Pfluger H, Lefkovits L, et al. Myocardial fibrosis predicts appropriate device therapy in patients with implantable cardioverter-defibrillators for primary prevention of sudden cardiac death. J Am Coll Cardiol. 2011;57:821-8.
45. Georgiopoulou VV, Kalogeropoulos AP, Borlaug BA et al. Left ventricular dysfunction with pulmonary hypertension: Part 1: epidemiology, pathophysiology, and definitions. Circ Heart Fail. 2013 Mar;6(2):344-54
46. Guazzi M, Borlaug BA. Pulmonary hypertension due to left heart disease. Circulation. 2012 Aug 21;126(8):975-90
47. Hsia HH, Haddad F. Pulmonary hypertension: a stage for ventricular interdependence? J Am Coll Cardiol. 2012 Jun 12;59(24):2203-5
48. McKenzie JC, Kelley KB, Merisko-Liversidge EM et al. Developmental pattern of ventricular atrial natriuretic peptide (ANP) expression in chronically hypoxic rats as an indicator of the hypertrophic process. J Mol Cell Cardiol. 1994 Jun;26(6):753-67.

49. Tea BS1, Dam TV, Moreau P et al. Apoptosis during regression of cardiac hypertrophy in spontaneously hypertensive rats. Temporal regulation and spatial heterogeneity. Hypertension. 1999 Aug;34(2):229-35
50. Kuribayashi T, Roberts WC. Myocardial disarray at junction of ventricular septum and left and right ventricular free walls in hypertrophic cardiomyopathy. Am J Cardiol. 1992 Nov 15;70(15):1333-40.
51. Saleh S, Liakopoulos OJ, Buckberg GD. The septal motor of biventricular function. Eur J Cardiothorac Surg. 2006 Apr;29 Suppl 1:S126-38
52. Beek AM, Kühl HP, Bondarenko O et al. Delayed contrast-enhanced magnetic resonance imaging for the prediction of regional functional improvement after acute myocardial infarction. J Am Coll Cardiol. 2003 Sep 3;42(5):895-901.
53. Caforio AL, Pankuweit S, Arbustini E, et al. Current state of knowledge on aetiology, diagnosis, management, and therapy of myocarditis: A position statement of the european society of cardiology working group on myocardial and pericardial diseases. Eur Heart J. 2013;34:2636-48, 2648a-2648d
54. Blauwet LA, Cooper LT. Myocarditis. Prog Cardiovasc Dis. 2010;52:274-88
55. Deluigi CC, Ong P, Hill S et al. Ecg findings in comparison to cardiovascular mr imaging in viral myocarditis. Int J Cardiol. 2013;165:100-6
56. Di Bella G, Florian A, Oreto L, et al. Electrocardiographic findings and myocardial damage in acute myocarditis detected by cardiac magnetic resonance. Clin Res Cardiol. 2012;101:617-24
57. Punja M, Mark DG, McCoy JV. Electrocardiographic manifestations of cardiac infectious-inflammatory disorders. Am J Emerg Med. 2010;28:364-77

58. Morgera T, Di Lenarda A, Dreas L et al. Electrocardiography of myocarditis revisited: Clinical and prognostic significance of electrocardiographic changes. Am Heart J. 1992;124:455-67
59. Nucifora G, Miani D, Di Chiara A, et al. Infarct-like acute myocarditis: Relation between electrocardiographic findings and myocardial damage as assessed by cardiac magnetic resonance imaging. Clin Cardiol. 2013;36:146-52
60. Ukena C, Mahfoud F, Kindermann I et al. Prognostic electrocardiographic parameters in patients with suspected myocarditis. Eur J Heart Fail. 2011;13:398-5
61. Jhamnani S, Fuisz A, Lindsay J. The spectrum of electrocardiographic manifestations of acute myocarditis: An expanded understanding. J Electrocardiol. 2014;47:941-7
62. Migliore F, Zorzi A, Marra MP et al. Myocardial edema underlies dynamic t-wave inversion (wellens' ecg pattern) in patients with reversible left ventricular dysfunction. Heart Rhythm. 2011;8:1629-34
63. Migliore F, Zorzi A, Perazzolo Marra M et al. Myocardial edema as a substrate of electrocardiographic abnormalities and life-threatening arrhythmias in reversible ventricular dysfunction of takotsubo cardiomyopathy: Imaging evidence, presumed mechanisms, and implications for therapy. Heart Rhythm. 2015 Aug;12(8):1867-77
64. Perazzolo Marra M, Zorzi A, Corbetti F et al. Apicobasal gradient of left ventricular myocardial edema underlies transient t-wave inversion and qt interval prolongation (wellens' ecg pattern) in tako-tsubo cardiomyopathy. Heart Rhythm. 2013;10:70-7
65. Zorzi A, Perazzolo Marra M, Migliore F, et al. Relationship between repolarization abnormalities and myocardial edema in atypical tako-tsubo syndrome. J Electrocardiol. 2013;46:348-51

66. Cooper LT, Baughman KL, Feldman AM et al. The role of endomyocardial biopsy in the management of cardiovascular disease: a scientific statement from the American Heart Association, the American College of Cardiology, and the European Society of Cardiology. Endorsed by the Heart Failure Society of America and the Heart Failure Association of the European Society of Cardiology. J Am Coll Cardiol. 2007;50(19):1914-31
67. Inoue S, Murakami Y, Ochiai K, Kitamura J, Ishibashi Y, Kawamitsu H, et al. The contributory role of interstitial water in gd-dtpa-enhanced mri in myocardial infarction. J Magn Reson Imaging. 1999;9:215-19
68. Madias JE. Transient attenuation of the amplitude of the QRS complexes in the diagnosis of Takotsubo syndrome. Eur Heart J Acute Cardiovasc Care 2014;3:28-36
69. Hayek E, Gring CN, Griffin BP. Mitral valve prolapse. Lancet 2005 365: 507–18
70. Freed LA, Levy D, Levine RA, et al. Prevalence and clinical outcome of mitral-valve prolapse. N Engl J Med 1999; 341:1–7
71. Freed LA, Benjamin EJ, Levy D, et al. Mitral valve prolapse in the general population: the benign nature of echocardiographic features in the Framingham Heart Study. J Am Coll Cardiol 2002; 40: 1298-304
72. Nishimura RA, McGoon MD, Shub C, Miller FA Jr, Ilstrup DM, Tajik AJ. Echocardiographically documented mitral-valve prolapse. Long-term follow-up of 237 patients. N Engl J Med. 1985;313:1305-9
73. Düren DR, Becker AE, Dunning AJ. Long-term follow-up of idiopathic mitral valve prolapse in 300 patients: a prospective study. J Am Coll Cardiol. 1988;11:42-7.
74. Marks AR, Choong CY, Sanfilippo AJ, Ferré M, Weyman AE. Identification of high-risk and low-risk subgroups of patients with mitral-valve prolapse. N Engl J Med. 1989;320:1031-6.

75. Davies MJ, Moore BP, Braimbridge MV. The floppy mitral valve. Study of incidence, pathology, and complications in surgical, necropsy, and forensic material. Br. Heart J 1978;40:468–481
76. Kligfield P, Levy D, Devereux RB, Savage DD. Arrhythmias and sudden death in mitral valve prolapse. Am Heart J 1987; 113:1298–1307
77. Vohra J, Sathe S, Warren R, Tatoulis J, Hunt D. Malignant ventricular arrhythmias in patients with mitral valve prolapse and mild mitral regurgitation. Pacing Clin Electrophysiol 1993;16:387–93.
78. Bharati S, Granston AS, Liebson PR, Loeb HS, Rosen KM, Lev M. The conduction system in mitral valve prolapse syndrome with sudden death. Am Heart J 1981;101:667-70.
79. Burke AP, Farb A, Tang A, Smialek J, Virmani R. Fibromuscular dysplasia of small coronary arteries and fibrosis in the basilar ventricular septum in mitral valve prolapse. Am. Heart J.1997; 134:282–291
80. Campbell RW, Godman MG, Fiddler GI, Marquis RM, Julian DG. Ventricular arrhythmias in syndrome of balloon deformity of mitral valve. Definition of possible high risk group. Br Heart J 1976 38:1053-1057.
81. Chugh SS, Jui J, Gunson K, Stecker EC, John BT, Thompson B et al. Current burden of sudden cardiac death: multiple source surveillance versus retrospective death certificate-based review in a large U.S. community. J Am Coll Cardiol 2004 44:1268-1275.
82. Winkle RA, Lopes MG, Popp RL, Hancock EW. Life-threatening arrhythmias in the mitral valve prolapse syndrome. Am J Med 1976 60:961-967.
83. Savage DD, Levy D, Garrison RJ, Castelli WP, et al. Mitral valve prolapse in the general population. 3. Dysrhythmias: the Framingham Study. Am Heart J 1983 106:582-586.
84. Devereux RB, Perlolf JK, Reichek N, et al. Mitral valve prolapse. Circulation 1976 54:3-14

85. Hancock EW, Cohn K. The syndrome associated with midsystolic click and late systolic murmur. Am J Med 1966 41:183-96.
86. Shappell SD, Marshall OE, Brown RE, et al.. Sudden death and the familial occurrence of mid-systolic click, late systolic murmur syndrome. Circulation 1973 48:1128-34.
87. Chesler E, King RA, Edwards JE. The myxomatous mitral valve and sudden death. Circulation. 1983;67:632-9.
88. Pocock WA, Bosman CK, Chesler E, Barlow JB, Edwards JE. Sudden death in primary mitral valve prolapse. Am Heart J 1984;107:378-82.
89. Dollar AL, Roberts WC. Morphologic comparison of patients with mitral valve prolapse who died suddenly with patients who died from severe valvular dysfunction or other conditions.J Am Coll Cardiol. 1991;17:921-31
90. Jeresaty RM. Sudden death in the mitral valve prolapse-click syndrome. Am J Cardiol 1976 37:317-318.
91. Corrado D, Basso C, Nava A, et al. Sudden death in young people with apparently isolated mitral valve prolapse. G Ital Cardiol 1997 27:1097-1105.
92. Topaz O, Edwards JE. Pathologic features of sudden death in children, adolescents, and young adults. Chest 1985 87:476-482.
93. Wei JY, Bulkley BH, Schaeffer AH, et al. Mitral valve prolapse syndrome and recurrent ventricular tachyarrhythmias: a malignant variant refractory to conventional drug therapy. Ann Intern Med 1978 89:6–9.
94. Boudoulas H, Schaal S, Stang M, et al. Mitral valve prolapse sudden death long term survival JACC 1986 (Supp) 7: 29A
95. Sriram CS, Syed FF, Ferguson E, et al. Malignant bileaflet mitral valve prolapse syndrome in patients with otherwise idiopathic out-of-hospital cardiac arrest. JACC 2013 62:222-230

96. Gulotta SJ, Gulco L, Padmanabhan V, et al. The syndrome of systolic click, murmur, and mitral valve prolapse-a cardiomyopathy? Circulation 1974 49:717-728.
97. Crawford MH, O'Rourke RA. Mitral valve prolapse: a cardiomyopathic state? Prog Cardiovasc Dis 1984 27:133-139.
98. Cobbs BW, King SB 3rd. Ventricular buckling: a factor in the abnormal ventriculogram and peculiar hemodynamics associated with mitral valve prolapse. Am Heart J 1977 93:741-758.
99. Wilde AM, Duren DR, Hauer RNW, et al. Mitral Valve Prolapse and Ventricular Arrhythmias: Observations in a Patient with a 20-Year History. Journal of Cardiovascular Electrophysiology 1997 8:307-16 .
100. Criley JM, Zeilenga DW, Morgan MT. Mitral dysfunction: a possible cause of arrhythmias in the prolapsing mitral leaflet syndrome. Trans Am Clin Climatol Assoc 1974 85:44-53.
101. Rizzon P, Biasco G, Brindicci G et al. Familial syndrome of midsystolic click and late systolic murmur. British Heart Journal 1973 35:245-259
102. Zabel M. Roller B. Franz MR: Amplitude and polarity of stretch-induced voltage changes depend on the timing of stretch: A means to characterize stretch-activated channels in the intact heart. (Abstract) PACE 1993 16:886.
103. Basso C, Perazzolo Marra M, Rizzo S, et al. Arrhythmic Mitral Valve Prolapse and Sudden Cardiac Death. Circulation. 2015;132:556-66.
104. Hutchins GM, Moore GW, Skoog DK. The association of floppy mitral valve with disjunction of the mitral annulus fibrosus. N Engl J Med. 1986;314:535-40.
105. Eriksson MJ, Bitkover CY, Omran AS, et al. Mitral annular disjunction in advanced myxomatous mitral valve disease: echocardiographic detection and surgical correction. J Am Soc Echocardiogr. 2005;18:1014-22.

106. Weis AJ, Salcedo EE, Stewart WJ, et al. Anatomic explanation of mobile systolic clicks: implications for the clinical and echocardiographic diagnosis of mitral valve prolapse. Am Heart J. 1995;129:314-20.
107. Mathey DG, Decoodt PR, Allen HN et al. The determinants of onset of mitral valve prolapse in the systolic click-late systolic murmur syndrome. Circulation. 1976;53:872-8.
108. Carmo P, Andrade MJ, Aguiar C et al. Mitral annular disjunction in myxomatous mitral valve disease: a relevant abnormality recognizable by transthoracic echocardiography. Cardiovasc Ultrasound. 2010;8:53.
109. Han Y, Peters DC, Salton CJ, et al. Cardiovascular magnetic resonance characterization of mitral valve prolapse. JACC Cardiovasc Imaging. 2008;1:294-303.
110. Zia MI, Valenti V, Cherston C, et al. Relation of mitral valve prolapse to basal left ventricular hypertrophy as determined by cardiac magnetic resonance imaging. Am J Cardiol. 2012;109:1321-5.
111. Han Y, Peters DC, Kissinger KV, et al. Evaluation of papillary muscle function using cardiovascular magnetic resonance imaging in mitral valve prolapse. Am J Cardiol. 2010 Jul 15;106:243-8.
112. Gilbert BW, Schatz RA, VonRamm OT, et al. Mitral valve prolapse. Two-dimensional echocardiographic and angiographic correlation. Circulation. 1976;54:716-23.
113. Lin LI.A concordance correlation coefficient to evaluate reproducibility. Biometrics. 1989 Mar;45:255-68.
114. Silbiger JJ, Anatomy, mechanics, and pathophysiology of the mitral annulus. Am Heart J 2012;164:163-76.
115. Levine RA, Hagége AA, Judge DP, et al. Mitral valve disease-morphology and mechanisms. Nat Rev Cardiol. 2015;12:689-710.

116. Scampardonis G, Yang SS, Maranhão V, et al. Left ventricular abnormalities in prolapsed mitral leaflet syndrome. Review of eighty-seven cases. Circulation. 1973;48:287-97.
117. Crawford MH, O'Rourke RA. Mitral valve prolapse: a cardiomyopathic state? Prog Cardiovasc Dis. 1984;27:133-139.
118. Haikal M, Alpert MA, Whiting RB, et al. Increased left ventricular mass in idiopathic mitral valve prolapse. Chest. 1982;82:329-33.
119. Maron BJ, Sherrid MV, Haas TS, et al. Novel hypertrophic cardiomyopathy phenotype: segmental hypertrophy isolated to the posterobasal left ventricular free wall. Am J Cardiol. 2010;106:750-2.
120. Nutter DO, Wickliffe C, Gilbert CA, et al. The pathophysiology of idiopathic mitral valve prolapse. Circulation. 1975;52:297-305.
121. Ehlers KH, Engle MA, Levin AR, et al. Left ventricular abnormality with late mitral insufficiency and abnormal electrocardiogram. Am J Cardiol. 1970;26:333-40.
122. Liedtke AJ, Gault JH, Leaman DM, et al. Geometry of left ventricular contraction in the systolic click syndrome. Characterization of a segmental myocardial abnormality. Circulation. 1973;47:27-35.
123. Farry JP, Simon AL, Ross AM, et al. Quantitative angiographic assessment of the mitral annulus in the prolapsing leaflet syndrome. Circulation. 1975; 52 (suppl II): 11-12.
124. Jeresaty RM. The syndrome associated with mid-systolic click and-or late systolic murmur. Analysis of 32 cases. Chest. 1971;59:643-7.
125. Gooch AS, Vicencio F, Maranhao V, et al. Arrhythmias and left ventricular asynergy in the prolapsing mitral leaflet syndrome. Am J Cardiol. 1972;29:611-20.
126. Noseworthy PA, Asirvatham SJ. The knot that binds mitral valve prolapse and sudden cardiac death. Circulation. 2015;13:551–552.

127. Vaidya VR, DeSimone CV, Damle N, et al. Reduction in malignant ventricular arrhythmia and appropriate shocks following surgical correction of bileaflet mitral valve prolapse. J Interv Card Electrophysiol. 2016 Aug;46(2):137-43
128. Barlow JB, Bosman CK. Aneurysmal protrusion of the posterior leaflet of the mitral valve. An auscultatory-electrocardiographic syndrome. Am Heart J. 1966;71:166-178.
129. Barlow JB, Bosman CK, Pocock WA, et al. Late systolic murmurs and non-ejection ("mid-late") systolic clicks: an analysis of 90 patients. Br Heart J. 1968;30:203-218
130. Jeresaty RM. Mitral valve prolapse-click syndrome. Progr Cardiovasc Dis. 1973;15:623-652
131. Adolph RJ. In defense of the stethoscope. Chest. 1998;114:1235-7
132. Levine RA, Handschumacher MD, Sanfilippo AJ, et al. Three-dimensional echocardiographic reconstruction of the mitral valve, with implications for the diagnosis of mitral valve prolapse. Circulation. 1989;80:589-98
133. Savage DD, Garrison RJ, Devereux RB, et al. Mitral valve prolapse in the general population. 1. Epidemiologic features: the Framingham Study. Am Heart J. 1983;106:571-6.
134. De Lazzari M, Zorzi A, Baritussio A, et al. Relationship between T-wave inversion and transmural myocardial edema as evidenced by cardiac magnetic resonance in patients with clinically suspected acute myocarditis: clinical and prognostic implications. J Electrocardiol. 2016 Jul-Aug;49(4):587-95.
135. Perazzolo Marra M, Basso C, De Lazzari M, et al. Morphofunctional Abnormalities of Mitral Annulus and Arrhythmic Mitral Valve Prolapse. Circ Cardiovasc Imaging. 2016 Aug;9(8):e005030.